ELECTRODELESS CONDUCTANCE MEASUREMENTS USING TOROIDAL INDUCTORS
MARTIN, ROBERT ARNOLD, JR.
ProQuest Dissertations and Theses; 1971; ProQuest Dissertations & Theses Global

71-23,941

MARTIN, Jr., Robert Arnold, 1943-
ELECTRODELESS CONDUCTANCE MEASUREMENTS USING
TOROIDAL INDUCTORS.

University of Pittsburgh, Ph.D., 1971
Chemistry, analytical

University Microfilms, A XEROX Company, Ann Arbor, Michigan

ELECTRODELESS CONDUCTANCE MEASUREMENTS USING TOROIDAL INDUCTORS

by

rnold
Robert A. Martin, Jr.

B. S., Dickinson College, 1965

Submitted to the Graduate Faculty of
Arts and Sciences in partial fulfillment
of the requirements for the degree of
Doctor of Philosophy

University of Pittsburgh
1971

UNIVERSITY OF PITTSBURGH

FACULTY OF ARTS AND SCIENCES

This thesis was presented

by

Robert A. Martin, Jr.

It was defended on

April 22, 1971

and approved by

Dr. C. E. Wilson

Dr. R. S. Craig

Dr. C. L. Stevens

Dr. J. J. Taber

Dr. H. W. Safford Chairman

FOREWORD

The author wishes to express his gratitude to Dr. H. W. Safford for suggesting the research reported herein; his counsel in the interpretation of experimental results and in the preparation of this thesis are deeply appreciated.

Many thanks are also due to Miss Lillian Abernethy whose ability to type this thesis from the author's undecipherable penmanship greatly facilitated the completion of this work.

Acknowledgment is also made to the National Science Foundation for a Graduate Traineeship and to the University of Pittsburgh for a Graduate Student Teaching Assistantship.

TABLE OF CONTENTS

Page

FOREWORD ii

I. INTRODUCTION 1

A. Purpose and Scope 1

B. Electrical Circuit Concepts 3

1. Definitions 3

2. Resonant Circuits 3

3. Q Factor 5

4. Toroidal Inductors 6

5. Mutual Inductance 7

C. Low Frequency Conductometric Analysis 10

1. Basic Principles 10

2. Applications 11

3. Limitations and Sources of Error 11

D. High Frequency Conductometric Analysis 13

1. Basic Principles 13

2. Instrument Response 14

3. Limitations and Sources of Error 16

E. Historical Background 18

1. Development of Theory and Instrumentation 18

2. Applications 21

II. APPARATUS AND REAGENTS 23

A. Signal Generators 23

1. General Considerations 23

2. The Heath Sine - Square Wave Generator, Model IG-82 23

Page

3. The Knight Sine - Square Wave Generator, Model KG-688 23

B. Voltmeters 24

1. The Heath Vacuum Tube Voltmeter, Model IM-21 . . . 24

2. Eico AC VTVM, Model 255 24

C. The Heath Decade Resistance Box, Model IN-11 25

D. The Heath Decade Capacitance Box, Model IN-21 25

E. The Sargent Model V Oscillometer, Catalog No. S-29180 26

F. The Beckman Instruments Conductivity Bridge, Model RC-16B2 26

G. Triad Transformer Corp. Toroidal Inductors 26

H. Indiana General Corp. Toroidal Cores 26

I. J. W. Miller Co. Toroid Cores 28

J. FET Amplifier 29

K. The "Sidearm" Measuring Apparatus 30

L. Magnetic Induction Probes (Dipping Type) 32

M. Reagents 35

1. Deionized Water 35

2. Chemicals 35

III. EXPERIMENTAL AND RESULTS 36

A. Introduction 36

1. Limitations of Present Contactless Conductance Methods 36

2. Preliminary Investigations 37

3. Importance of the Toroidal Resonant Frequency . . 38

Page

B. Immersion Method 39

1. Introduction 39

2. Experimental Procedure 39

3. Preliminary Experiments and Results 40

a. Volume Effect 40

b. Direct Response Curves at the Toroidal Resonant Frequency 40

c. Capacitive Response Using the Sargent Oscillometer 42

4. Further Evidence for the Impedimetric Nature of the Immersion Response 45

a. Frequency Shift Effects 45

b. Correlation of Response Curve Midpoints with Low Frequency Conductances. 45

c. Effect of Intertoroidal Distance on Response 47

d. Effect of Frequency on Response 50

5. Determination of Optimum Operating Frequency . . . 50

6. Differential Techniques 53

a. Introduction 53

b. Procedure 53

c. Results Using the Differential Method 54

d. Magnetic Response 57

7. Applications 57

a. Acid-Base Titration 57

b. Dielectric Measurements 58

8. Summary 58

Page

C. Sidearm Method 63
  1. Introduction 63
  2. Experimental Procedure 63
  3. Preliminary Investigations 63
    a. Importance of a Closed Solution Loop 63
    b. Direct Response Curves at the Toroidal Resonant Frequency 64
  4. Further Evidence for the Impedimetric Nature of the Sidearm Response 66
    a. Correlation of the Concentrations at the Response Curve Peaks with Low Frequency Conductance Values 66
    b. Effect of Intertoroidal Distance Upon Response 66
    c. Effect of Frequency Upon Response 66
  5. Determination of Optimum Operating Frequency . . . 69
  6. Concentration Ranges Obtainable with the Sidearm Apparatus 69
  7. Differential Techniques 72
    a. Introduction and Procedure 72
    b. Results Using the Differential Method 72
  8. Applications 72
  9. Magnetic Response at High Concentrations 75
    a. Direct Response 75
    b. Differential Response 75
  10. Summary 78

Page

D. Magnetic Induction Method 80

  1. Introduction 80

    a. Scope 80

    b. Review of Magnetic Induction Principles 80

    c. Frequencies Employed in Previous Work 81

    d. Reported Lower Limits of Conductance Measurement by the Magnetic Induction Method 82

  2. Features of Magnetic Probe Design 83

  3. Experimental Connections and Procedure 84

    a. Electrical Connections for Direct Response Mode 84

    b. Electrical Connections for Differential Mode 85

    c. The "Delta Millivolt" Differential Method . . . 85

    d. Miscellaneous Procedures 86

      i. Use of a Series Capacitor 86

      ii. Use of FET Amplifier 87

      iii. Temperature 87

      iv. Method of Stirring 87

      v. Conductance Tables 87

  4. Preliminary Investigations 87

    a. Volume Effect 87

    b. Response to Dielectric Changes 88

    c. Direct Response of Probe A 88

    d. Effect of Solution Loop Variables 88

      i. Effect of Core Volume on Response 88

Page

ii. Effect of Container Width Upon Response . . 91

iii. Effect of Intertoroidal Distance 93

5. Effect of Varying Frequency, Amperage, and Turns Ratio Upon Response 93

a. Effect of Varying Amperage at Constant Frequency 95

b. Effect of Varying Frequency at Constant Amperage 95

c. Effect of Turns Ratio 95

d. Conclusions 98

6. Determination of Optimum Conditions for Probe Operation 100

a. Determination of i·f Maximum for Probe A . . . 101

b. Determination of the i·f Product for Probe D 101

c. Conclusions 106

7. Studies of Probe C 106

a. Determination of i·f Product 106

b. Response of Probe C 107

i. Null Response to Pure Resistance 107

ii. Null (R_{box}) Response to Solutions 107

iii. Delta Millivolt Response to Pure Resistance 110

iv. Delta Millivolt Response to Solutions . . . 112

v. Conclusions 112

c. Low Level Response and Precision Using Probe C 113

d. Signal to Noise Ratio at Different Conductance Levels 113

Page

- e. Precision and Accuracy Obtainable 113
- f. Determination of the Cell Constant of Probe C 113
- g. Effect of the Number of Null Windings 117
- h. Solution Heating Effect of Probe C 117
- i. Effect of Temperature on the Response of Probe C 119

8. Studies of Probe F 120
   - a. Determination of i·f Product 122
   - b. Response of Probe F 123
     - i. Null Response to Pure Resistance 123
     - ii. Null (R_{box}) Response to Solutions 123
     - iii. Delta Millivolt Response to Pure Resistance 123
     - iv. Delta Millivolt Response to Solutions . . . 126
     - v. Conclusions 126
   - c. Low Level Response and Precision Using Probe F 126
   - d. Signal to Noise Ratio at Different Conductance Levels 126
   - e. Precision and Accuracy Obtainable 129
   - f. Determination of the Cell Constant of Probe F 129
   - g. Determination of N_s x n_s Product 129
   - h. Solution Heating Effect of Probe F 130
9. Limitations and Sources of Error 130
10. Chemical Applications 131
    - a. Introduction 131

Page

b. Probe C - Titrations at Low Solution Conductances 132

i. Acid-Base Titrations 132

(a) Strong Acid 132

(b) Weak Acid 133

ii. Precipitation Titrations 133

iii. Compleximetric Titrations. 136

iv. Conclusions 136

c. Probe C - Titrations in the Presence of Foreign Electrolytes 136

i. Acid-Base Titration 139

ii. Precipitation Titration 139

iii. Compleximetric Titration 142

(a) Zn(II) with EDTA 142

(b) TiO^{2+} with EDTA 144

iv. Redox Titrations 146

(a) Titration of Ferrous Iron with Permanganate 146

(b) Standardization of HCl Using KIO_3 . . . 147

(c) Standardization of $Na_2S_2O_3$ with KIO_3. . 147

(d) Titration of $Na_2S_2O_3$ with I_2 in KI. . . 150

(e) Standardization of I_2 with As_2O_3. . . . 150

(f) Assay of Potassium Ferrocyanide Using Cerate 153

d. Probe F - Titrations at Very Low Solution Conductances 157

i. Titration of $AgNO_3$ with NaCl using Probe F 158

Page

ii. Titration of $AgNO_3$ with KI 160

iii. Titration of 3.33×10^{-5} M $AgNO_3$ with KI . . 162

iv. Conclusions. 164

e. Probe F - Titrations in the Presence of Foreign Electrolyte 164

i. Titration of $AgNO_3$ with KI 164

ii. Conclusions 168

11. Literature Specifications and Applications 170

a. Commercial Salinometers 170

b. Applications 171

12. Summary and Conclusions 171

E. Summary 175

APPENDIX A 177

APPENDIX B 178

APPENDIX C 179

APPENDIX D 180

REFERENCES CITED 181

BIBLIOGRAPHY 184

I. INTRODUCTION

A. Purpose and Scope

For almost a century, classical low frequency conductance measurements have been employed as a useful analytical technique for following experimental variables which cause a change in the resistance of an electrolyte solution. Using relatively simple apparatus, the technique responds singularly, within wide concentration limits, to the resistance of a solution contained between two platinum electrodes.

Beginning in the early nineteen-forties, interest focused on contactless methods of determining solution conductance using radio frequency techniques. By removing the metal electrodes from direct contact with the solution being studied, the uncertainties of electrode fouling and polarization phenomena are avoided. This field is now referred to as high frequency conductometric analysis.

However, high frequency methods have several disadvantages. The measuring circuitry is more complex than that used in low frequency conductometric analysis. High frequency instruments usually respond to the total impedance of a solution rather than to its resistance alone. The response of these instruments is generally nonlinear as a function of electrolyte concentration. At best, a linear response can be obtained only within one order of magnitude of electrolyte concentration. Finally, the use of high radio frequencies (1 to 460 MHz) is involved and may lead to problems of shielding and circuit instability.

To overcome some of the aforementioned disadvantages, workers turned to an electrodeless conductance measuring system in which the electrolyte solution provides a means of magnetic coupling between toroidal inductors. Using moderately low frequencies (1 to 50 kHz) and highly conducting solutions (usually greater than 0.1 molar), measurements accurate to 0.1% are obtainable.

Publications describing this technique are few and oftentimes contain seemingly conflicting statements regarding the effects of certain variables on the observed conductometric response. In these few papers, data showing the effect of solution and circuit variables on the system's response are virtually nonexistent.

Therefore the primary objectives of the present work are threefold. First, an attempt will be made to discover those variables which affect this magnetic induction response, since no comprehensive work on overall system response has been published. Secondly, attempts will be made to extend the useful response of the toroidal induction system to include solution concentrations at the micromolar level. Finally, it would be of interest to investigate some chemical applications of this electrodeless conductance measuring system, not only in areas where low frequency conductometric techniques are applicable, but also in situations where small conductance changes are occuring in the presence of large amounts of foreign electrolyte.

B. Electrical Circuit Concepts

1. Definitions

In order to facilitate the description of the work presented in this dissertation, an explanation of several electronic terms and concepts is necessary. It is assumed that the fundamental quantities of resistance, capacitance, and inductance are understood.[1,2]

Capacitors and inductors react with an a.c. signal to provide a frequency-dependent opposition to the flow of current. Capacitive reactance is defined as $X_C = 1/2\pi fC$ (in ohms), and inductive reactance is defined as $X_L = 2\pi fL$ (in ohms), where f is the frequency of the a.c. voltage, C is the value of the capacitance in farads and L is the inductance of the coil in henries. The reciprocal of reactance is called the susceptance, B; likewise, the reciprocal of the resistance, R, is the conductance, G.

The vector sum of resistance and reactance, i.e., the total opposition to current flow in an AC circuit containing R, C, and L, is termed the impedance of the circuit and is given the symbol Z. Its inverse quantity is the admittance, Y.

For the purposes of this dissertation an oscillator or signal generator will be defined simply as a source of alternating or periodic voltage.

2. Resonant Circuits

In circuits containing R, C, and L there are two important cases to be considered. In the series case, depicted in Figure 1 below, I is

---

[1] "The Radio Amateur's Handbook," 44th ed., American Radio Relay League (publisher), 1967.

[2] H. V. Malmstadt et al., "Electronics for Scientists," W. A. Benjamin, Inc., New York, 1963.

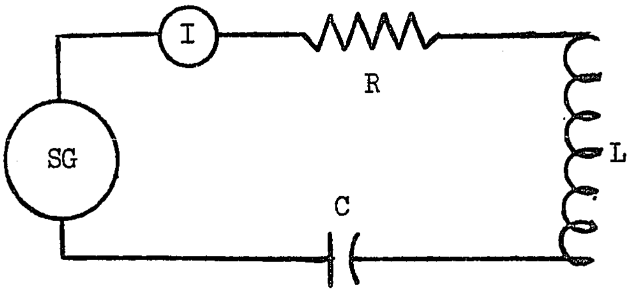

Figure 1. Series Resonant Circuit

an ammeter and SG represents a signal generator. At one particular frequency the reactances of the coil and capacitor will be exactly equal in magnitude but opposite in sign to one another, i.e., their reactances will cancel. At this frequency, equal to $1/2\pi\sqrt{LC}$, the line current as indicated by I is at a maximum and ideally is limited only by R. The circuit is said to be at series resonance or tuned to resonance when the above conditions are fulfilled.

For the parallel case depicted in Figure 2 below, there will

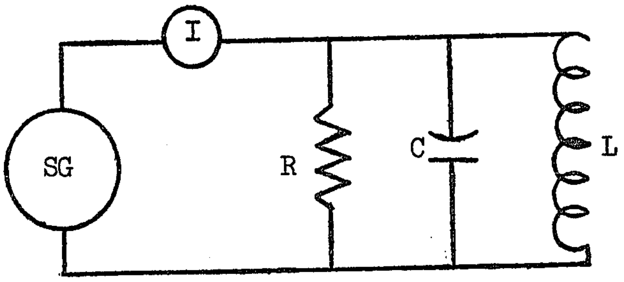

Figure 2. Parallel Resonant Circuit

also exist a frequency at which X_L and X_C are equal in magnitude, but opposite in sign to one another. At this frequency, the line current I is found to be a minimum, the impedance of the circuit a maximum, and the circuit is parallel resonant. The resistance R in many cases is not an actual resistor, but may be the series resistance of the coil "transformed" to a large equivalent parallel resistance.[1]

It should be pointed out that all coils possess distributed capacitance. This capacitance is due to the close proximity of successive wire windings to one another. The net result is that every coil has a self-resonant frequency due to the parallel combination of its own inductance and distributed capacitance.

3. Q Factor

Mention is often made of the "Q factor" of a resonant circuit. In every inductor there exists some resistance due to the resistance of the wire used to wind the coil. This resistance alters the response shape of a tuned resonant circuit. Hence, a quality factor or sharpness index called the Q of the circuit has been defined such that:

$$Q_{series} = \frac{X}{r} \quad \text{and}$$

$$Q_{parallel} = \frac{Z_r}{X},$$

where X is the reactance (in ohms) of either the inductor or capacitor at resonance, r is the resistance of the coil and Z_r is the "transformed" value of r mentioned earlier in the discussion of parallel resonant circuits. The concept of Q is depicted graphically in Figure 3 below.

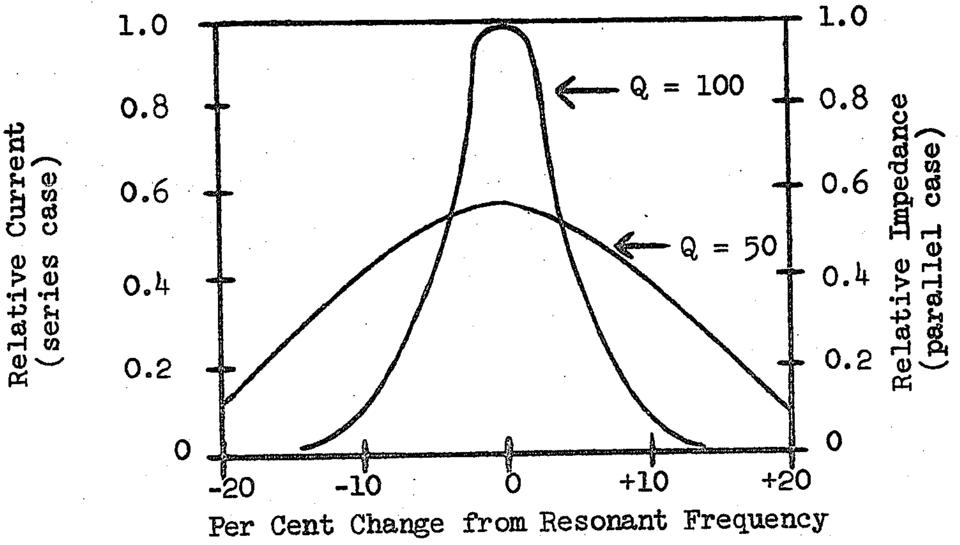

Figure 3. Q Concept

From a practical standpoint, the higher the Q value of a circuit, (and this is governed almost exclusively by the resistance of the inductor used), the narrower the band of frequencies to which the resonant circuit will respond. Hence, frequencies different from the resonant frequency are totally rejected by the circuit.

4. Toroidal Inductors

Inductors are commonly wound in solenoidal fashion using either an air or iron core. If the ends of a solenoid are bent around in a circle and joined together, the resulting inductor is known as a toroid. Winding an inductor in this shape confines the expanding and collapsing magnetic field due to current oscillations almost entirely to the ring of the toroid as shown in Figure 4. Hence a toroid is self-shielding by virtue of its shape; it is therefore less prone to the pickup of extraneous signals. Furthermore, toroids can be made with very high Q values.

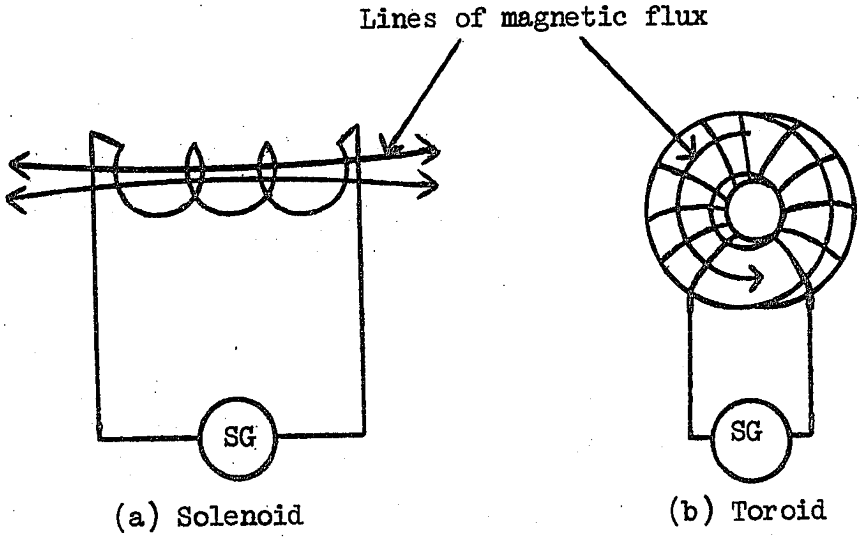

(a) Solenoid (b) Toroid

Figure 4. Magnetic Flux Lines in Inductors

5. Mutual Inductance

If two coils are arranged coaxially as shown in Figure 5, and an alternating current is made to flow in the primary coil, an induced voltage will be read on the meter connected to the secondary coil. This occurs because the magnetic lines of force set up by one coil "cut" the turns of the other coil. This response results from the mutual inductance between the two coils.

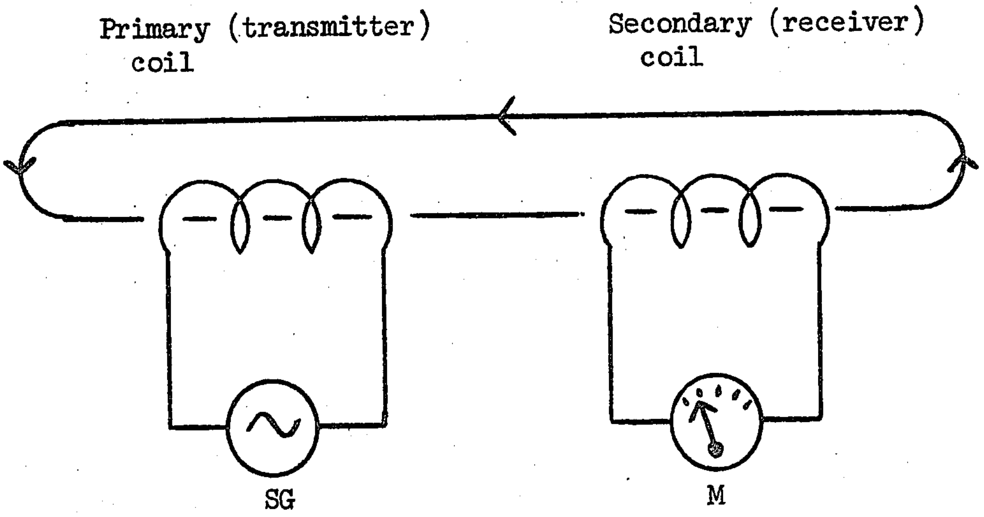

Figure 5. Principle of Mutual Inductance

The magnitude of the voltage induced in the secondary coil is found to depend upon the number of turns of the coils, N, and the time rate of change of the magnetic flux (the product of amperage times frequency) linking the two coils. Mathematically,[3]

$$\bar{E}_{\text{induced}} = -N_1 \frac{\Delta\varphi}{\Delta t}$$

where $\bar{E}_{\text{induced}}$ is the average value of the induced voltage, φ is the magnetic flux linking the two circuits, and t is the time in seconds. Since φ is directly proportional to the current in a given coil, and if the geometric spacing between the coils remains unchanged, then,

---

[3] R. L. Weber et al., "Physics for Science and Engineering," McGraw-Hill Book Co., Inc., New York, 1959, p. 409.

$$\bar{E}_{\text{induced}} = -N_2 \frac{\Delta i}{\Delta t} = -M \frac{\Delta i}{\Delta t}.$$

The symbol M is called the coefficient of mutual inductance between the two coils.[3]

Although the magnetic field of a toroid is ideally confined to its core, mutual inductance can be provided between two toroids by threading a closed loop of wire through the holes in the center of the toroids. Apparently there exists some "stray" flux in the center hole of a toroid because the magnetic field is larger near the inside radius than at the outside radius.[4] This stray flux in the primary toroid can then induce a current in the single wire winding; this current in the wire, in turn induces a current in the second toroid using the same principle. This is illustrated in Figures 6 and 7 below.

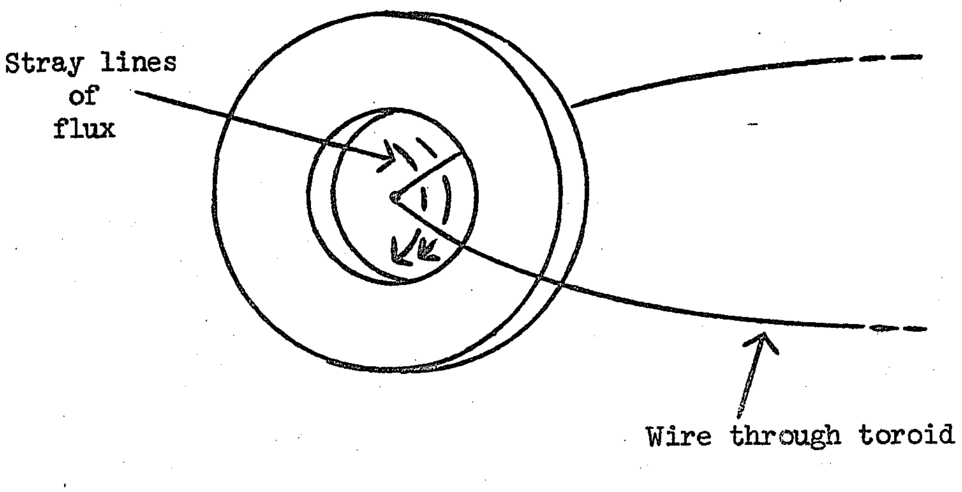

Figure 6. Magnetic Induction Mechanism of a Toroid

---

[4] ibid., p. 349.

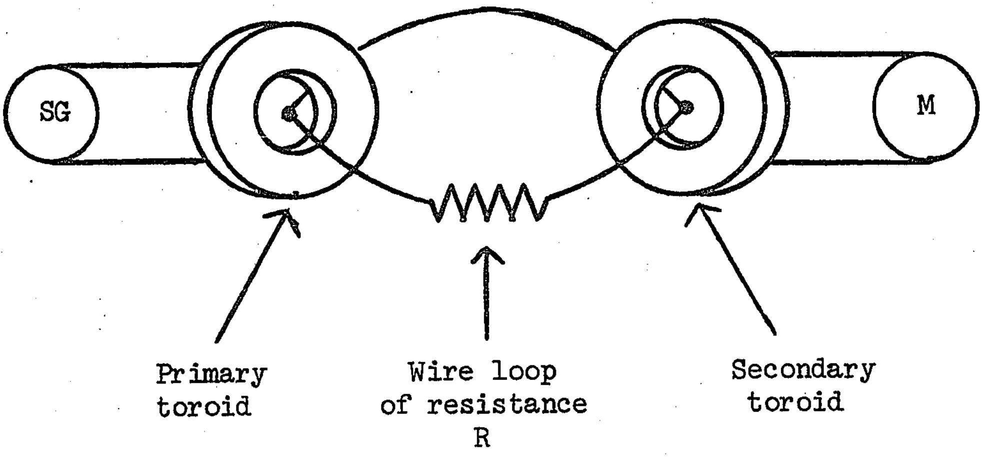

Figure 7. Mutual Inductance Between Two Toroids

The amount of mutual coupling between the two toroids is mainly dependent upon the voltage applied to the primary toroid and the resistance of the wire loop. From a physical viewpoint there is no reason why the loop of wire cannot be replaced by a closed loop of electrolyte solution. Hence one could measure the resistance of a solution without using electrodes.

It is noteworthy that the solenoidal winding configuration (Figure 4) does not lend itself to inducing a current in a wire or solution loop. A wire through the core of a solenoid is coaxial with the cutting flux, but for a current to be induced, the magnetic flux must "cut" the wire at some angle.

C. Low Frequency Conductometric Analysis

1. Basic Principles

In order that comparisons may be made with measurements reported later in this work, a brief discussion of classical low frequency conductance measurements will be presented.

Low frequency conductometric analysis involves the measurement of the resistance, R, in ohms, of an electrolyte solution. The reciprocal quantity G, the conductance, is expressed in mhos or ohm^{-1}.

If a constant voltage is applied to two metal electrodes, usually of platinum, which are immersed in a solution of electrolyte, the measured resistance will depend upon the area of and the distance between the electrodes, the number and charge of the ions present, the mobilities of the ions, the degree of ionization of the electrolyte, and the temperature of the solution.

The electrodes, solution, and container comprise the conductometric cell. The resistance of the solution is commonly measured by making the cell one arm of a Wheatstone bridge which is energized by 60 or 1000 Hz alternating current. Since the resistance of a conductor is directly dependent upon its length but inversely proportional to its cross-sectional area, the measured resistance, R, is given by

$$R = \rho \cdot d/A,$$

where d is the distance between the two identical electrodes of area A. The proportionality constant ρ is the specific resistance. The reciprocal of ρ is k which is termed the specific conductance (expressed in mhos/cm), and represents the conductance of a cube of the solution one cm on an edge. Thus,

$$k = \frac{1}{\rho} = \frac{d}{A} \cdot \frac{1}{R} = G \cdot \frac{d}{A} = G\theta \ ,$$

where θ (cm^{-1}) is called the cell constant. Using solutions of known specific conductance (usually KCl), the value of θ can be easily determined for a given cell.

2. Applications

Since there exists a linear relationship between the concentration of a given ion and its contribution to the total conductance of the solution, conductance measurements are often used to follow the change in concentration of a species during a titration. Up to the end point one is removing the ion being determined, whereas after the end point one is adding excess titrant. Hence if one plots conductance values as a function of titrant volume, two intersecting lines are obtained and the point of intersection is the end point. Typical values of accuracy and precision range from 0.1 to 2%.

Conductometry finds many uses in acid-base, precipitation and complex formation analyses, as well as being a tool in determining solubility product constants and the degree of ionization of various electrolytes.

3. Limitations and Sources of Error

The most severe drawback is that conductance is a nonspecific property in solutions containing two or more electrolytes. A second difficulty concerns the use of the Wheatstone bridge. Ideally only the resistance of the solution is measured. However, stray capacitances and inductances often result in a poor null reading, yielding imprecise resistance values.

The electrodes may give rise to sources of error for the following reasons. In precipitation reactions, the metal electrodes often become fouled, resulting in a change in the cell constant.

Polarization phenomena at the electrode surfaces can occur even when one uses alternating current. Thirdly, the light coating of platinum black applied to the electrodes for the purpose of reducing polarization effects may give rise to catalytic effects with species in the solution. Finally, there is a periodic need for replatinization of the electrode surfaces and rechecking the cell constant, both of which necessitate inconvenient electrode maintenance.

D. High Frequency Conductometric Analysis

1. Basic Principles

A brief discussion of high frequency theory and some typical instrumental response characteristics are presented to aid in understanding certain experimental responses to be described in a later section. Several texts and monographs[5-9] are available which describe the high frequency technique in more detail. The presentation which follows is primarily due to Timnick.[10]

High frequency analysis, often called oscillometry, involves placing the solution to be analyzed either between the plates of the capacitor or in the field of the inductor which forms the resonant circuit of an oscillator circuit operating in the megahertz frequency range. As the composition of the solution changes, the operating parameters of the oscillator circuit change, as evidenced by a shift in operating frequency or a change in grid or plate current of the oscillator tube. In effect, the instrument measures changes in the total impedance of the sample resulting from changes in the dielectric constant and/or the conductance of the solution.

---

[5] C. N. Reilley in P. Delahay, "New Instrumental Methods in Electrochemistry," Interscience Publishers Inc., New York, 1954.

[6] W. G. Berl (ed.), "Physical Methods in Chemical Analysis," Vol. 3, Academic Press Inc., New York, 1956.

[7] I. M. Kolthoff and P. J. Elving (ed.), "Treatise on Analytical Chemistry," Part I, Vol. 4, Interscience Publishers Inc., New York.

[8] E. Pungor, "Oscillometry and Conductometry," Pergamon Press, Oxford, 1965.

[9] C. L. Wilson and D. W. Wilson (ed.), "Comprehensive Analytical Chemistry," Elsevier Publishing Co., New York, 1964.

[10] A. Timnick *et al.*, Chemistry in Canada *12*, 23 (1960).

2. Instrument Response

To a good approximation, the properties of a high frequency *capacitance type* cell containing an electrolyte solution may be represented by the *equivalent electrical circuit* shown below in Figure 8(a). In the diagram, C_g represents a capacitance due to the cell walls, C_s is a capacitance due to the dielectric constant of the solution and R_s is the resistance of the electrolyte solution. This circuit may be simplified to that shown in Figure 8(b), where C_p is called the equivalent parallel capacitance and R_p is the equivalent high frequency resistance.

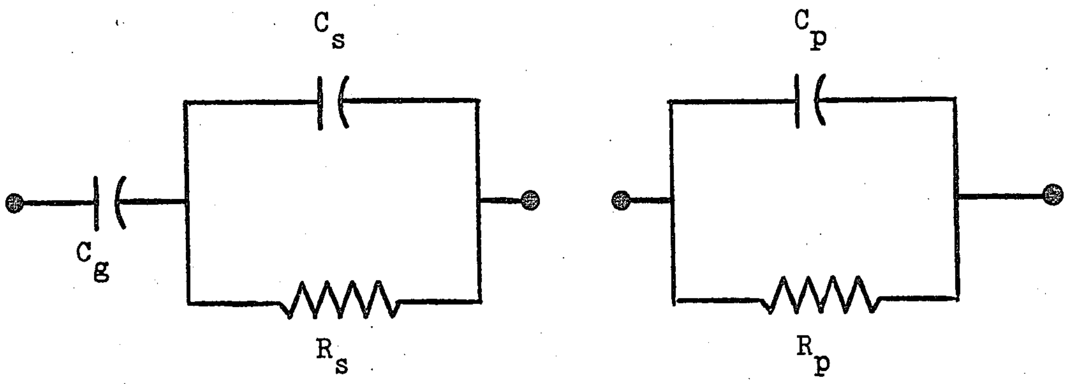

(a) Equivalent circuit (b) Simplified equivalent circuit

Figure 8. High Frequency (Impedimetric) Cell Circuit

If a high frequency alternating voltage is applied to the solution (represented by Figure 8(b)), an admittance current will flow. The admittance, Y, is the sum of two terms: G, the conductance, and B, the susceptance, both of which operate independently of one another. In equation form, $Y = G + jB$ where $j = \sqrt{-1}$. In terms of the equivalent circuit parameters in Figures 8(a) and 8(b), it can be shown[5-9] that,

$$G_{hf} = 1/R_p = \frac{\frac{1}{R} w^2 C_g{}^2}{\left[\frac{1}{R}\right]^2 + w^2 (C_g + C_s)^2}$$

where $w = 2\pi f$, and G_{hf} is the high frequency conductance. Now since $1/R = G$, the low frequency conductance of the solution, then

$$G_{hf} = \frac{Gw^2C_g^{\,2}}{G^2 + w^2(C_g + C_s)^2} \quad . \qquad (1)$$

It may be seen from Equation 1 that for a given set of cell parameters and assuming the C_s is independent of G, G_{hf} is a unique function of G, the low frequency conductance. Also, since G_{hf} approaches zero for large or small values of G, there is a peak for G_{hf} when plotted as a function of G. Differentiating Equation 1, setting the result equal to zero and solving,

$$G_{peak} = w(C_g + C_s) \; .$$

Thus, the low frequency conductance value at which the high frequency peak occurs is directly proportional to frequency, so that in order to analyze concentrated electrolyte solutions, high frequencies must often be used. The aforementioned concepts are shown graphically in Figure 9.

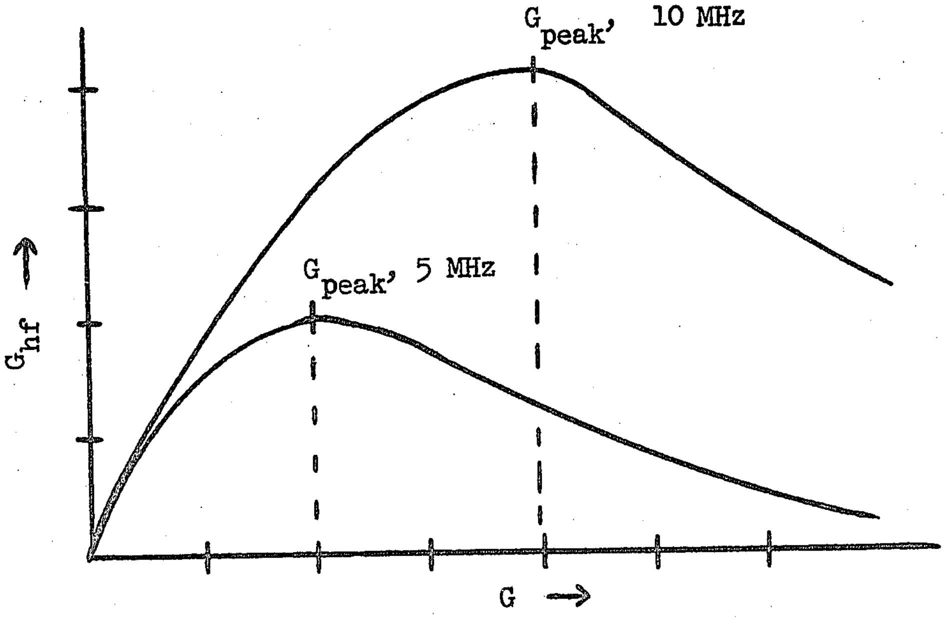

Figure 9. Relationship of High Frequency Conductance to Low Frequency Conductance

Now the susceptance term B is equal to wC, and it may be derived[5-9] that

$$C_{hf} = C_p = \frac{C_g G^2 + w^2 C_g C_s{}^2 + w^2 C_g{}^2 C_s}{G^2 + w^2(C_g + C_s)^2} . \tag{2}$$

From Equation 2 it is apparent that when G is large, C_{hf} approaches C_g and when G is small, C_{hf} approaches the value $C_g C_s/(C_g + C_s)$. Consequently when C_{hf} is plotted as a function of G, a sigmoid curve results. It is found that the value of G at the midpoint of the curve = $w(C_g + C_s)$ and that the conductance value at the midpoint occurs at the same low frequency conductance value as does the C_{hf} peak. These concepts are illustrated in Figure 10 below.

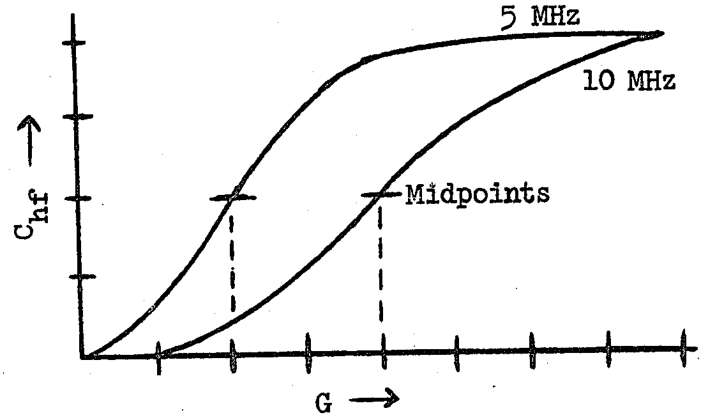

Figure 10. Relationship of High Frequency Capacitance to Low Frequency Conductance

Experimentally it is found that those high frequency instruments which are primarily responsive to changes in cell capacitance give curves similar to those of Figure 10, while instruments measuring cell conductance changes give response curves resembling those of Figure 9.

3. Limitations and Sources of Error

Although possessing the advantage that the measuring electrodes are not in contact with the sample, high frequency conductance techniques have several disadvantages. The cell is usually part of an oscillator circuit element; hence oscillator operation often becomes critical if high sensitivity is required; also there exists the possibility that under certain conditions, depending on the properties of the solution, the oscillator may cease functioning entirely.

It was mentioned previously that if solutions of high conductivity are to be measured, a high oscillator frequency (or a change in the cell constant) is required. Higher frequencies bring about problems of shielding and frequency stability. In general, high concentrations of foreign electrolytes cannot be tolerated.

The response curves in Figures 9 and 10 are nonlinear, whereas a low frequency response curve is linear. This leads to such phenomena as titration curve inversions and nonlinear end point extrapolations, the latter giving rise to poor precision and accuracy in analyses.

Finally, the range over which a linear response can be achieved for a given frequency is usually only one order of magnitude of concentration or specific conductance values. Hence one must adjust solution concentrations within fairly narrow limits in order to achieve the most favorable instrument response for a particular application.

E. Historical Background

1. Development of Theory and Instrumentation

Probably the first demonstration of a contactless method for measuring the conductivity of an electrolyte solution was given by Piccard and Frivold[11] in 1920. Ruben[12] later described a system composed of 2 coils, one of which is connected to a signal generator and the other to a meter readout, in which the conductance of an electrolyte solution contained in a test tube threading both coils is measured.

Between 1933 and 1945 Blake[13] developed several methods of measuring solution conductance using both capacitive and inductive coupling arrangements. In this country Jensen and Parrack[14] initiated work in what is now referred to as "High Frequency Analysis". Between 1946 and 1955 a rigorous theory was developed to explain the response behavior of capacitive type measuring cells. Theoretical explanations of the coil-type high frequency behavior continue to appear.[15]

At the height of interest in high frequency analysis, two publications[16,17] appeared describing measured responses differing from that of coil-type impedimeters. The method is based on the principle of mutual inductive coupling between two coils as influenced by a sample solution placed between them. In addition to a typical high frequency impedimetric type response at low solute concentrations, these publications described another region of sensitivity beginning at 0.1 M HCl and continuing to higher concentrations. The apparatus was similar to that of Ruben.[12] Frequencies from 2.5 to 10 MHz were used and high gain amplification before detection by a meter was employed.

---

[11] Piccard and Frivold, "Archives des Sciences Physiques et Naturelles" (Series 5) 2, 264 (1920); cited in U. S. Patent 2,542,057.

[12] S. Ruben, U. S. Patent 1,610,971, Dec. 14, 1926.

[13] G. G. Blake, "Conductimetric Analysis at Radio Frequency," Chemical Publishing Co., Inc., New York, 1952.

[14] F. W. Jensen and A. L. Parrack, Ind. Eng. Chem., Anal. Ed. 18, 595 (1946).

[15] A. Bellomo, J. Electroanal. Chem. 27, 267 (1970).

[16] S. Fujiwara and S. Hayashi, Anal. Chem. 26, 239 (1954).

[17] Y. Kamura, Yakugaku Zasshi 74, 1 (1954).

In 1956 publications concerning the use of magnetic induction devices employing toroidal inductors for measuring the conductivity of an electrolyte solution began to appear. Actually from a chronological viewpoint such a measuring system was first described by Relis[18] in 1951. The system employs two toroidal inductors spaced coaxially in an electrolyte solution. One toroid, connected to an oscillator, sends a high audio frequency signal through the solution. The second toroid receives this signal and, after suitable amplification, the signal is sent to a meter. The magnitude of the signal is reported to be directly related to the conductance of the electrolyte solution. Both direct readout and differential (null) methods for determining solution conductivity are described. Recently this apparatus has appeared commercially in the form of contactless sea water salinometers.[19,20]

---

[18] M. J. Relis, U. S. Patent 2,542,057, Feb. 20, 1951.

[19] Beckman Instruments Co., Inc., Cedar Grove, New Jersey, Model RS7-B.

[20] Hytech Marine Products, San Diego, California, Model 6220.

Gupta and coworkers[21] described a similar magnetic induction device called a transformer bridge. Operating at audio frequencies and using moderately to highly conducting solutions (≥ 0.1 M salts), the reproducibility of measurement is better than 0.02%.

A more detailed description of the features and advantages of such a bridge for electrodeless conductance measurements appeared in a definitive paper by Calvert and coworkers.[22] The conductances of divalent salt solutions as low as 5 millimolar were measured with 0.1% accuracy. Articles describing nearly identical transformer bridge circuits have since appeared[23-28] with one attempt[28] to extend the response to solutions of low conductance by using higher frequencies than employed before and varying the ratio of the number of primary to secondary windings. However, the attempt was unsuccessful and no null balance was obtainable. Another paper[27] claimed success in a similar attempt.

A simplified toroidal conductance analyzer has been described by Johnson and Hart.[29,30] The aim of the work was to examine and optimize certain physical and electrical parameters of their device.

---

[21] S. R. Gupta et al., J. Sci. Instr. 33, 313 (1956).

[22] R. Calvert et al., J. Phys. Chem. 62, 47 (1958).

[23] V. S. Griffiths, Anal. Chim. Acta 18, 174 (1958).

[24] V. S. Griffiths, Talanta 2, 230 (1959).

[25] B. Lavagnino and B. Alby, Ann. Chim. 49, 1272 (1959).

[26] N. L. Brown and B. V. Hamon, Deep-Sea Research 8, 65 (1961).

[27] V. I. Lopatnikov, Soviet Physics (Eng. trans.) 6, 505 (1961).

[28] M. De Rossi, Sci. Tec. 6, 31 (1962); C. A. 61, 3754 (1964).

[29] C. M. Johnson and G. E. Hart, Rocky Flats Internal Report RFP-657, U. S. Atomic Energy Commission, 1966.

[30] C. M. Johnson and G. E. Hart, Anal. Instrum. 4, 23 (1967).

The development of another conductance measuring instrument employing toroids, which is capable of measuring dilute electrolyte solutions whose specific conductances are 10 micromhos/cm with a precision of ± 2 %, has been recently described.[31] The authors claim that at least one order of magnitude more dilute solutions can be measured, but with less accuracy. However, no data are given to corroborate these claims.

A recent review[32] of the present state of contactless analysis describes possible analytical uses of these toroidal conductance measuring devices.

2. Applications

Probably the most frequent use of toroidal conductivity analyzers has been the measurement of the salinity of sea water for various oceanographic purposes.[19,20,26,33] Park[33] and associates have applied such an instrument to the determination of the alkalinity of sea water. The results compared favorably to more conventional methods considering that the alkalinity of sea water represents only a fraction of the total sample conductance.

Other uses for this means of conductance measurement have been the determination of the equivalent conductances of several salts at high concentrations,[21,22] the measurement of the specific conductance of concentrated NaCl solutions,[25] and the monitoring of the nitric acid concentrations of radioactive wastes.[29,30]

---

[31] A. E. Hackl and H. Deisinger, Allgemeine and Praktishe Chemie 19, 229 (1968).

[32] L. Pazsitka et al., Z. Anal. Chem. 245, 103 (1969).

[33] K. Park et al., Anal. Chem. 35, 1549 (1963).

It should be obvious that few analytical applications of this new method of contactless conductance measurement have been attempted.

II. APPARATUS AND REAGENTS

A. Signal Generators

1. General Considerations

The two signal sources to be described possess the following advantages for use in this research. Both are capable of producing a continuous sine wave output (to 1 MHz, Heath, or 2 MHz, Knight) at high voltage levels (10 vrms). Also, both generators have coarse and fine output attenuator controls for convenient level adjustments in experimental use. The square wave sections of these two instruments were not used.

2. The Heath Sine - Square Wave Generator, Model IG-82*

Specifications:

Frequency Range - 20 Hz to 1 MHz in 5 decade ranges.

Frequency Response - 20 Hz to 1 MHz ± 1.5 db.

Frequency Accuracy - ± 5% of dial setting.

Output Voltage (rms) - 0 to 10 v in four decade ranges.

Output Impedance - 600 ohms ± 10% on the 0.01, 0.1, and 1 volt ranges and 10 kilohms on the 10 volt range.

Distortion - 0.25%.

Attenuators - switch selected decade ranges with fine output level control.

3. The Knight Sine - Square Wave Generator, Model KG-688**

Specifications:

Frequency Range - 20 Hz to 2 MHz in 5 decade ranges.

---

*The Heath Company, Benton Harbor, Michigan.

**Allied Radio Co., Chicago, Illinois.

Frequency Response - 20 Hz to 2 MHz ± 2 db.

Frequency Accuracy - ± 3% from 100 Hz to 1 MHz and ± 5% above and below these frequencies.

Output Voltage (rms) - 0 to 7.5 v into loads of 10 kilohms or higher; 0 to 6.5 v into 600 ohms.

Output Impedance - nominally 600 ohms ± 10%.

Distortion - 0.25%.

Attenuators - switch selectable in 1 db steps from 0 to -41 db plus a fine output level control.

B. Voltmeters

1. The Heath Vacuum Tube Voltmeter, Model IM-21

Specifications:

Frequency Response - ± 1 db from 10 Hz to 500 kHz; ± 2 db from 10 Hz to 1 MHz, applicable to all voltage ranges.

Voltage Ranges - 10 mv to 300 volts (rms) full scale in 10 switch selected ranges.

Input Impedance - 10 megohms shunted by 22 pf on all ranges.

Accuracy - ± 5% of full scale voltage.

Modifications - output jacks to permit monitoring the rectified meter voltage (a portion of which may be used for output to a recorder) were installed on the rear of the instrument.

2. Eico AC VTVM, Model 255*

Specifications:

Frequency Response - 10 Hz to 600 kHz ± 0.5 db on all voltage ranges.

---

*Electronic Instrument Co., Flushing, New York.

Voltage Ranges - 1 mv to 300 volts (rms) full scale in 12 switch selected ranges.

Input Impedance - 10 megohms shunted by 15 pf on all ranges.

Accuracy - ± 3% of full scale voltage.

C. The Heath Decade Resistance Box, Model IN-11

Specifications:

Range - 1 ohm to 999,999 ohms in 1 ohm steps, switch selected.

Resistors - 1/2% accuracy up to 0.5 watt power dissipation.

Residual Resistance - 0.043 ohms minimum at the terminals with all switches in their zero positions.

Shunt Capacitance - approximately 56 pf* from either terminal to the case; the exact value depends on the decades used.

D. The Heath Decade Capacitance Box, Model IN-21

Specifications:

Range - 100 pf to 0.111 μfd in increments of 100 pf using switch selected silver mica capacitors.

Accuracy of Incremental Capacity - ± 1%.

Residual Capacitance - 10 to 15 pf at the terminals.

---

*experimentally determined.

E. The Sargent Model V Oscillometer, Catalog No. S-29180*

This instrument was used as a capacitance measuring device in various experiments. It is known from previous work[34] that each dial division (of a total of 32,000 available divisions) corresponds to 0.0052 pf.

F. The Beckman Instruments Conductivity Bridge, Model RC-16B2**

The instrument is essentially a Wheatstone bridge with integral null detector. Conductance values from 0.4 to 5,000,000 micromhos may be measured at either of two selected frequencies, 60 Hz or 1 kHz. Accuracy is 1% of the dial reading.

G. Triad Transformer Corp. Toroidal Inductors***

The following toroids are available commercially in several sizes and with a choice of two protective coatings. Table I lists some important properties of these inductors. The core material of these toroids is composed of a powdered nickel alloy.

H. Indiana General Corp. Toroidal Cores****

The following core forms, composed of magnetic iron oxide compounds called ferrites, were obtained. Their relevant properties

---

*E. H. Sargent and Co., Inc., Chicago, Illinois.

[34] R. F. Zarilla, "New Instrumentation for Analysis by High Frequency Techniques," thesis, University of Pittsburgh, 1966.

**Beckman Instruments, Inc., Cedar Grove, New Jersey.

***Triad Transformer Corporation, Huntingdon, Indiana.

****Indiana General Corporation, Keasley, New Jersey.

TABLE I

Specifications of Triad Toroids

Toroid type no.	Inductance, millihenries, ± 2%	Self-resonant freq. in air, kHz ±10%	Outside diameter, inches ± 20%	Inside diameter, inches ± 20%	Thickness (height), inches
†					
EA-001	1	460	1	5/16	3/8
EA-005	5	190	1	5/16	3/8
EA-010	10	140	1	5/16	3/8
EA-050	50	55	1	5/16	3/8
EA-070	70	40	1	5/16	3/8
EA-100	100	35	1	5/16	3/8
EA-150	150	29	1	5/16	3/8
EA-500	500	16	1	5/16	3/8
EA-1000	1,000	9.5	1	5/16	3/8
EC-5000	5,000	3.1	1 1/4	7/16	5/8
EC-10,000	10,000	3.4	1 1/4	7/16	5/8
EK-010	10	115	1 15/16	9/16	7/8
EK-100	100	35.5	1 15/16	9/16	7/8
EK-5000	5,000	3.8	1 15/16	9/16	7/8
EA-100A	100	32	1 1/16	3/16	1/2

[†] All toroids are covered with a plastic coating except toroid EA-100A which is encapsulated in epoxy resin.

are given in Table II. The 0-5 core material was chosen for its high permeability (μo = 3000 at 100 kHz) and its upper usable frequency limit of 400 kHz.

TABLE II

Indiana General Toroidal Cores

Toroid form, type number	Core material designation	Outside diameter, inches	Inside diameter, inches	Thickness, inches
CF-114	0-5	1 1/4	3/4	3/8
CF-117	0-5	1 7/8	1 3/8	3/8

I. J. W. Miller Co. Toroid Cores

A set of toroids was constructed using the cup cores of a commercial radio transformer. A core form was made by slicing the closed cylindrical end from one (of two) cup core of a J. W. Miller model 1463-PC interstage transformer* with the aid of a glass cutting saw. The resulting toroidal form measures 9/16" OD x 13/32" ID x 5/16" thick. When this core form is filled tightly with a single layer of Belden No. 28 A.W.G. enameled magnet wire (Catalog No. 8040**), the resulting toroid has a self resonant frequency slightly over 2 MHz. The resonant frequency was lowered to 2.0 MHz by connecting 255 pf in parallel across the terminals of the toroid. Two such toroids were made, and the inductance of each toroid measured 26 μh. These toroids will hereafter be designated as J-26.

---

*J. W. Miller Co., Los Angeles, California.

**Belden Corporation, Chicago, Illinois.

J. FET Amplifier

A simple, high input impedance, field effect transistor amplifier was constructed to boost the input voltage from the (later described) receiver toroid before presentation to the VTVM. A choice of two source bypass capacitors enables one to choose a wide or narrow band amplification factor. The amplifier schematic and its frequency response characteristics are presented in Figures 11 and 12.

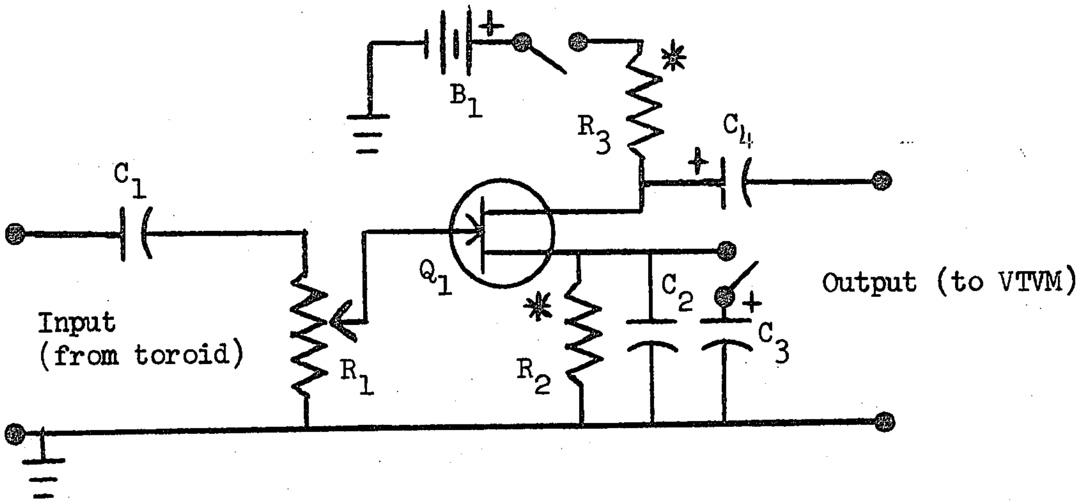

Figure 11. FET Amplifier Schematic

Q_1 = MPF 105 junction field effect transistor, N-channel (Motorola).

R_1 = 1 megohm pot. with spst on-off switch.

R_2 = 33 k ohm carbon resistor 1/2 w 10%.

R_3 = 47 k ohm carbon resistor 1/2 w 10%.

* - chosen for highest gain and lowest distortion.

C_1 = 0.025 μfd 600 VDC Mylar capacitor.

C_2 = 0.005 μfd 1 KVDC ceramic capacitor.

C_3, C_4 = 10 μfd 25 VDC electrolytic capacitor.

B_1 = 15 v battery, Burgess U10 or equivalent.

Chassis = Bud "mini-box", No. CU-3000-A,

dimensions = 2 3/4" L x 2 1/8" W x 1 5/8" D.

Gain at 1 kHz = 0-25 (C_3 in), 0-2.5 (C_3 out).

Maximum input before clipping = 100 mvrms (C_3 in).

Frequency response (C_3 connected) - flat 20 Hz to 200 kHz, - 3 db at 225 kHz.

Current drain - approximately 150 microamperes.

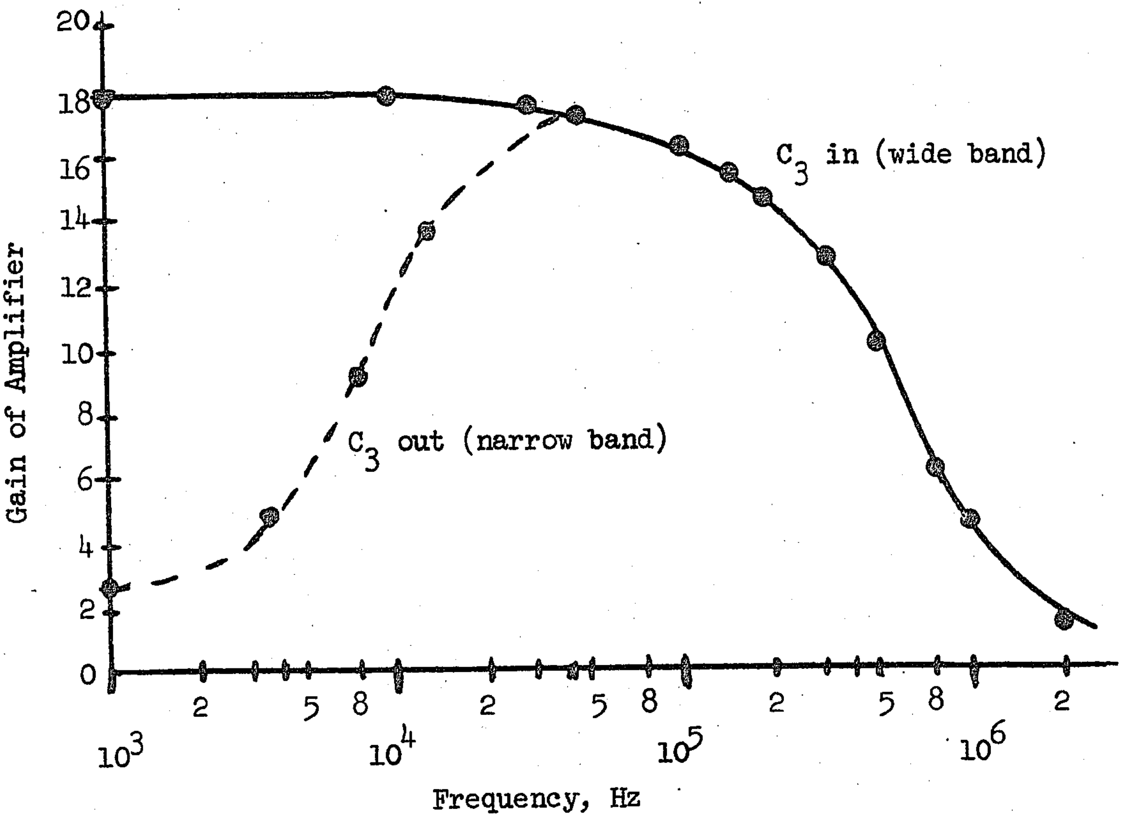

Figure 12. Frequency Response of FET Amplifier

K. The "Sidearm" Measuring Apparatus

The following apparatus, because of its physical layout, is called the "Sidearm" configuration. It is a closed loop of pyrex glass with polyvinyl chloride tubing joints and passes through the holes of two toroids. Electrolyte is made to flow through the glass loop by means of a "Ministaltic Pump".* The toroids sit upon the ridge of the tubing connectors, and the exchange of one type of toroid for another is easily accomplished. Both toroids are enclosed in aluminum mini-boxes** to provide maximum shielding from one another. Figure 13 shows this apparatus.

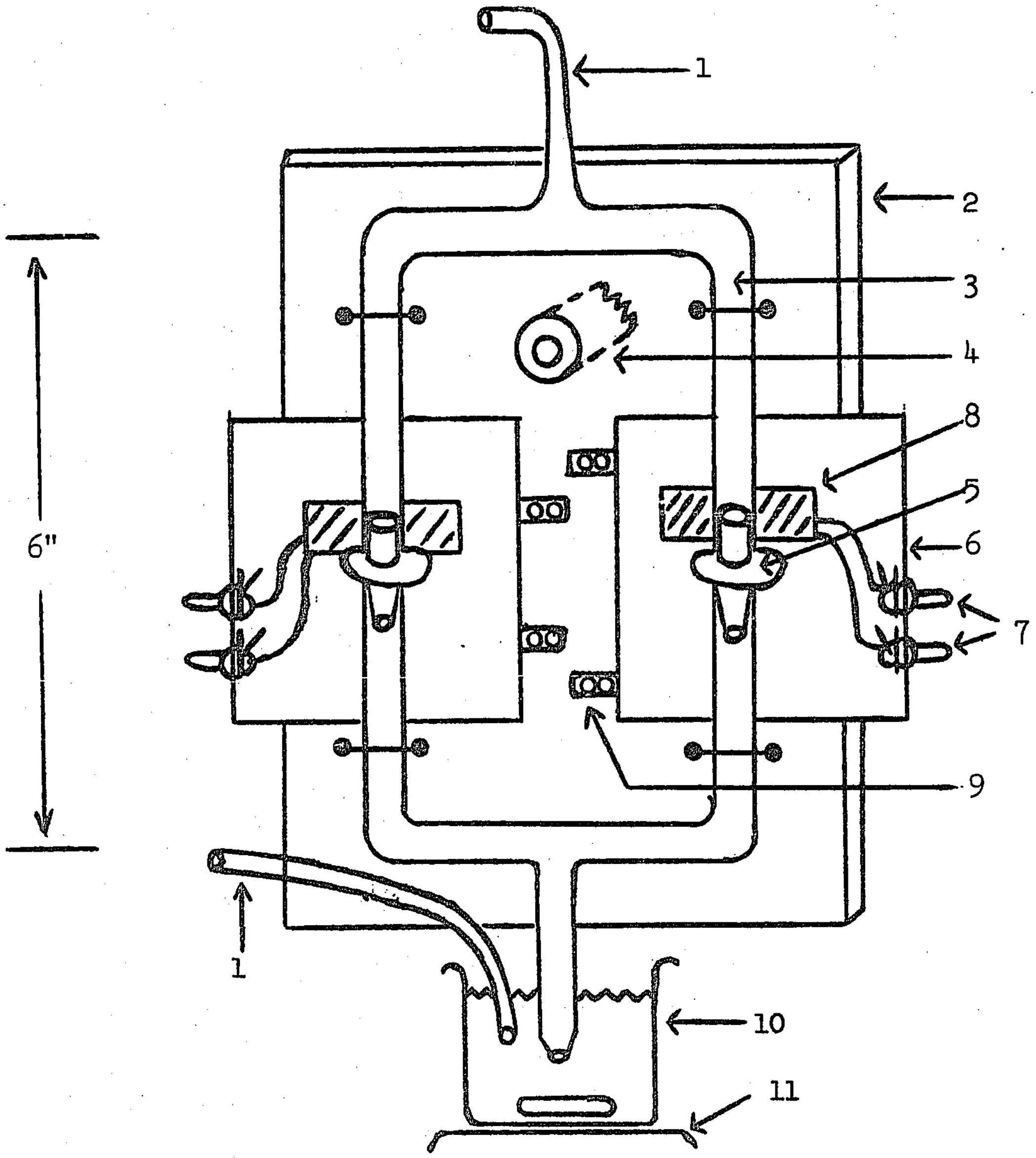

Figure 13. Sidearm Apparatus

---

*Manostat Corporation, New York, New York.

**Bud Catalog No. CU-3000-A.

1. 1/8" O D nylon tubing, to and from pump.
2. 6" L x 3" W x 1/4" D plastic mounting frame.
3. 6 mm O D pyrex tubing loop.
4. 1/2" plastic rod for clamping the apparatus to a support rod.
5. Bel-Art polyethylene tubing reducer-connector, catalog No. 19507*.
6. Bud "mini-box" shield, No. CU-3000-A.
7. Banana plugs - the toroid leads are connected to the plugs through Fahnestock clips mounted on the inside of the removable mini-box shield.
8. Toroids.
9. "L" brackets for binding the miniboxes to the plastic frame.
10. Solution beaker.
11. Magnetic stirrer.

L. Magnetic Induction Probes (Dipping Type)

The method of construction of the four probes used in the magnetic induction section is presented in Figure 14.

In all cases, the toroidal inductors are wound single layer with a given size of enameled magnet wire. These windings are closely placed so as to obtain the highest inductance possible from a given core material and a given wire size. The main secondary winding leads have a braided shield wire around them as they are routed up the plastic tube (part No. 6 in Figure 14) in order to keep stray pickup from the primary winding leads to a minimum.

In Table III the pertinent data concerning the five probes which were constructed are tabulated.

---

*Bel-Art Products, Pequannock, New Jersey

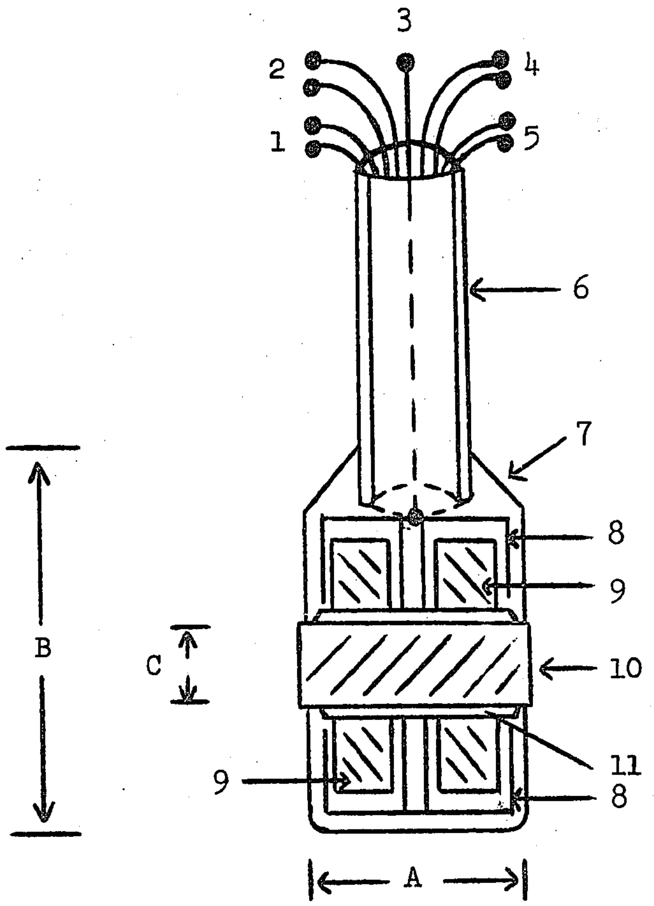

Figure 14. Magnetic Induction Probe

1. Leads to main primary toroidal winding (from signal generator).
2. Leads to null windings (2 turns) wound around the main primary winding.
3. Shield ground wire.
4. Leads from main secondary toroidal winding (to VTVM).
5. Leads to null windings (2 turns) wound around the main secondary winding.
6. Plastic tubing 3/8" OD x 1/4" ID x 3 1/2" L.
7. Silicone Rubber protective coating; GE RTV Adhesive, Catalog No. RTV-108* or Dow Corning Bathtub Caulk.**

---

*General Electric Co., Waterford, New York.

**Dow Corning Corporation, Midland, Michigan.

8. Copper or aluminum foil electrostatic shields.
9. Toroidal core with windings.
10. Bakelite plastic or pyrex glass tubing inserted into the holes of the two toroids.
11. Copper foil shield placed around the tubing of item 10 above.

The shields of items 8 and 11 above are connected to ground wire 3.

TABLE III

Magnetic Induction Probes

Probe designation	Core material	Dimension in mm			Wire size, A.W.G.		Inductance* in mh		Self-resonant* freq., kHz		Remarks
		A	B	C	Pri.	Sec.	Pri.	Sec.	Pri.	Sec.	
A	Cores of EA-005 toroids from Triad	22	27	10	28	28	0.90	0.90	585	585	(a)
B	EC-5000 toroids, shielded, encased in silicone rubber	16	35	8	-	-	5000	5000	3.1	3.1	(b)
C	EA-005 cores	22	27	10	28	34	0.90	3.15	585	234	(c)
D	Identical to Probe A but with null windings.										
F	CF-117	31	56	28	22	22	38	38	56	56	(d)

*Measured in accordance with Heathkit Technical Application Bulletin 9C, 1953.

(a) No null windings.

(b) Two probes whose primary to secondary distance is variable.

(c) Secondary coil has approximately twice as many turns as the primary coil.

(d) For very dilute solutions.

M. Reagents

1. Deionized Water

Deionized water for all experiments was obtained by passing deionized water from the central "house" system through a Fisher Scientific mixed bed ion resin cartridge, catalog No. 9-035-25.* The specific conductance of this water always measured less than 1 micromho per centimeter, which compares favorably with literature values for good quality water in equilibrium with atmospheric carbon dioxide.

2. Chemicals

All chemicals used were of analytical reagent quality. Solutions of HCl, NaOH, and $AgNO_3$ were made by dilution of Fisher Certified Reagent* solutions.

---

*Fisher Scientific Co., Pittsburgh, Pennsylvania.

III. EXPERIMENTAL AND RESULTS

A. Introduction

1. Limitations of Present Contactless Conductance Methods

Conventional techniques of contactless conductance measurement have several important limitations. The classical high frequency conductometric method, hereafter referred to as the impedimetric method, has a limited range over which its response to solution conductance is linear. Also, high operating frequencies must often be used for work with highly conducting solutions (assuming that the design of the measuring cell must remain fixed). Finally, the measuring elements, either capacitor plates or inductance coil, are usually parts of the frequency-determining network of the oscillator; this can produce problems of oscillator instability at high operating frequencies.

Conductance measurements based on the magnetic induction principle produce good results at high electrolyte concentrations, but little data concerning low concentrations of electrolyte have been published. Only one response curve depicting a magnetic induction response versus solution composition has appeared.[29]

It is therefore the intention in this present work to determine and evaluate those experimental variables basic to the response of the magnetic induction method. Hopefully, the versatility of the method at high electrolyte concentrations can be extended to include solutions in the micromolar range. Finally, possible chemical applications using this method will be examined.

2. Preliminary Investigations

Originally it was planned to follow the techniques of Griffiths[23] and Calvert and coworkers[22] in order to become familiar with the magnetic induction measurement technique. In simplest form these authors describe an apparatus consisting of two insulated toroidal coils dipping into a solution whose conductance is desired. One toroid (the transmitter) is connected to a signal generator, and the second toroid (the receiver) is connected to a VTVM. This setup was duplicated, and it was planned to measure the direct response of the system versus solution composition before attempting a differential technique. The above mentioned authors concerned themselves with differential techniques only.

It was soon apparent that the response curves obtained by the direct measurement approach resembled more closely a classical impedimetric type response rather than an expected linear magnetic induction response. However, these preliminary results appeared interesting and had not been reported in the literature. Work to confirm the predominantly impedimetric nature of these initial toroidal responses was therefore undertaken. In Sections III B and III C following, two experimental toroidal configurations are described which give responses that can best be explained by impedimetric theory and the results obtained by workers using conventional impedimetric methods. The work to be reported in these sections ultimately leads to a toroidal configuration whose response can be described entirely by the laws of magnetic induction (Section III D).

3. Importance of the Toroidal Resonant Frequency

Although it is not known whether Griffiths[23] and Calvert et al.[22] made their conductance measurements at the resonant frequency of their toroids, in the work which follows (Sections III B and III C) the natural self-resonant frequency of the receiver toroid was used initially. Operation at the resonant frequency was deemed important both by Fujiwara and Hayashi[16] and Johnson and Hart.[29] The latter authors stated that maximum energy transfer between two identical toroids occurs at the self-resonant frequency of the pair. Furthermore, Owen[35] has shown that the coefficient of mutual inductance between two coils rises rapidly as the resonant frequency of the secondary coil is approached. Actually this resonant frequency may be the natural self-resonant frequency of the secondary coil alone or with the coil plus added parallel capacitance.

---

[35] D. Owen, "Alternating Current Measurements at Audio and Radio Frequencies," Methuen and Co. Ltd., London, 1957, p. 102.

B. Immersion Method

1. Introduction

Each of the Triad toroids is covered by a thin (1/32 inch) plastic coating which proved highly resistant to attack by aqueous electrolyte solutions. This covering is less resistant to organic solvents such as benzene and carbon tetrachloride and is attacked readily by acetone, ethanol, and especially methanol. However, the covering was considered adequate long-term protection for the toroid so that it could be dipped directly into an electrolyte solution; hence a direct response version of the technique of Griffiths[23] and Calvert et al.[22] mentioned previously could easily be attempted.

2. Experimental Procedure

The two toroids to be used were placed inside a shielded container, usually a beaker wrapped with aluminum foil, the foil being grounded to an earth ground. The leads of each toroid were routed over the top of the container and affixed to a suitable length of RG-58 C/U shielded cable. The cable leads of one toroid were connected to the signal generator, and the leads of the other toroid were connected to the Heath AC VTVM. The Eico AC VTVM was connected to the signal generator in such a way that either the input voltage or input current to the transmitter toroid could be monitored; the current was measured as a voltage drop across a standard resistor.

In the interest of reducing noise pickup, all grounds were made to a common earth ground. It was found that grounding the case of the VTVM connected to the receiver toroid was sufficient to reduce the inherently small noise pickup of the toroid (due to its high Q) to an immeasurably low value. Figure 15 shows in detail the experimental connections.

The usual procedure for recording solution composition changes was as follows: the particular toroids to be used were connected to the shielded leads of the signal generator and output VTVM, respectively. The container was then filled with water to a level approximately 1 cm above the top of the toroids; then sufficient voltage at or near the resonant frequency of the receiver toroid was applied to the transmitter toroid so that a convenient voltage reading (usually 2 mv) was observed on the lowest scale of the output VTVM; electrolyte was then added in increments to the stirred solution, and the change in voltage indicated by the output VTVM was noted following each addition.

3. Preliminary Experiments and Results

a. Volume Effect. It was observed that the readings of the output VTVM increased greatly with the level of water added to the beaker until the tops of both toroids were below the level of the water. This effect, hereafter called the volume effect, was easily minimized by adjusting the initial volume of water so that the tops of the toroids were at least 1 cm below the level of water.

b. Direct Response Curves at the Toroidal Resonant Frequency. Using the EA-100 toroids, response curves were obtained for solutions of HCl, NaOH, and NaCl at constant receiver toroid resonance; i.e., after each addition of electrolyte, the signal generator required retuning to a lower frequency in order to achieve maximum output from the receiver toroid. A response curve was constructed by plotting output millivolts versus the concentration of the species in solution

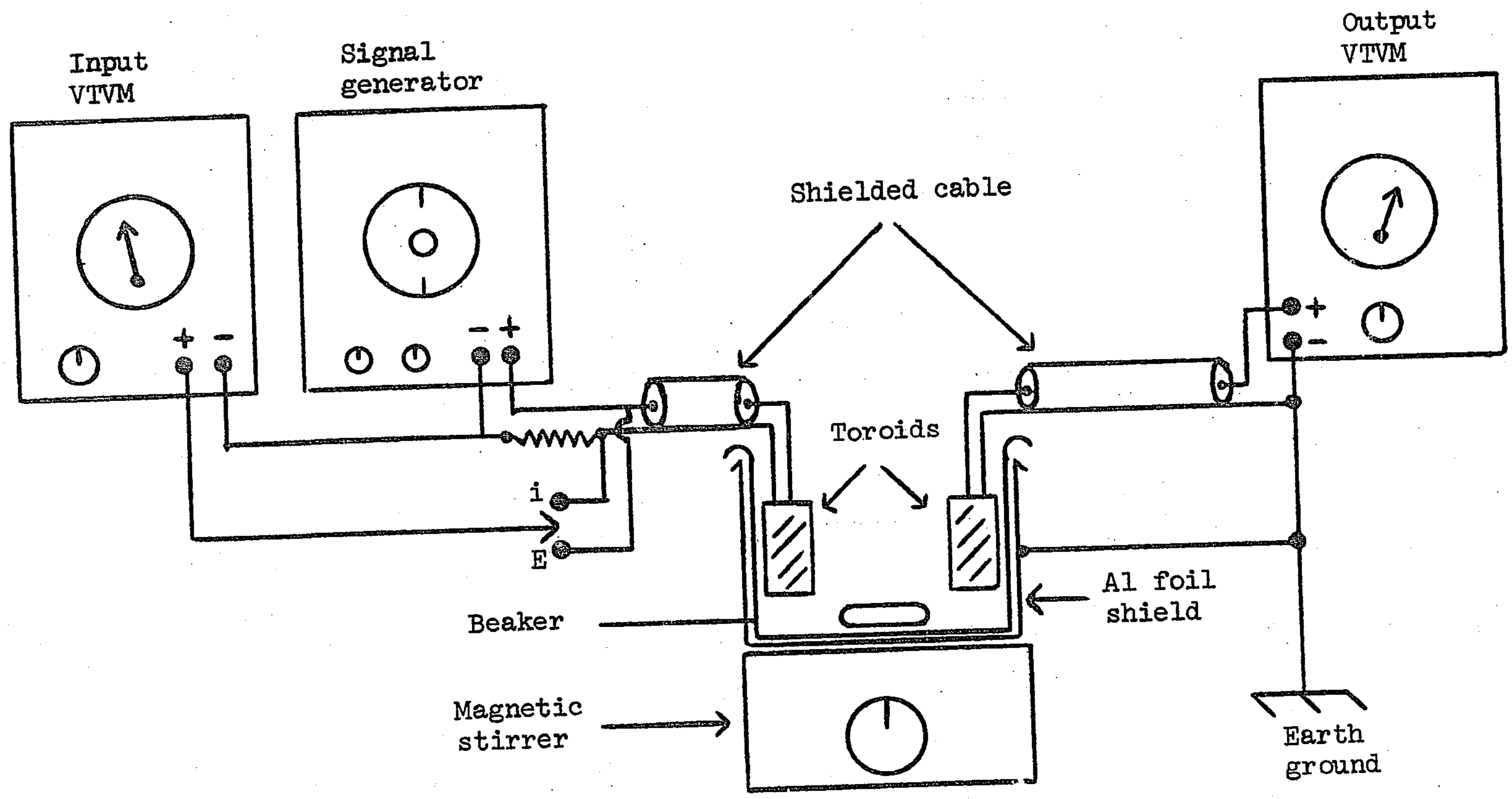
Input
VTVM
Signal
generator
+
−
− +
Shielded cable
Output
VTVM
+
−
Toroids
i
E
Beaker
Magnetic
stirrer
Al foil
shield
Earth
ground

Figure 15. Electrical Connections

(or milliliters of reagent added). The results* are shown in Figure 16.

An examination of Figure 16 reveals that little change in output voltage occurs after the addition of 1 milliliter of reagent (concentration of solution = 1.25×10^{-4} M). If the toroidal response were predominantly magnetic in nature, one would expect output voltage changes to occur at higher electrolyte concentrations; yet under the above mentioned experimental conditions all response changes occurred at low electrolyte levels. Also, the curves in Figure 16 appear similar to the response curves obtained with capacitance type impedimeters (Figure 10, Section I D). The above facts strongly suggested that the experimental quantity actually being measured was the capacitance of the solution contained between the two toroids.

c. Capacitive Response Using the Sargent Oscillometer. In order to gain insight into the nature of the above responses, the following experiment was performed using the Sargent Oscillometer which operates at 5 MHz and responds mainly to capacitive changes occurring between its output leads. Changes in solution capacitance were measured, first using the Sargent cell, and then using two EA-100 toroids. In the latter case the two leads of each toroid were soldered together. Then one toroid was connected to the "hot" output lead of the Oscillometer and the other to the ground lead. The toroids were then placed in a shielded beaker and changes in capacitance between the toroids were recorded. These results are shown in Figure 17.

---

*The actual millivolt values which appear on the ordinate will differ among the many figures to be presented due to the use of different solution containers and the nature of the shielding employed.

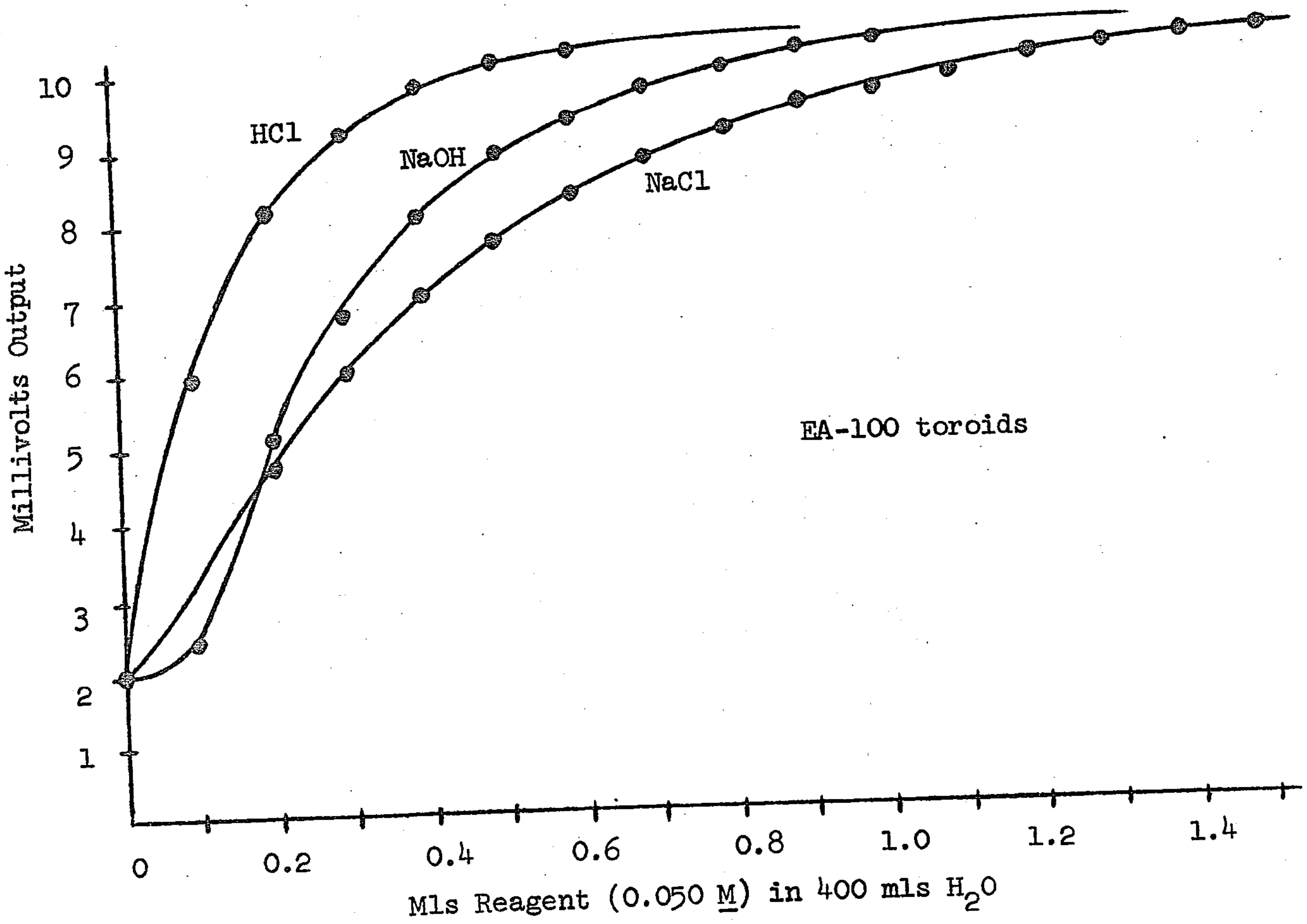

Figure 16. Immersion Method Response Curves

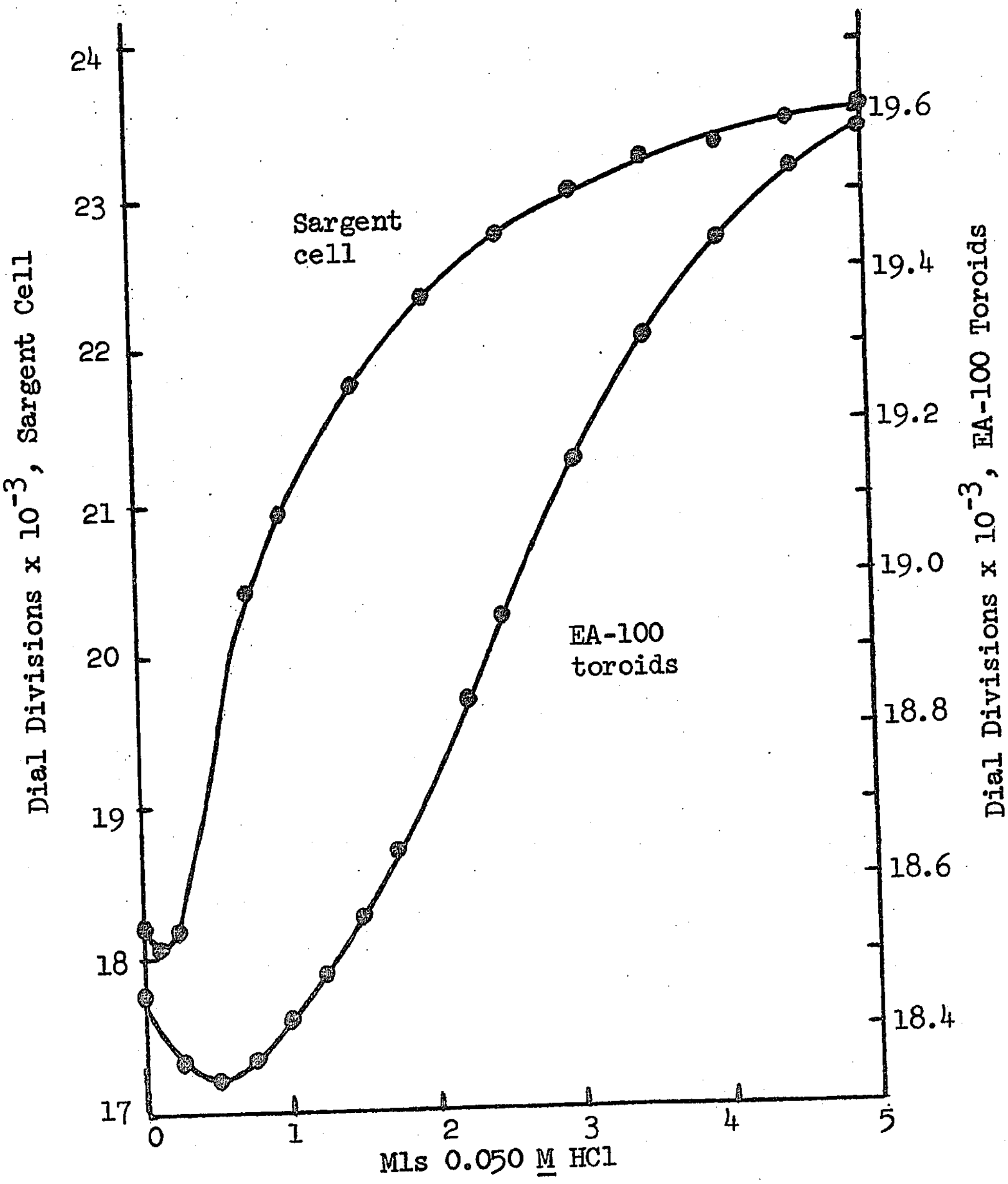

Figure 17. Capacitive Response Using Sargent Oscillometer

4. Further Evidence for the Impedimetric Nature of the Immersion Response

a. Frequency Shift Effects. It has been mentioned that to obtain response curves at constant resonance, the signal generator must be retuned after each addition of electrolyte. The nature and magnitude of these frequency shifts were examined for air, water and solutions containing known amounts of added electrolyte. Using the EA-010 toroids, plots of receiver toroid output versus frequency were made near the toroidal resonant frequency. The results appear in Figure 18. The resonant frequency peak shifted from 140 kHz for air to 115 kHz for water and finally to 108.5 kHz for 1.25×10^{-4} M HCl.* A similar shift of the resonant frequency has been noted by others using coil type impedimeters. Reilley[5] has proposed that the mode of coupling between coil and solution is actually electrostatic, i.e., capacitive, and not magnetic in nature. Hamme,[36] and Ladd and Lee,[37] attributed the frequency shift to an increase in the distributed capacity of the coil caused by the addition of electrolyte; in other words, the value of solution dielectric between adjacent turns of each toroid is increased as the medium is changed from air to water to dilute HCl, thus lowering the toroidal resonant frequency.[1]

b. Correlation of Response Curve Midpoints with Low Frequency Conductances. It is an experimental fact of impedimetric work, that the

---

*A table which correlates HCl solution concentrations used in Sections III B and III C to their specific conductivities appears in Appendix A.

[36] H. W. Hamme et al., J. Chem. Phys. 22, 944 (1954).

[37] M. F. C. Ladd and W. H. Lee, Talanta 12, 941 (1965).

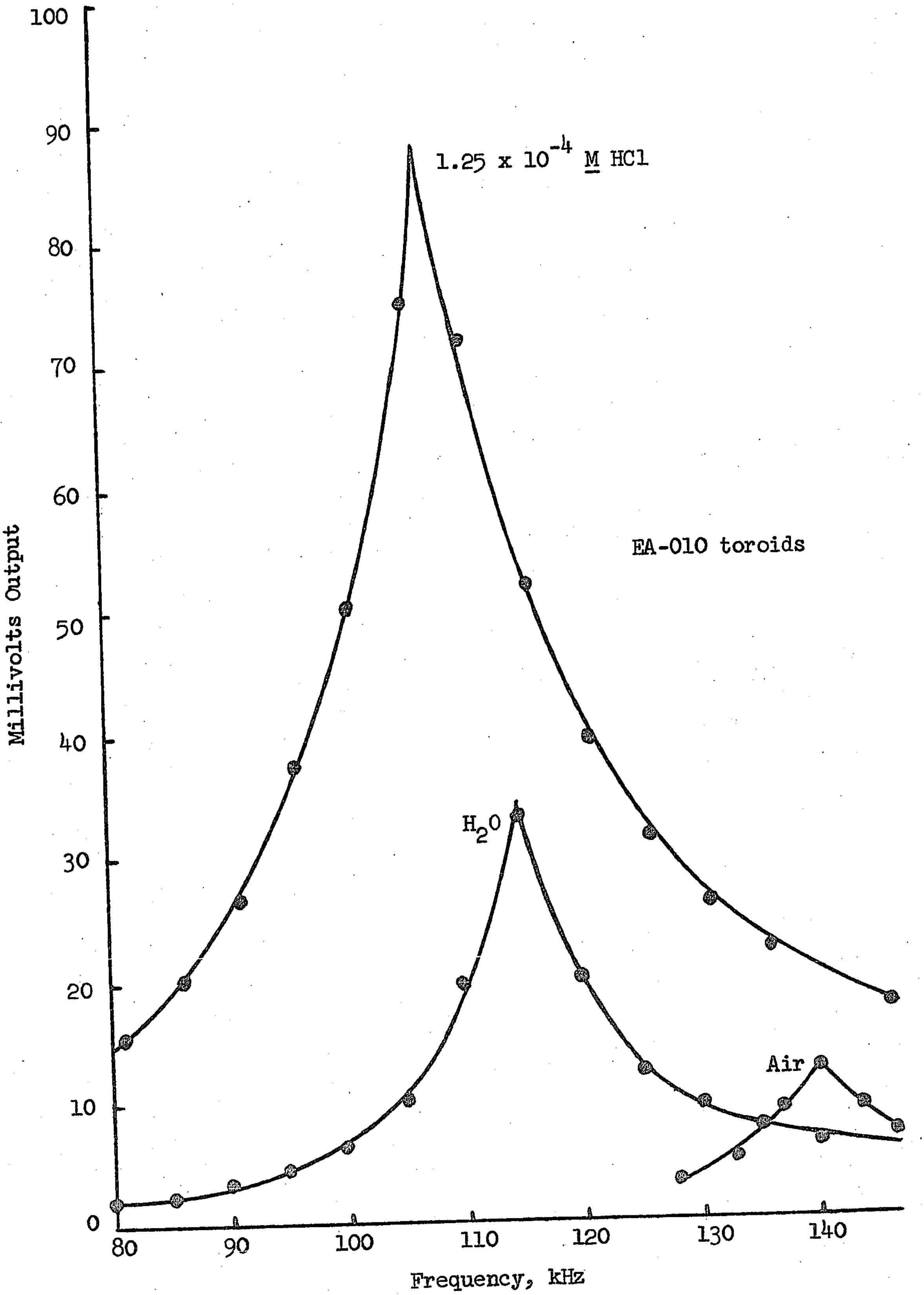

Figure 18. Frequency Shift Effects

midpoints of capacitive response curves, such as in Figure 19, occur at the same low frequency conductance value.[38] Using the EA-001 toroids this fact was checked. In Figure 19 the midpoints for HCl and NaCl occur at 1.75×10^{-4} M and 6.20×10^{-4} M, respectively. The relative low frequency conductivities at these concentrations (the cell constant was not used) were 27,500 micromhos for HCl and 8,600 micromhos for NaCl. For each electrolyte, the product of the concentration at the midpoint of the response curve times the conductance at that concentration should be a constant.[38] Thus for HCl, $1.75 \times 10^{-4} \times 27{,}500 = 4.8$ and for NaCl, $6.20 \times 10^{-4} \times 8{,}600 = 5.3$.

The agreement of the results (10%) was considered sufficient for the purpose of the experiment.

c. Effect of Intertoroidal Distance on Response. By increasing the distance between the capacitor plates of an impedimetric apparatus, an increase in response sensitivity versus concentration can be effected.[34,39,40] This distance increase also has the same effect as increasing the operating frequency, with the result that the midpoints of the capacitive response curves are shifted to higher concentrations (Figure 10, Section I D). This is analogous to a change in cell constant using low frequency conductance techniques. Figure 20 confirms the experimental effect of increased intertoroidal distance upon the midpoint of the response curve, using the EA-001 toroids.

---

[38] J. L. Hall, Anal. Chem. 24, 1236 (1952).

[39] C. N. Reilley and W. H. McCurdy, Jr., Anal. Chem. 25, 86 (1953).

[40] S. C. Clayton *et al.*, Anal. Chim. Acta 14, 269 (1956).

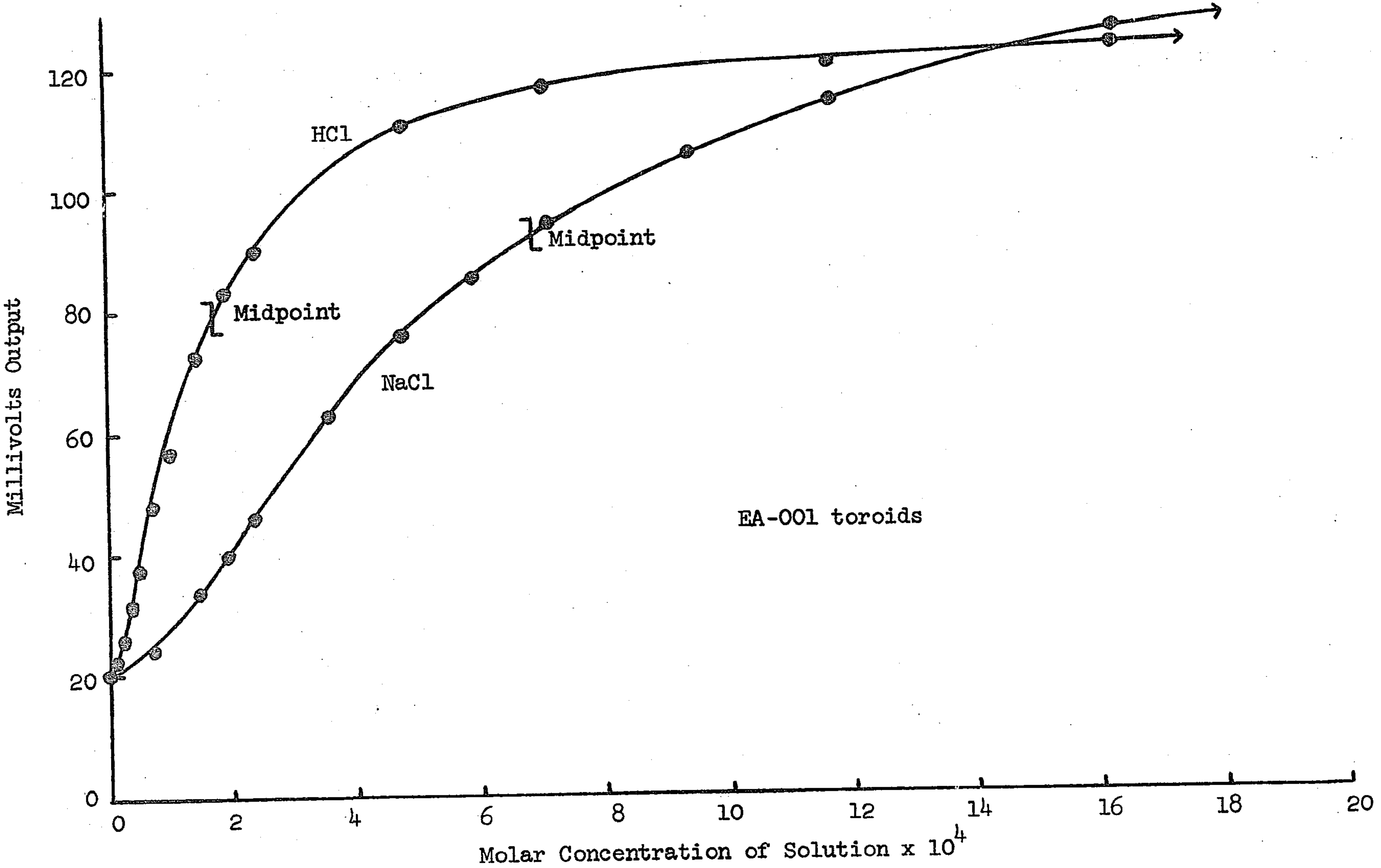

Figure 19. Determination of Response Curve Midpoints

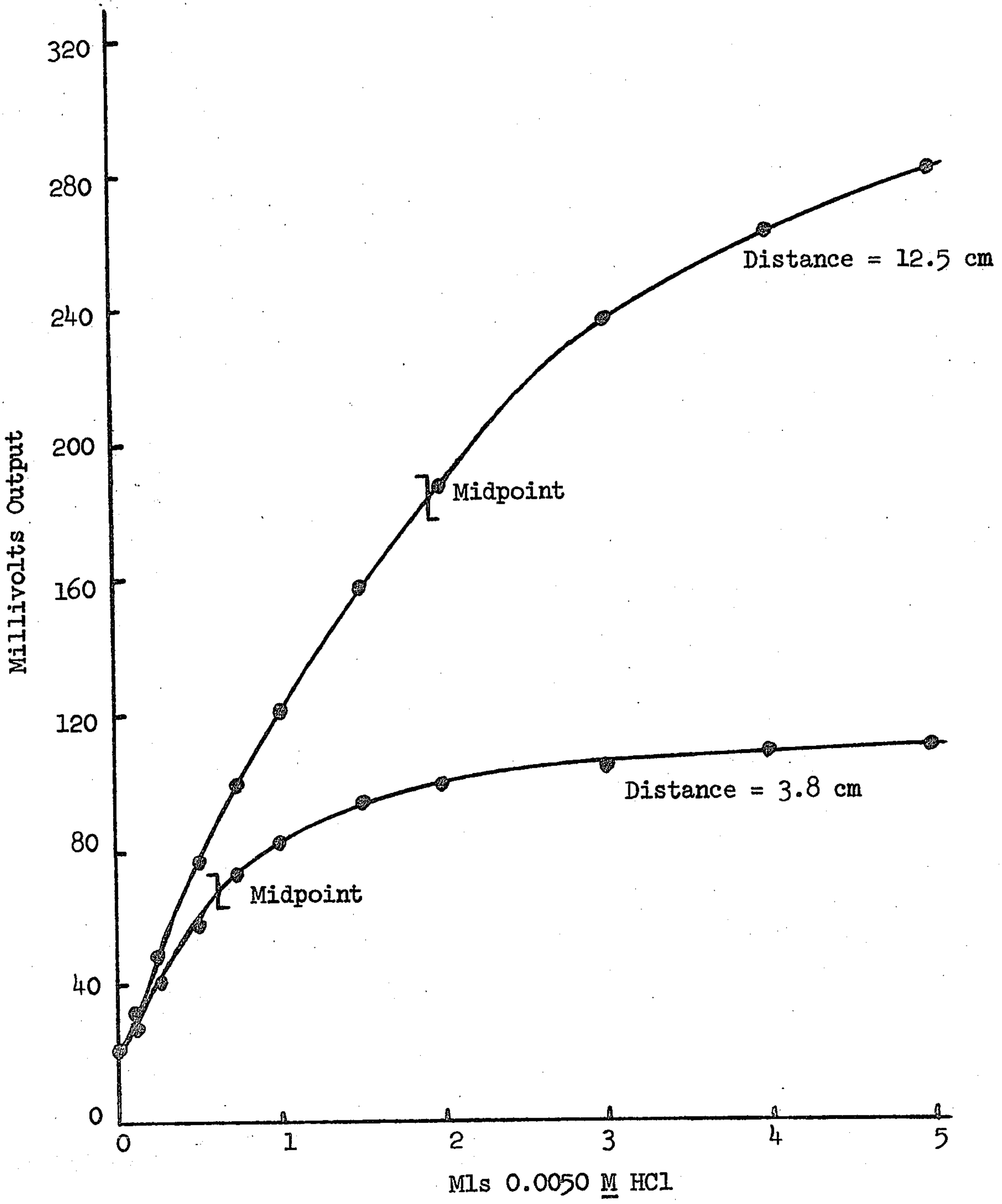

Figure 20. Effect of Intertoroidal Distance

d. Effect of Frequency on Response. According to impedimetric theory (Section I D), an increase in frequency extends the useful response of the system to higher values of electrolyte concentration. Figure 21 shows this effect using toroids whose resonant frequencies differ by an order of magnitude.

5. Determination of Optimum Operating Frequency

The aforementioned frequency shifts which occurred using this Immersion Method suggested that frequencies other than the resonant frequency might result in greater system sensitivity to concentration changes.

Accordingly, response curves were made at several frequencies near resonance. The resonant frequency was applied to two identical toroids and the VTVM reading noted. Then the signal frequency was either lowered or raised until the VTVM reading dropped to 1/2, 1/4 or 1/10 of its resonant frequency voltage reading. With the frequency then remaining unchanged, electrolyte was added and the response curve plotted. The above voltage fractions represent, in radio terminology, frequencies which are 6 db, 12 db or 20 db off resonance.[1] This decibel notation will be used hereafter.

In Figure 22 the results of using frequencies other than the resonant frequency are shown for the EA-100 toroids. It is observed that the greatest sensitivity is available using frequencies which are 6 or 12 db lower than the toroidal resonant frequency.

When identical experiments were performed using the epoxy encapsulated EA-100A toroids, no improvement in sensitivity could be obtained at frequencies different from resonance. Apparently the

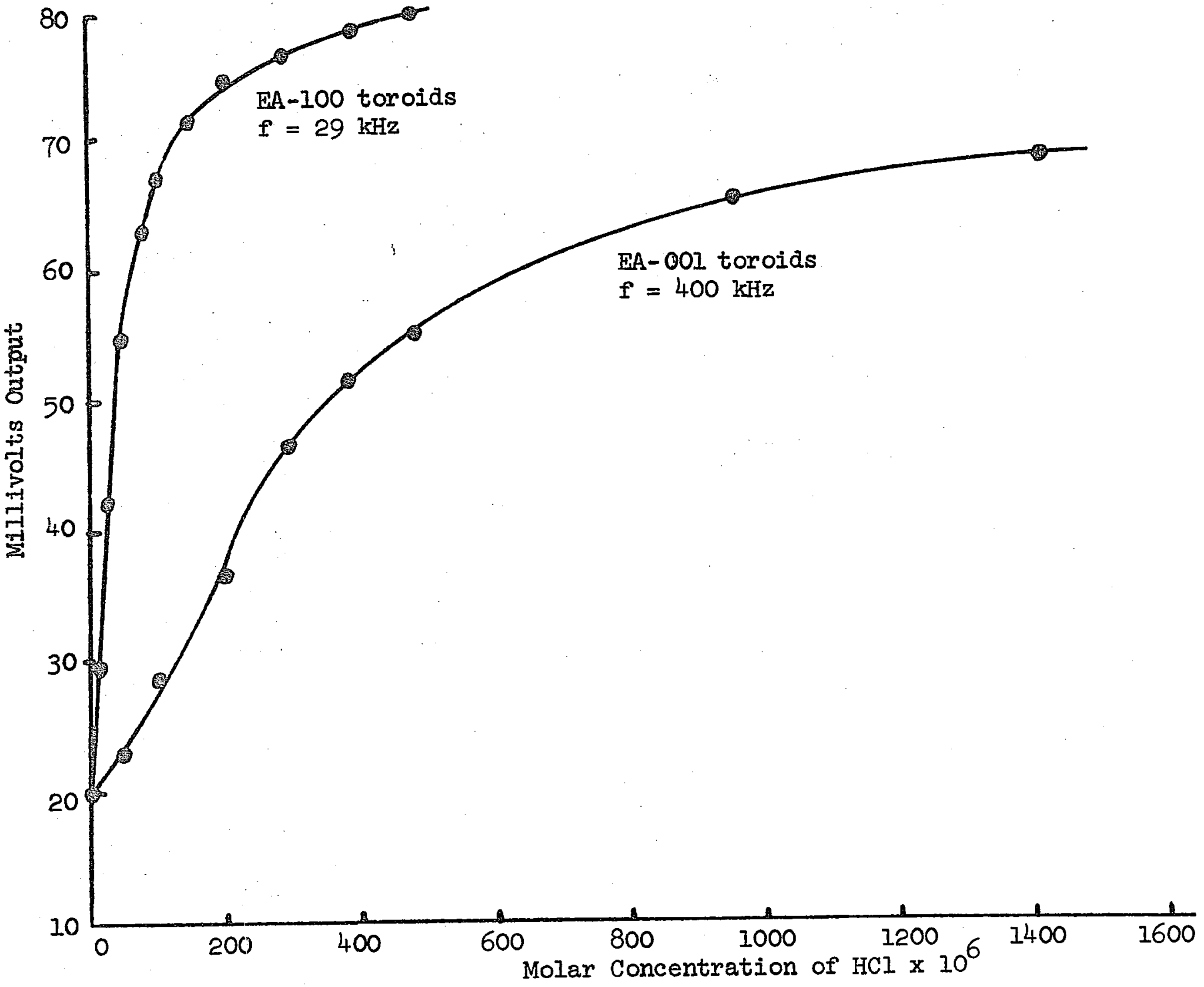

Figure 21. Effect of Frequency upon Response

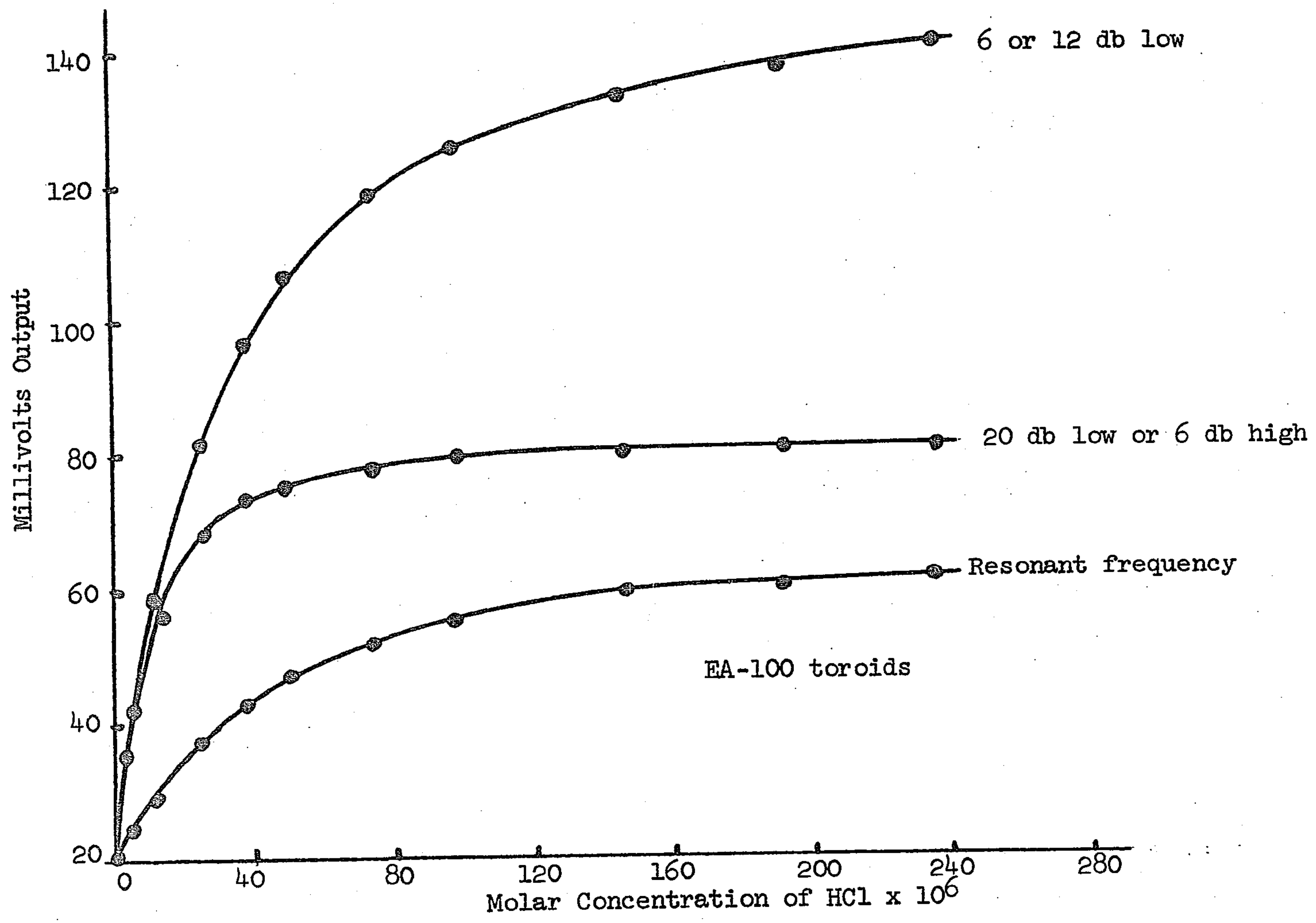

Figure 22. Determination of Optimum Operating Frequency

thicker (3/32 inch) epoxy coating prevents the toroid windings from interacting with the solution dielectric to such an extent that no increase in distributed capacitance results; hence, the response remains unaffected by using frequencies different from resonance; this is in agreement with the experimental observation that little or no returning of the signal generator was necessary when a constant resonance experiment was performed using the EA-100A toroids as compared to using the thin plastic covered EA-100 toroids. These results are also consistent with the known fact that when the thickness of a capacitor dielectric is increased, the capacitance value (and by analogy, any capacitive effect) is diminished.

As a result of the above investigations all later experiments using the plastic covered toroids were performed at 12 db off resonance on the low frequency side.

6. Differential Techniques

a. Introduction. Titrations performed using the direct response mode of the Immersion Method resulted in poor accuracy and precision. These faults resulted from the necessity of reading small voltage changes superimposed upon large voltage values. A differential, rather than direct, means of voltage measurement would greatly enhance the accuracy and precision of the results. Therefore the differential technique described by Griffiths[23] and Calvert et al.[22] was attempted.

b. Procedure. The connections remained essentially the same as in Figure 15, except for two extra turns of 20 gauge plastic covered hookup wire which were wound upon the existing windings of each toroid. One lead from each of these extra null windings was routed to the terminals of the Heath Decade Capacitance Box and Heath Decade Resistance Box, which were wired in parallel. The one remaining lead of the receiver toroid null winding was connected to the remaining null winding of the transmitter toroid. These connections are shown in Figure 23.

If the phase relationships of Figure 23 were correct, a null reading on the VTVM was obtained upon switching in the necessary values of resistance and capacitance; if not, leads 3 and 4 or 2 and 1 were interchanged. A null reading at some value of resistance (R) and capacitance (C) was then possible.

The actual number of null windings is arbitrary in that different multiples of capacitance and resistance are required depending upon the number of windings used.[22-24,26] Two null windings resulted in convenient values of R and C within the range of the two decade boxes. A finer degree of null could be obtained if small fixed capacitors (<100 pf) were added in parallel with the Heath Capacitance Box.

It was found necessary to ground the cases of both decade boxes to eliminate body capacitance effects. Using 10 volts input to the transmitter toroid, a null ratio of 200:1 was possible; i.e., with no null windings, an output of 1 volt appeared on the VTVM; with a complete null using the differential setup, the residual noise was less than 5 mv.

c. Results Using the Differential Method. Using EA-001 toroids provided with null windings, response curves similar to Figure 24 were obtained.

It can be seen that when this differential procedure is used, the previous direct response can be separated into two component parts,

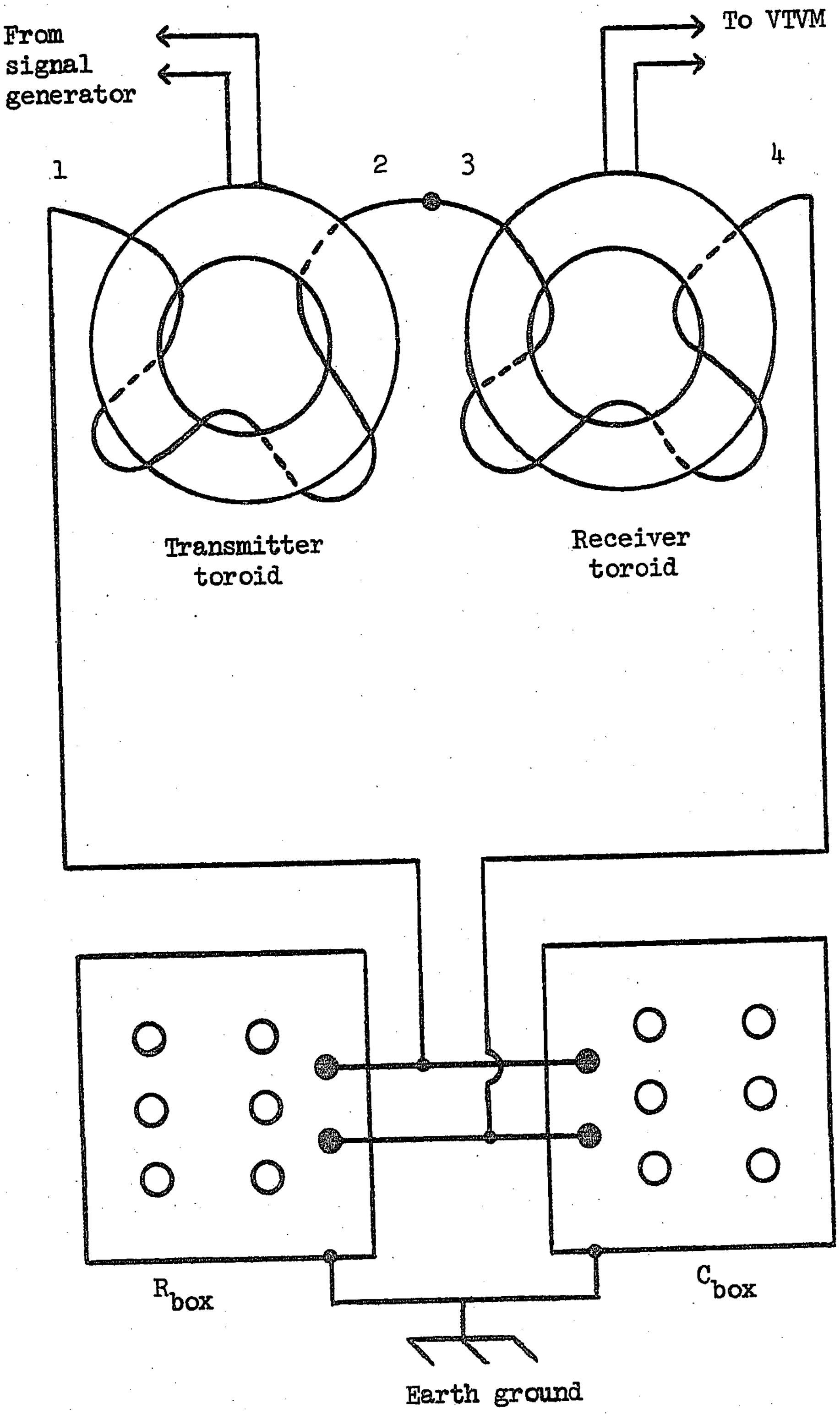
From
signal
generator
To VTVM
1
2
3
4
Transmitter
toroid
Receiver
toroid
R_{box}
C_{box}
Earth ground

Figure 23. Differential Mode Electrical Connections

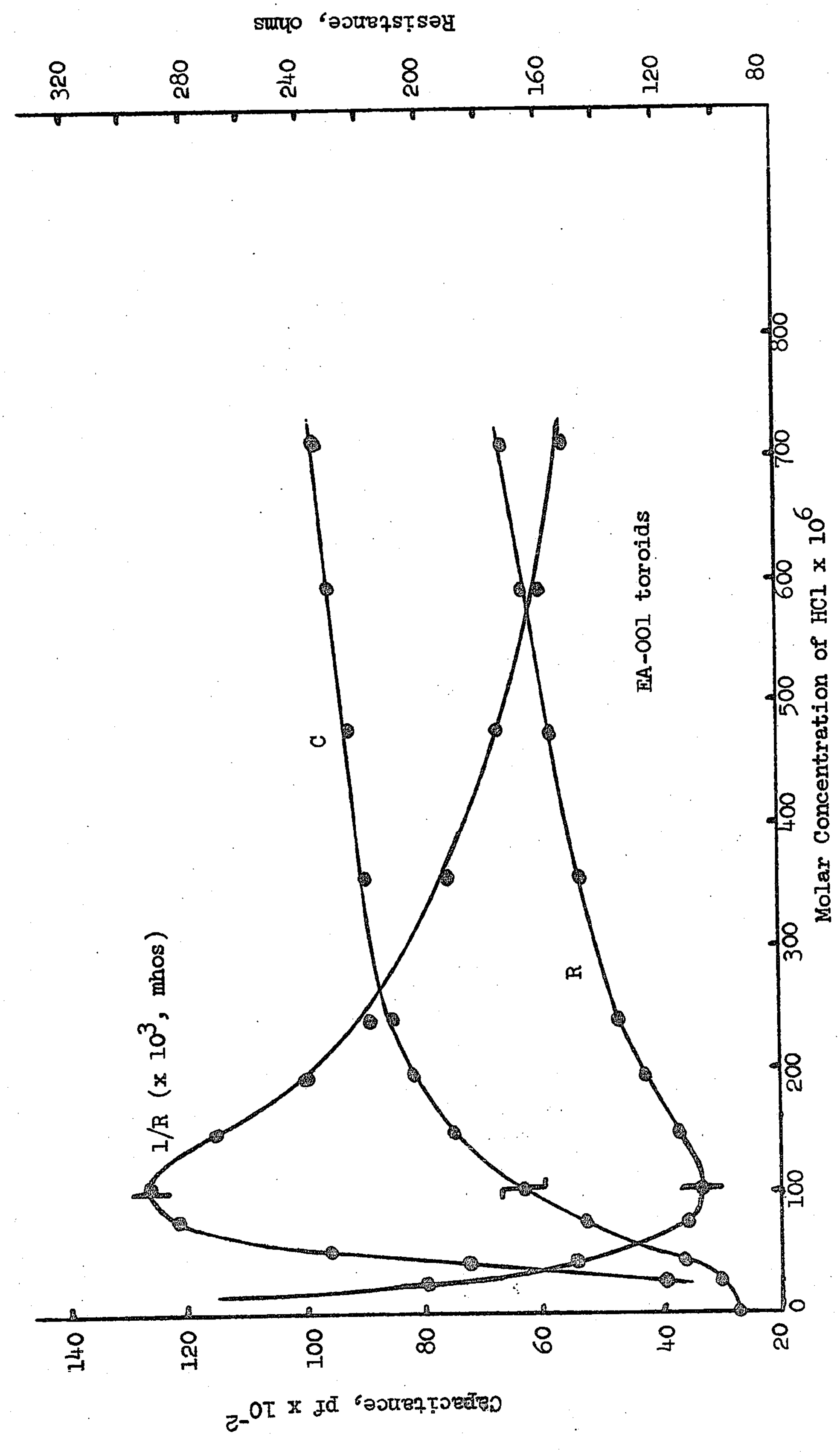

Figure 24. Differential Mode Response Curves

one due to solution capacitance and the other due to solution conductance (1/R). The two response curves are identical in meaning to those presented in Section I D (Figures 9 and 10) concerning classical impedimetric response curves. In agreement with theory, the peak of the 1/R curve occurred at the same concentration as the midpoint of the capacitance curve. Thus using toroids in a differential arrangement, it is evident that the previous direct response was actually composed of proportions of capacitance and conductance (1/R) which together produced an overall capacitance-like impedimetric response curve.

d. Magnetic Response. Attempts were made to discover any magnetic response which might have been obscured by the impedimetric response. Using the differential technique, attempts to find a magnetic type response at high electrolyte concentrations were made. Even with a 2 M HCl solution, no response indicative of magnetic coupling could be obtained. Several of the available toroids were used to determine if such variables as frequency, core mass, and hole diameter had any effect. Also, further amplification was tried using the FET amplifier ahead of the output VTVM. However none of these attempts was successful in finding a magnetic type response. Only the previously found impedimetric response at low concentrations was obtainable.

7. Applications

a. Acid-Base Titration. Using the differential procedure, a simple neutralization titration was performed. Concentrations of acid or base were used, which from inspection of the response curve in Figure 24, lay on both sides of the 1/R peak. Hence, an inverted titration curve, many of which are reported in the impedimetric literature,[39] could be produced. Typical differential titrations are shown in Figures 25 and 26. In Figure 25, all solution conductances during the titration were to the left of the 1/R peak of Figure 24, whereas in Figure 26, all values were to the right of that peak. Titration curves corresponding to the differential changes in capacitance could be used as well.

b. Dielectric Measurements. Employing the differential technique, the EA-001 toroids were used to detect changes in dielectric constant. The results for several pure liquids and water-ethanol mixtures[41] are shown in Figure 27.

8. Summary

Attempts were made to obtain a direct magnetic induction response by immersion of two toroids into an electrolyte solution. It was found that with the toroids available, a usable response could be obtained only at concentrations less than 2 millimolar. The shape of the response curves resemble closely those obtained on classical impedimetric equipment; but equally important, the curves resemble those obtained by workers[16,17] who also measured low level solution conductance by the extent to which the solution coupled two closely spaced induction coils.

Early experiments using the resonant frequency of the toroids indicated an impedimetric type response at low concentrations; several

---

[41] L. Meites (ed.), "Handbook of Analytical Chemistry," McGraw-Hill Book Co., New York, 1963.

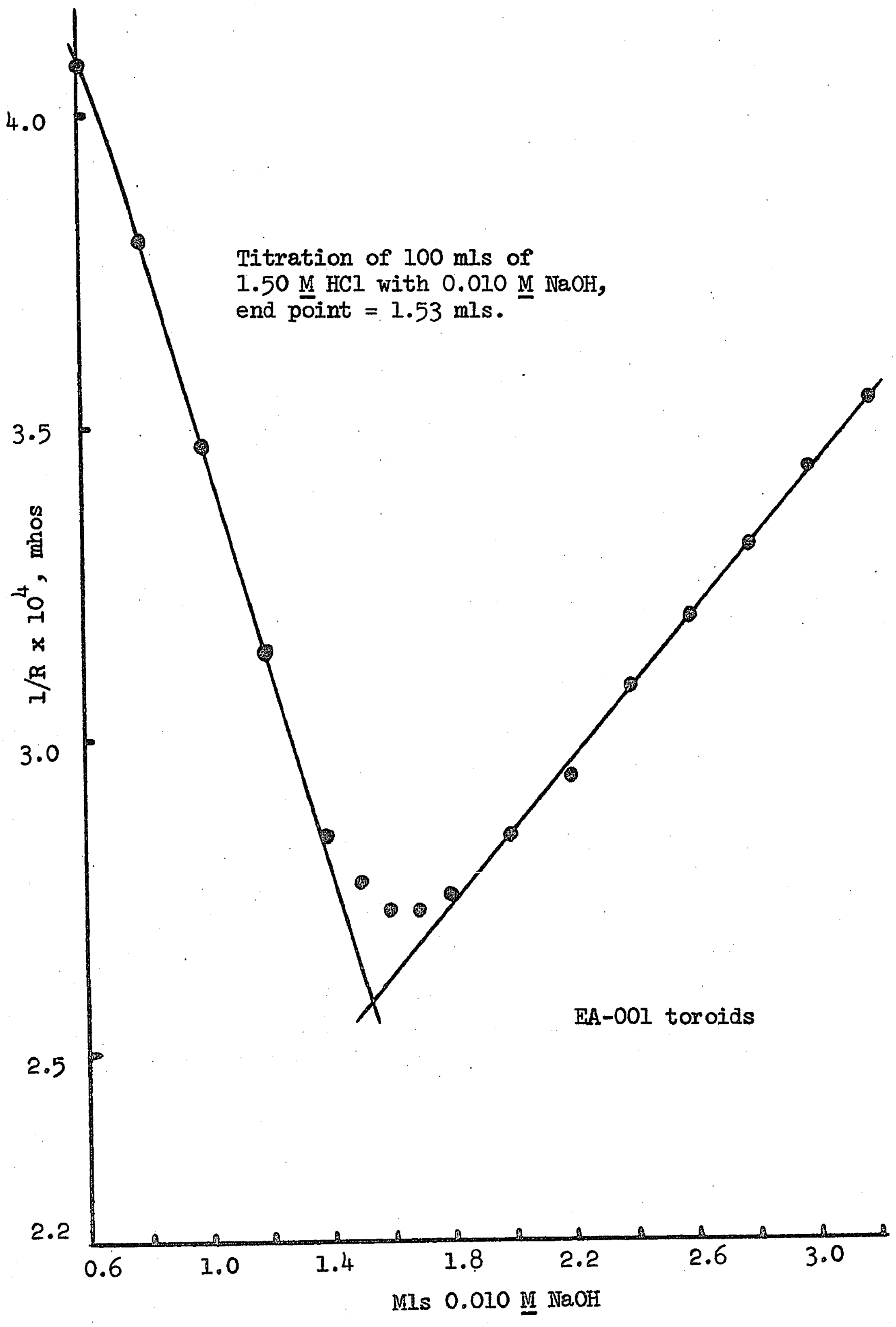

Figure 25. Acid-Base Titration

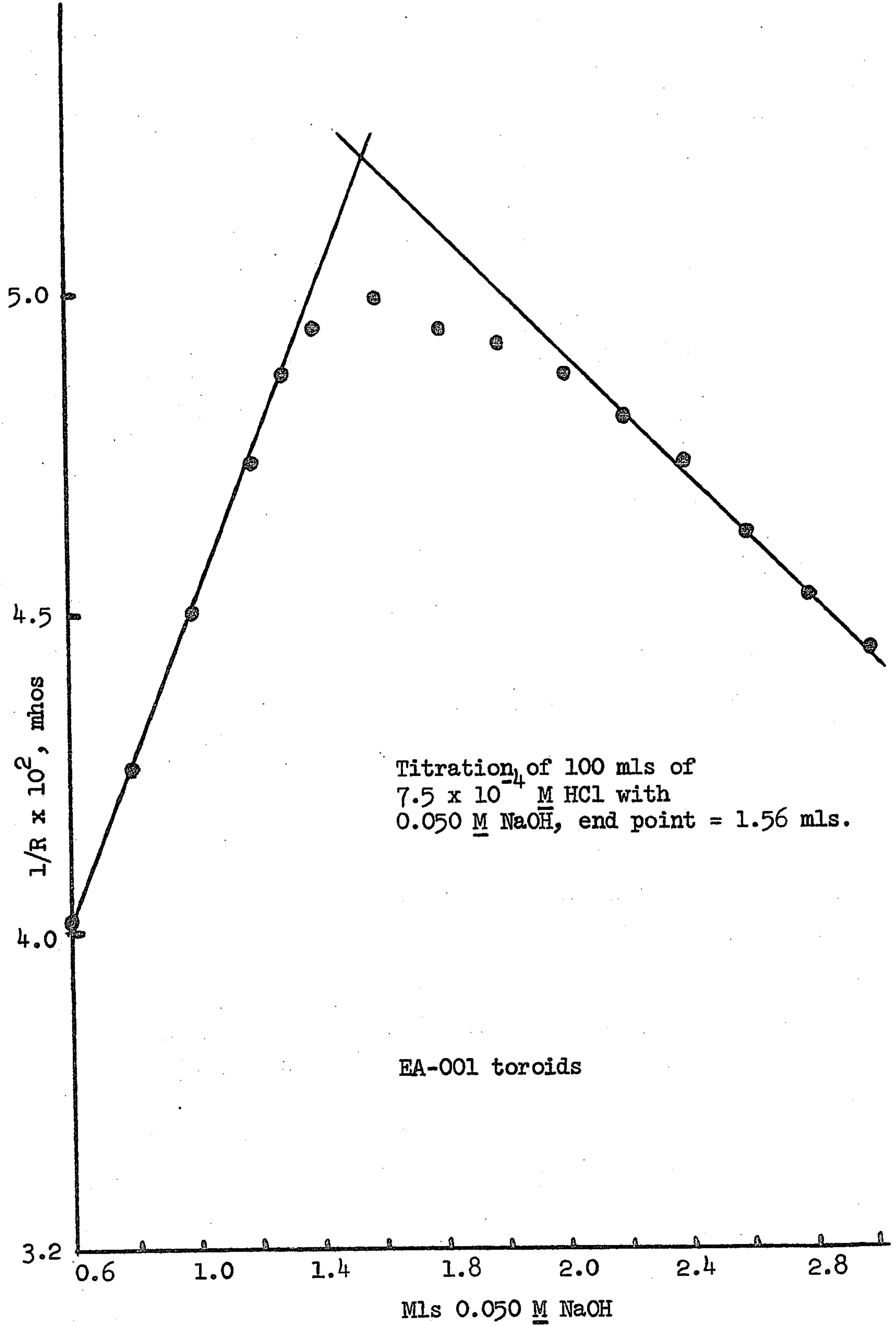

Titration of 100 mls of 7.5×10^{-4} M HCl with 0.050 M NaOH, end point = 1.56 mls.

EA-001 toroids

Figure 26. Acid-Base Titration

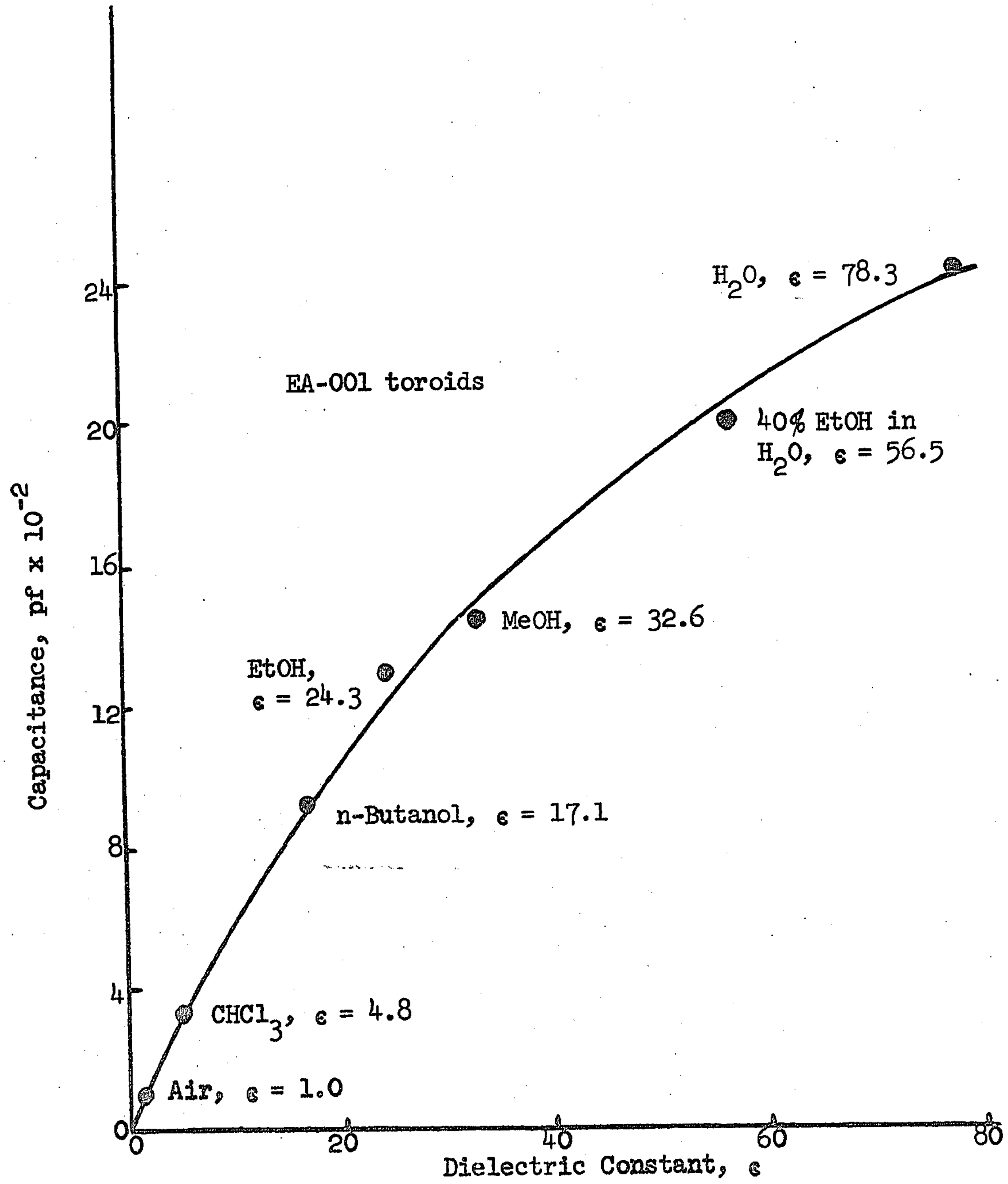

Figure 27. Dielectric Constant Measurements

experiments performed to confirm this idea proved successful. For this Immersion Method it was also concluded that the most sensitive response occurs using frequencies other than the resonant frequency, specifically a frequency 6 to 12 db on the low side of the toroidal frequency response curve.

Differential techniques used by others[22,23] at high concentrations proved equally applicable for the low electrolyte levels reported herein. Using simple apparatus, this technique provided a high sensitivity characteristic of most null methods, and allowed a convenient separation of the solution impedance into its basic quantities of resistance and capacitance. Applications of this technique included an acid-base titration and the measurement of dielectric constant values.

Attempts to discover a magnetic type response at high concentrations proved unsuccessful.

It is concluded that the response of this Immersion Method at low concentrations is due predominantly to impedimetric (electrostatic) coupling between the toroids. The existence of a small amount of magnetic coupling, which although unmeasurable, cannot be excluded; if some magnetic coupling is not present, it is difficult to understand the successful operation of the differential measurement technique which depends on the cancellation of magnetically out-of-phase signals.

C. Sidearm Method

1. Introduction

The Sidearm Apparatus described in Section II K was constructed to eliminate several disadvantages of the Immersion Method. The primary object in developing this method was to achieve greater toroidal isolation from the solution dielectric; i.e., it was thought that the removal of the toroidal windings from close contact with the solution might produce a response more dependent on the solution resistance than on its capacitance. To this end, the distance between the toroids was made large, and the toroids were provided with shields. Another reason for pursuing this design was to eliminate the deterioration of the plastic covering of the toroids; also, by not immersing the toroids directly into the solution, the volume effect could be eliminated; and finally, since the method still involves a closed loop of solution, a magnetic response might be observed.

2. Experimental Procedure

The apparatus has been described in Section II K. The shields were grounded to earth. The connections to the toroids and the operating procedure were identical to that described in Section III B for the Immersion Method.

3. Preliminary Investigations

a. Importance of a Closed Solution Loop. The purpose of the first experiment was to determine what effect "closing the loop" of the Sidearm Apparatus had upon the observed response. It was found that the observed response shape did not differ, whether the loop was closed (completely full of solution), or if the solution level was just above the top of the toroids in each arm of the loop. This suggested that the response, at least at low electrolyte concentrations, was impedimetric in nature, not magnetic; the latter would require a closed loop. The magnitude of the response actually decreased upon closing the loop. This fact suggested that loop closure changed the value of the impedimetric resistance and/or capacitance.

b. Direct Response Curves at the Toroidal Resonant Frequency. The nature of the direct response of this method was initially ascertained before differential techniques were considered. The response curves using EA-100 toroids are shown* for HCl, NaOH, and NaCl in Figure 28. The curves appear similar to those obtained with resistance measuring impedimeters (Section I D, Figure 9). During these experiments at constant resonance, it was noted that little or no retuning of the signal generator was required (<1% of initial frequency as compared to nearly 10% for the Immersion Method). Also, the particular toroidal resonant frequency was higher than that obtainable in the Immersion Method, a result of reducing the dielectric around the toroid windings from 78.3 for water to 1.0 for air. These observations were interpreted to mean that the Sidearm Apparatus had succeeded in affording a large degree of capacitive isolation between the toroids.

As further confirmation of the capacitive isolation, the Sargent Oscillometer, when connected to the toroids as in Section III B,

---

*The absolute mv readings may differ from one figure to another. This results from using different amounts of shielding; i.e. none, one, or both shields may have been grounded during a particular experiment; if insufficient output to the VTVM occurred even at full input voltage, one or more shields were ungrounded so that a readable output could be obtained.

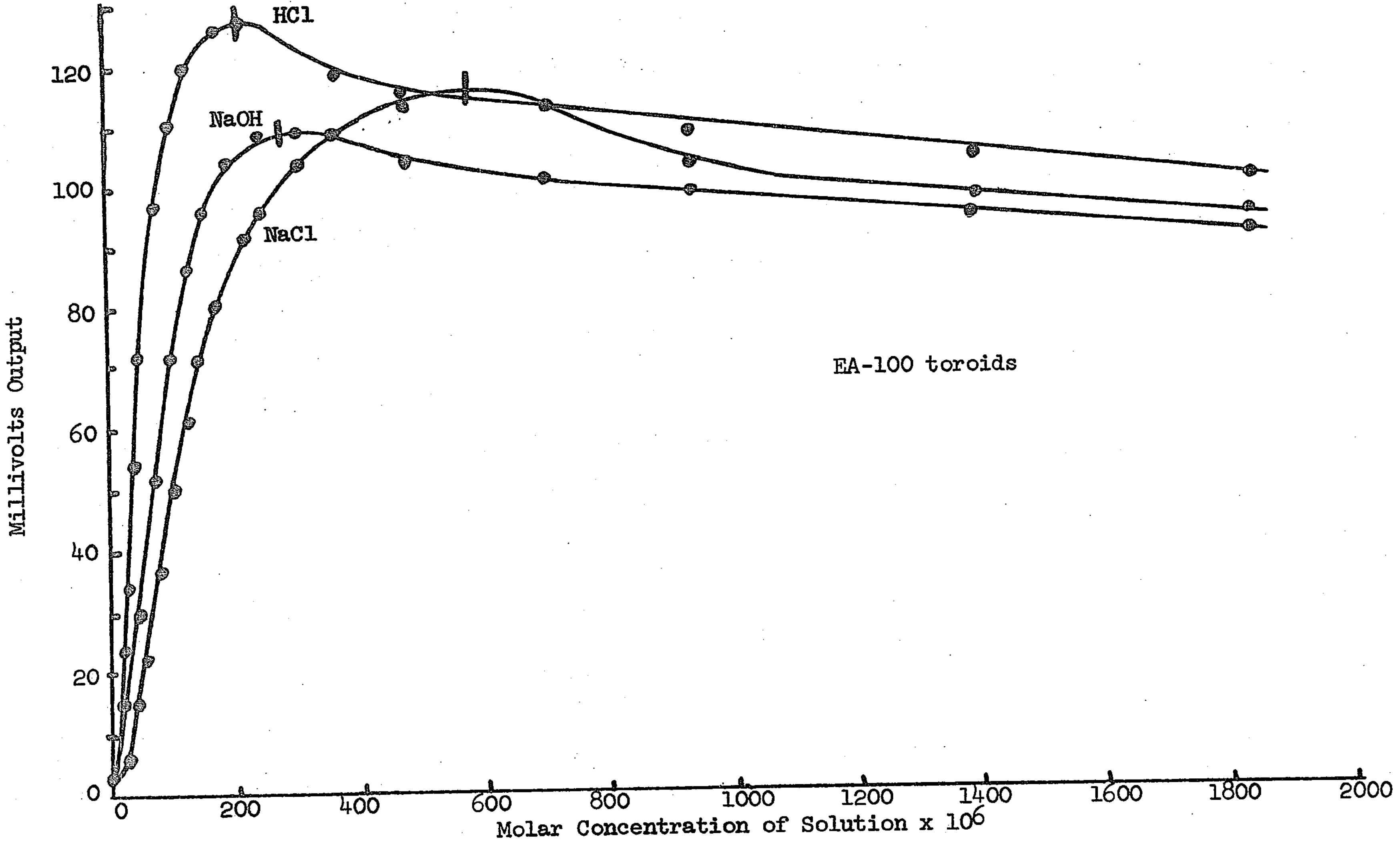

Figure 28. Sidearm Response Curves

showed extremely small changes in capacitance as the concentration of HCl in the loop was varied; it may be recalled that a large degree of capacitive coupling was found with the Immersion Method.

4. Further Evidence for the Impedimetric Nature of the Sidearm Response

a. Correlation of the Concentrations at the Response Curve Peaks with Low Frequency Conductance Values. The product of the solution concentration at the peak of each response curve (Figure 28) and the low frequency conductance at that concentration was a constant for the three electrolytes, in accord with impedimetric theory.[38]

b. Effect of Intertoroidal Distance Upon Response. Using EA-001 toroids, the response curve obtained using the conventional 18 cm toroidal separation of the Sidearm Apparatus was compared to that obtained when both toroids were on the same side of the loop, only 3 cm apart. According to impedimetric theory, the response peak should shift to higher concentration values with increasing separation. The results are plotted in Figure 29.

c. Effect of Frequency Upon Response. In accord with theory, if the operating frequency is increased, the peak of the response curve should also be shifted to higher values of electrolyte concentration. Confirmation of the linearity between frequency and concentration at the response peak, as stated in Section I D, is given in Table IV and Figure 30. The deviation of the data from linearity results from the imprecision of reading the concentration value at the broad response peak.

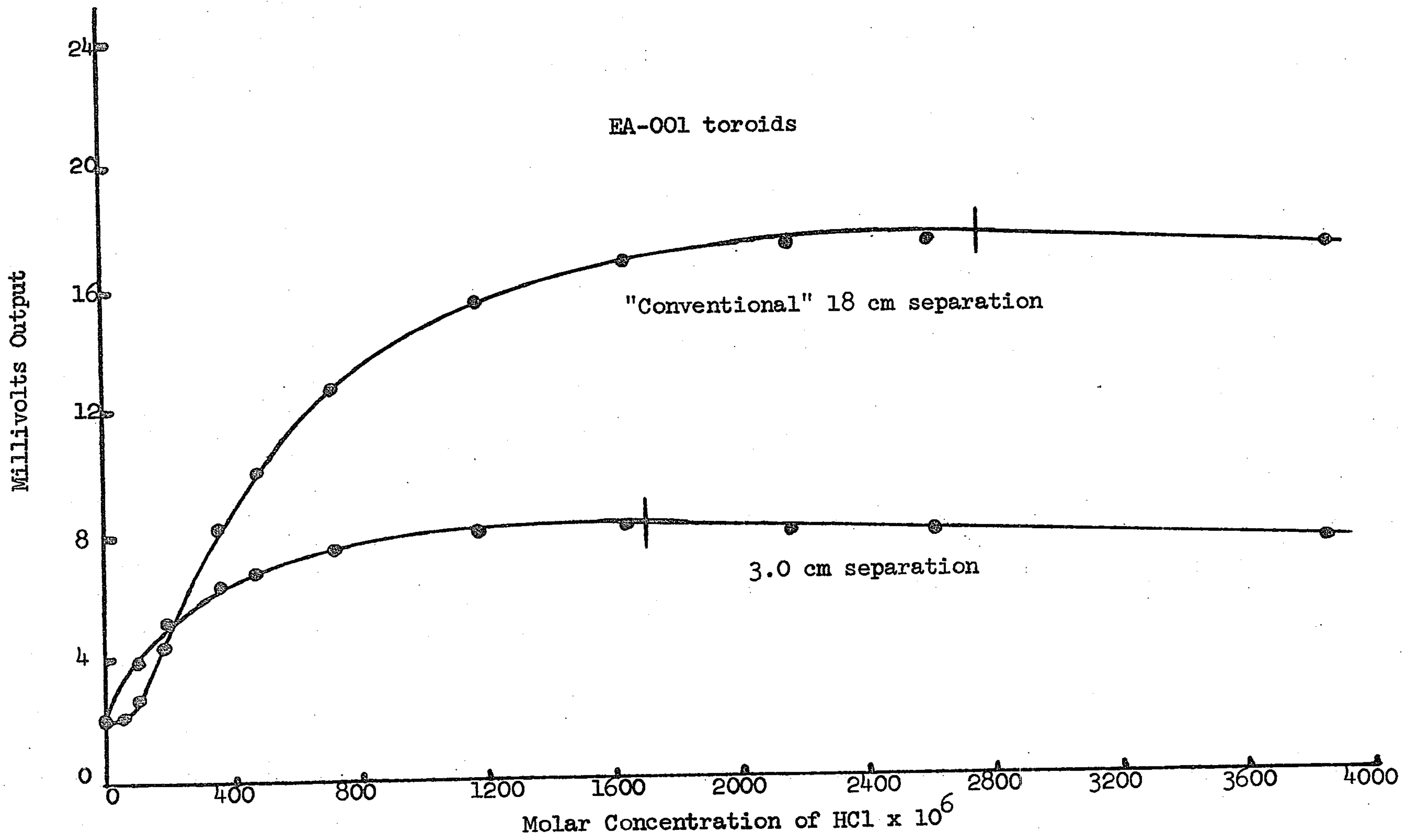

Figure 29. Effect of Intertoroidal Distance

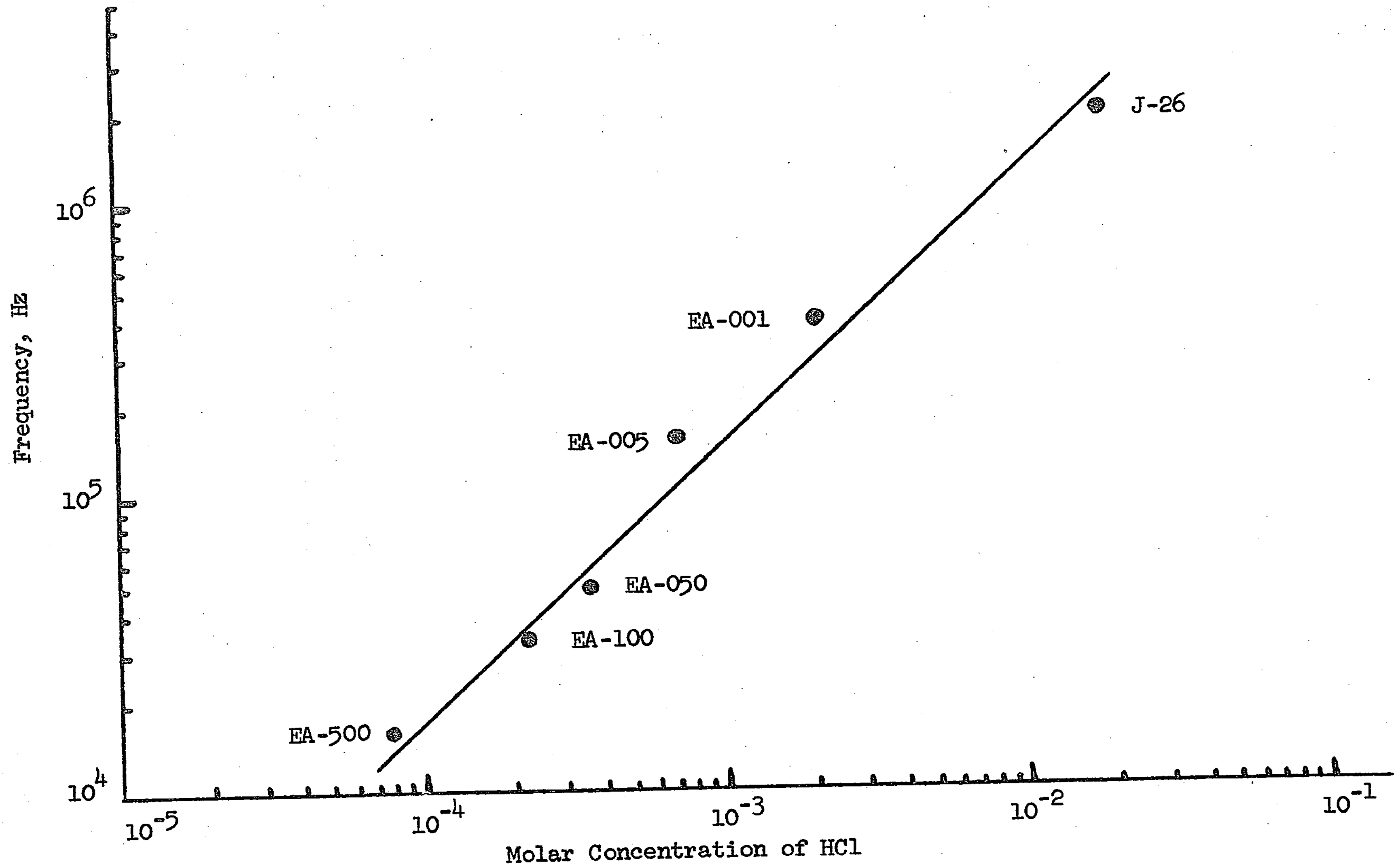

Figure 30. Effect of Frequency upon Concentration at Response Peak

TABLE IV

Concentration of HCl at the Response Curve Peak

Toroid	Frequency employed, kHz	Molar concentration of HCl at peak
EA-500	16	8.0×10^{-5}
EA-100	33	2.20×10^{-4}
EA-050	50	3.55×10^{-4}
EA-005	160	7.05×10^{-4}
EA-001	390	2.06×10^{-3}
J-26	2000	1.80×10^{-2}

5. Determination of Optimum Operating Frequency

The effect of operating the toroids at frequencies other than resonance was investigated in a manner identical to that reported in Section III B. With the Sidearm Apparatus it was found that a frequency 6 db low resulted in the greatest overall response sensitivity. The results are shown in Figure 31 for EA-001 toroids. In all future experiments reported in this section (III C), this frequency condition was used.

6. Concentration Ranges Obtainable with the Sidearm Apparatus

Using just three pairs of the toroids available, responses covering four orders of magnitude of HCl and NaCl concentration in overlapping ranges can be obtained. In general, the NaCl response peak occurs at a concentration approximately 3.5 times that of the HCl. The peaks, however, occur at the same values of low frequency specific conductance, as predicted by theory. Figure 32 shows the HCl concentration ranges obtainable with the toroids, and hence the versatility of the Sidearm Method.

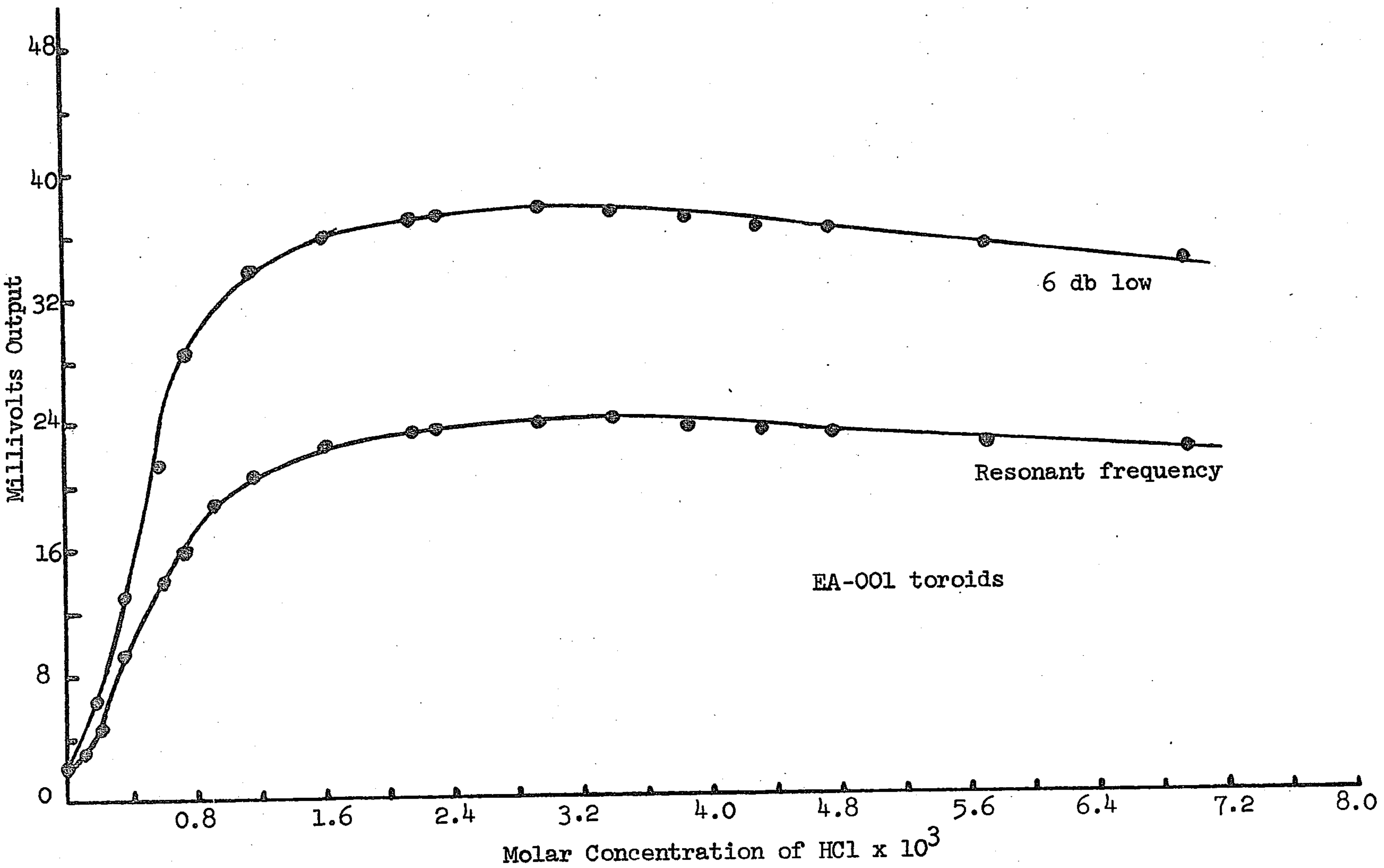

Figure 31. Determination of Optimum Operating Frequency

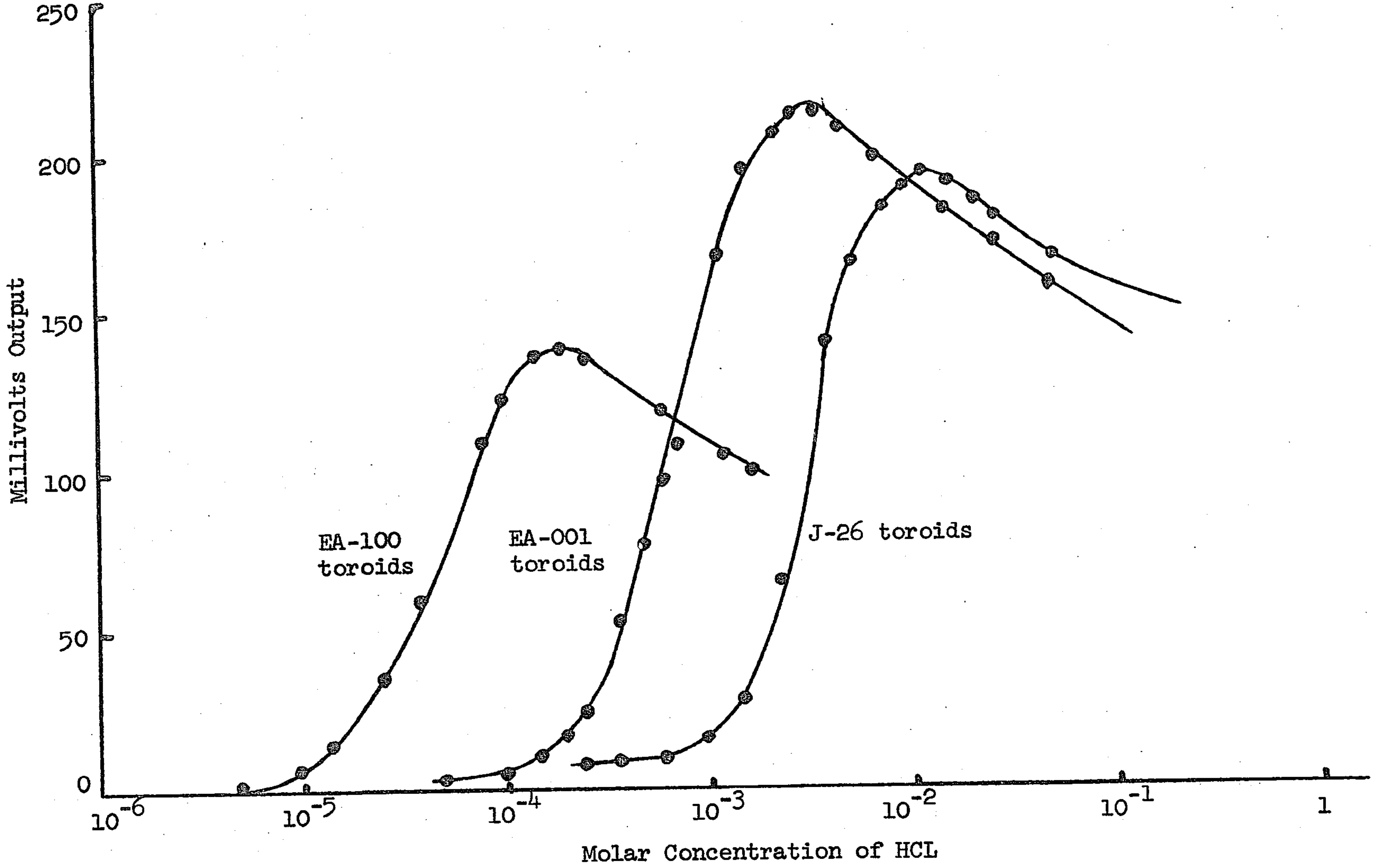

Figure 32. Concentration Ranges Obtainable with the Sidearm Method

As mentioned in Section III B, a conversion table for HCl concentration to low frequency specific conductance can be found in Appendix A.

7. Differential Techniques

a. Introduction and Procedure. The technique used with the Immersion Method (Section III B) was also employed with the Sidearm Apparatus, with but a single change. Only one null winding on each toroid was needed to bring the values of R and C required for a null into the range of the Heath Decade Boxes. Due to the high degree of isolation between the toroids, the FET amplifier was used before the VTVM so that a high null ratio (200:1) could be obtained.

b. Results Using the Differential Method. A separation of the direct Sidearm Method response into its resistive and capacitive components was achieved. The differential response using EA-001 toroids is shown in Figure 33. The reciprocals of resistance box readings (1/R) are also plotted. As before, the midpoint of the capacitive response occurs at the same concentration as the peak of the 1/R curve, which is in accord with impedimetric theory (Section I D).

8. Applications

An acid-base titration was performed using the differential technique. Although titrations can be performed on both sides of the 1/R peak, only the steep side to the left of the peak (Figure 33) was used. As before, titrations could also be performed using the values of null capacitance, but again these are omitted for brevity. Figure 34 shows the titration response using EA-001 toroids. The accurate

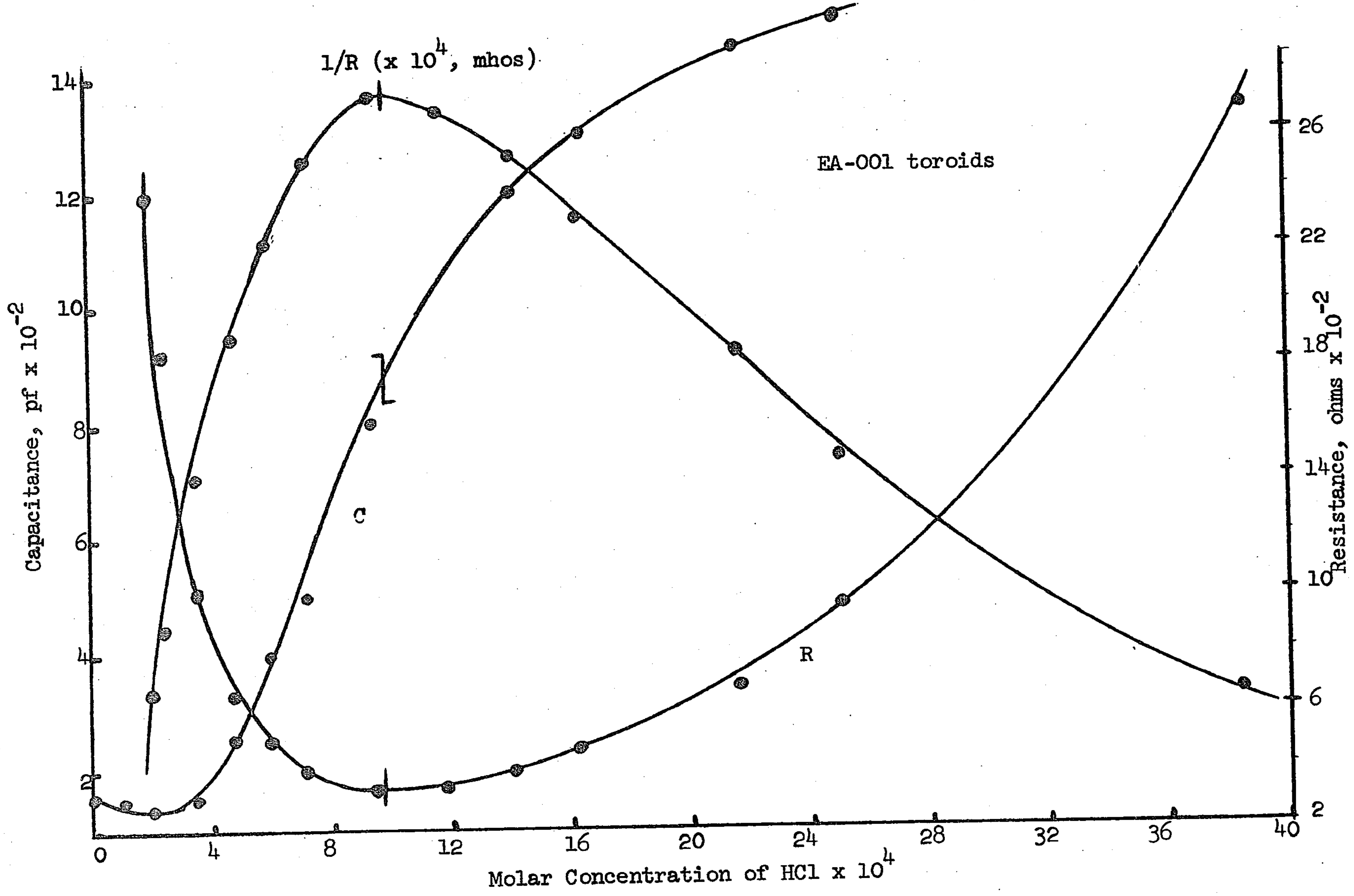

Figure 33. Differential Sidearm Response

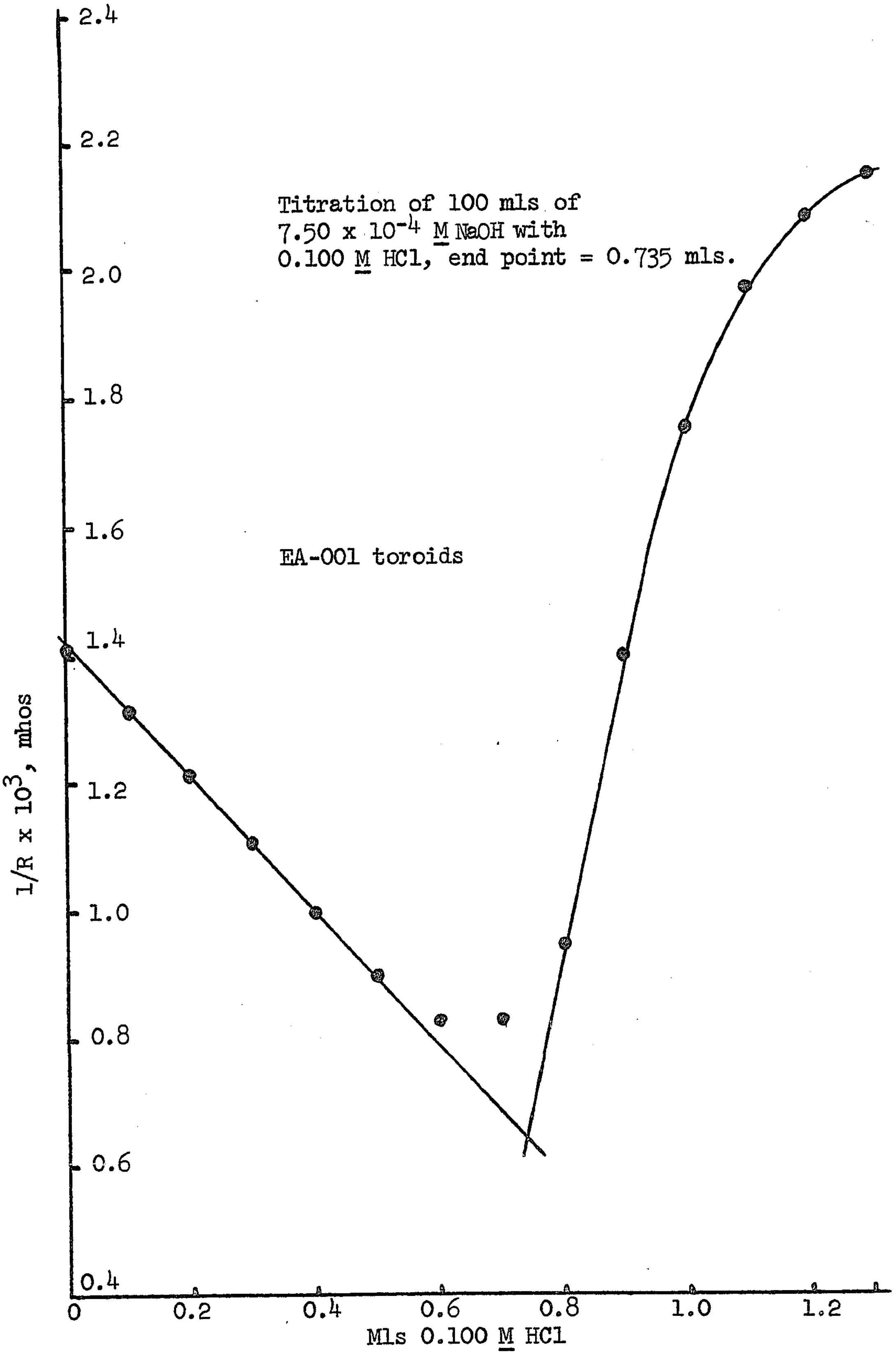

Figure 34. Acid-Base Titration

addition of small amounts of titrant was facilitated by the use of a Gilmont 2 ml micrometer syringe (Catalog No. 7844*).

Because of the excellent capacitive isolation between the toroids, dielectric constant measurements were not successful.

9. Magnetic Response at High Concentrations

a. Direct Response. Attempts to discover a magnetic response region at high HCl concentrations proved unsuccessful using the direct response mode.

b. Differential Response. Using the differential technique with EA-001 toroids, a second response region occurred beginning at 0.6 M HCl and continued to the highest concentration attempted (6 M HCl). The capacitance needed to secure a null remained nearly constant in this region, which suggested that the response obtained was predominantly magnetic in nature. This response is shown in Figure 35. The observed nonlinear response was due to the high concentrations of HCl used, i.e., the low frequency specific conductance is also not a linear function of HCl concentration.

If both the impedimetric and magnetic responses obtained by the differential method are plotted versus concentration, the total Side-arm Method response is obtained. This is shown in Figure 36 for the EA-001 toroids.

The total response curve is virtually identical to the measurements obtained by previous workers[16,17] using induction coil techniques. These authors reported that the responses obtained were due to the

---

*Cole-Parmer Co., Chicago, Illinois.

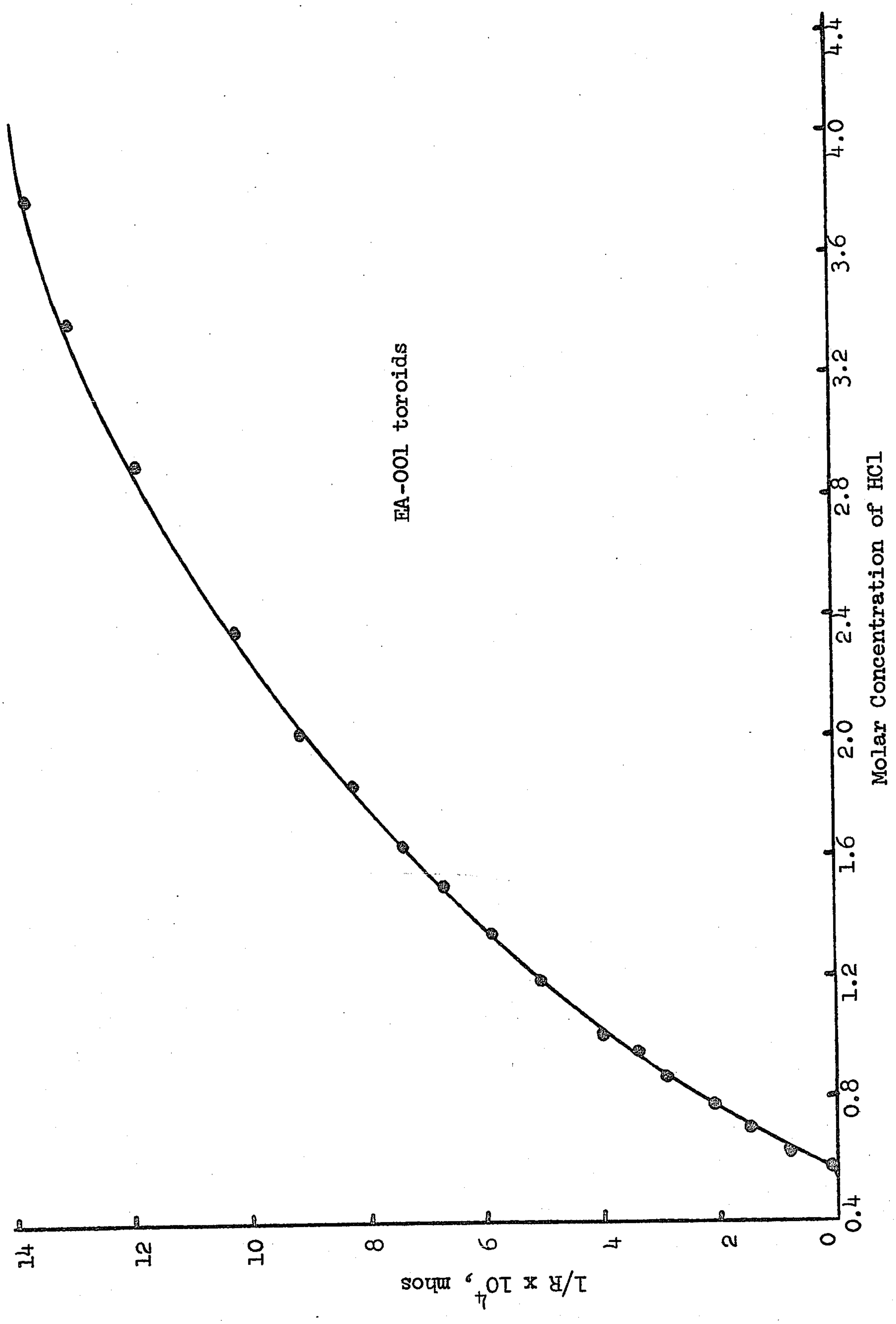

Figure 35. Sidearm Differential Magnetic Response

electromagnetic coupling between the two coils used in the measurement of the solution impedance.

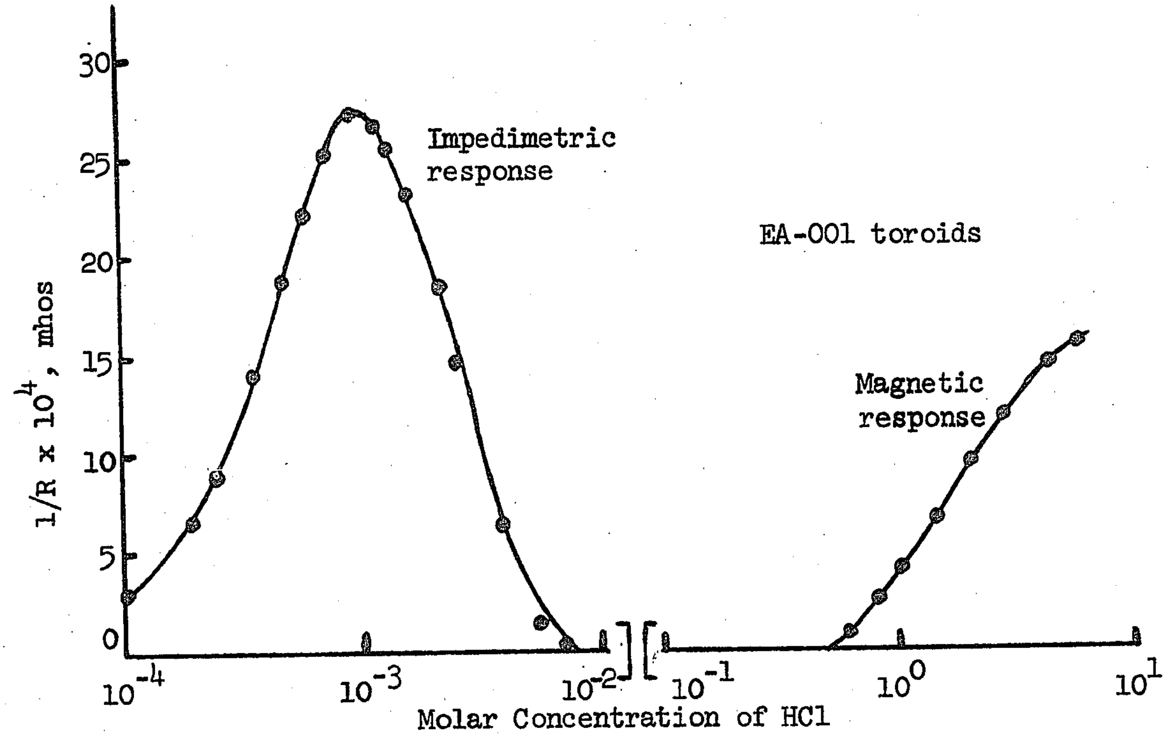

Figure 36. Total Differential Mode Sidearm Response

To further confirm the magnetic nature of the Sidearm response at high concentrations, the following experiment was performed. Aluminum foil shields were placed around the polyethylene tubing connectors upon which the toroids normally rested. (See Figure 13, Section II K). The toroids were then mounted as usual except that now the foil shield was between the toroid and the walls of the tubing loop. These extra shields were then grounded and the total response curve of Figure 36 was rerun. The impedimetric response was completely eliminated but the magnetic response remained. Thus, these extra shields had eliminated any capacitive (electrostatic) coupling with the solution, but had not substantially affected the magnetic response. This is the expected result of employing a Faraday shield.[5]

In order to obtain this magnetic response, it was found experimentally that the solution loop had to be closed; otherwise no measurable response at high concentrations could be obtained.

The magnetic response could not be extended to lower concentrations because of the physical limitations imposed by the toroids. A larger diameter solution loop is desirable to reduce the loop resistance for a given concentration, but the small inside diameters of the toroids themselves precluded using larger tubing with the Sidearm Apparatus. A new approach to the problem, rather than modification of the present apparatus was deemed necessary; the new approach is the subject of Section III D which follows.

10. Summary

Early experiments using the Sidearm Apparatus confirmed the excellent capacitive isolation between the two toroids. The response at low electrolyte concentrations was shown to be impedimetric in nature. For the same toroids, higher concentration levels could be reached with the Sidearm Method than with the Immersion Method, due to the long loop of small bore tubing used in construction of the loop. As mentioned before, the resistance of a conductor is directly proportional to its length and inversely proportional to its cross-sectional area; and for a given electrolyte concentration there is more resistance to the Sidearm loop then to the Immersion loop (which exists within the solution). The net effect of the Sidearm Method has been to change the cell constant, a change often used in impedimetric work[42,43] to permit work with highly conducting solutions.

---

[42] J. C. Clayton et al., Anal. Chim. Acta 14, 269 (1956).

[43] A. H. Collins, Analyst 87, 733 (1962).

It has been mentioned that the direct Sidearm response resembles an impedimetric 1/R response in shape. There is a resemblance, but as pointed out in Section I D, Figure 9, all impedimetric 1/R curves rise immediately upward from zero upon addition of even small amounts of electrolyte. Inspection of Figure 32 shows that this does not occur for the Sidearm Method. The actual response more closely resembles a capacitive sigmoid curve (Section I D, Figure 10) at the top of which a small 1/R type peak occurs. Thus the response obtained probably has a dual character; i.e., a 1/R type response occurring upon a basically capacitive type response; isolation of the toroids from the solution allows this 1/R type response to appear. This peak-shaped response was obtained in several configurations using toroids, and thus it is not a specific property of the Sidearm Method in itself.

As occurred in Section III B, a frequency 6 db low from the resonant frequency gave the highest system sensitivity.

Differential techniques proved equally applicable to this method, allowing a separation of the direct impedimetric response into its resistive and capacitive components. Using this technique, a simple acid-base titration was performed.

A magnetic response was finally discovered at high concentrations using the differential technique; evidence for the magnetic nature of the response was presented. The overall system response was shown to be extremely similar to the response curves obtained by others[16,17] who also used a pair of induction coils to sense changes in solution impedance.

D. Magnetic Induction Method

1. Introduction

a. Scope. It has been mentioned in Section I A that previously reported work using the Magnetic Induction Method of conductance measurement contains certain conflicting statements in regard to the effects of experimental variables upon the responses obtained. One of the main purposes of this study will be an attempt to resolve some of these conflicts. Attempts will also be made to extend the usable response range of the method to include solutions in the micromolar concentration range; work at these concentration levels has not been reported in the literature. These attempts will be described using data obtained from several magnetic induction probes which were constructed (Table III, Section II L, p. 34). Several chemical applications using these probes will be shown; titrations performed in the general areas of acid-base, compleximetric, precipitation and redox titrimetry will be described.

b. Review of Magnetic Induction Principles. In Section I B it was shown that for two closely spaced inductors,[3]

$$\bar{E}_{\text{induced}} = -M \frac{\Delta i}{\Delta t} , \qquad (3)$$

where $\bar{E}$ is the average voltage induced in the secondary, i is the current flowing in the primary, t is time, and M is the coefficient of mutual inductance, which is a function of the number of turns on each inductor. It is more convenient to express Equation 3 in the form,

$$E_s = MwI_p , \qquad (4)$$

where $w = 2\pi f$ (f = frequency in Hertz), I_p is the AC current flowing in the primary inductance coil, and E_s is the voltage induced in the secondary coil. Equation 4 predicts that the magnitude of the induced voltage will be directly proportional to the product of frequency, amperage, and the coefficient of mutual inductance M between the coils. The value of M can be optimized by winding a large number of turns on both coils and minimizing their separation from one another.

A convenient method of measuring M involves the use of Equation 4. By sending a known current of frequency f through the primary, and measuring the resulting induced secondary voltage, M can be calculated.[44]

c. Frequencies Employed in Previous Work. Only one publication describes the specific use of the resonant frequency of a set of toroids for conductance measurements. Johnson and Hart[29] state that "maximum energy transfer" occurs between toroidal inductors at this frequency. It was stated in Section I B concerning parallel resonant circuits that the least current flows in a parallel LCR network at resonance. Also, Equation 4 shows that the voltage induced in the secondary toroid is proportional to the current flowing in the primary toroid. It is therefore difficult to understand that these authors concluded that maximum system sensitivity occurred at the resonant frequency of their toroids, assuming (it is not stated in the article) that both toroids were operated as parallel LCR circuits.

A possible explanation may be that as the toroidal resonant frequency is approached, the increase in the frequency factor contribution (of Equation 4) more than offsets the decline of the primary toroidal current. Then too, it has been mentioned that the value of M increases near the self resonant frequency of the toroids.[35] Yet a third possible explanation concerns the lack of electrostatic shields around these authors' toroids. Capacitive coupling increases with increasing frequency (Section I B); hence, near the resonant frequency of their toroids more stray capacitive coupling may have given the appearance of an increase in inductive coupling. Since the authors used only a direct response technique, any energy coupling increase between the toroids might seem to result in greater system sensitivity.

---

[44] A. Campbell and E. C. Childs, "The Measurement of Inductance, Capacitance, and Frequency," Macmillan and Co. Ltd., London, 1935, p.203.

In the remaining publications to be considered, it is not known whether the toroids were operated at their self-resonant frequencies. Griffiths[23,24] and Calvert *et al.*[22] reported using frequencies in the range 1 to 50 kHz. The common statement concerning frequency found in all three of these papers is that it is important only in fixing the size of the magnetic measuring probe. However, Griffiths,[23] in a discussion section, reveals that the accuracy of the probe at 1 kHz is 0.5% while at 50 kHz the accuracy is better than 0.1%. The operating frequency of a probe was not investigated as a primary variable in the above mentioned articles.[22-24]

Lopatnikov[27] reports that the sensitivity of his probe is proportional to the *square* of the frequency used.

Lavagnino and Alby[25] report that for 15% solutions of NaCl in water, their results are independent of frequency from 0.5 to 10 kHz.

d. *Reported Lower Limits of Conductance Measurement by the Magnetic Induction Method*. At low electrolyte concentrations, the level of induced signal in the solution loop becomes very small, and a major problem is securing an adequate signal to noise ratio. A review of the literature reveals only one publication[31] which states the precision of measurements at a specified low value of conductance. The authors state that by using certain toroidal winding techniques (not explained), narrow band-pass filtering and high gain amplification, solution conductances of 10 x 10^{-6} mhos/cm can be measured with a precision of ± 2%; less precise results, they feel, can be made to 10^{-7} mhos/cm at reduced accuracy and precision. No data are presented.

Other authors report the lower limit of conductance measurements less precisely; DeRossi[28] finds the induction currents of his apparatus too small to measure below a certain undefined limit. Lopatnikov[27] offers that the quality of distilled water can be "estimated". Calvert _et_ _al_.[22] _suggest_ that loop impedances of 100 megohms can be measured, and that the accuracy of conductance measurements appears to be "better than 0.1% under the most unfavorable conditions".

2. Features of Magnetic Probe Design

In order to extend the magnetic response obtained with the Sidearm Apparatus to lower solution concentrations, the dipping probes described in Section II L (p. 32) were constructed. Several design features were considered especially desirable if success in measuring low solution conductivities was to be achieved.

The first decision was to incorporate the measuring toroids into the form of a dipping probe or probes rather than threading a glass loop of fixed dimensions through the toroids, as in the style of Gupta and coworkers.[21] It was thought that a more flexible and sensitive measuring system could be achieved in this way.

The toroids were constructed with copper or aluminum foil shields so that the measured response would indicate primarily the resistance of the solution; the probe, which is a simplified form of the transformer bridge of Calvert *et al.*,[22] responds to the total impedance of the solution loop if shields are not provided. Using shields, little or no capacitive balancing would be required in a differential measurement of solution conductance.

A further advantage of the probe type of design is that minimal toroidal separation is achieved; therefore the closed solution loop will provide the shortest possible path for the induced lines of magnetic flux; hence, the resistance of the loop will be small so that solutions of low conductance can be measured.

It is also desirable that the core diameter of the probe (dimension C in Table III, p. 34) be large, because the larger the diameter of the solution loop, the lower will be its resistance; again this facilitates the measurement of high resistance solutions.

3. Experimental Connections and Procedure

a. Electrical Connections for Direct Response Mode. The connections for any probe in Table III (p. 34) in a direct response mode of operation are identical to those reported for the Immersion Method, Section III B (p. 41). The probe shield lead and the negative (case) lead of the output VTVM were grounded to earth.

It was found that proper phasing of the toroids was helpful in securing the greatest response sensitivity (greatest output VTVM voltage change per unit conductance change). The primary and secondary leads of a particular probe were connected to signal generator and output

VTVM respectively; voltage was applied to the primary toroid and the VTVM reading noted. The toroid connections to the VTVM were then reversed and the VTVM reading again noted. Whichever connections gave the lower VTVM output as described above, gave the greatest response change per unit solution concentration change.

b. Electrical Connections for Differential Mode. The connections to signal generator and VTVM were made as above. One lead from each pair of differential windings was connected to the Heath Decade Resistance Box (see Figure 23); a small variable (trimmer) capacitor was wired in parallel with the decade box to compensate for capacitive leakage to the solution loop and between the toroids due to the imperfect shields. The two remaining differential leads were then connected together. If a null could not be secured using values of R and C, the connections of one pair of differential windings were reversed. A null could then be obtained.

After each concentration change the value of resistance on the decade box was changed to resecure a null on the VTVM. In general a change in trimmer capacitance was necessary only at high decade box resistance values (>10 kilohms). The reciprocals of these resistance values ($1/R$) were then plotted versus concentration (or solution conductance) changes to obtain a response curve.

c. The "Delta Millivolt" Differential Method. A simplified quasi-differential method was used on many occasions. After initially nulling the VTVM using the resistance box and trimmer capacitor, the voltage reading which occurred on the VTVM after each addition of electrolyte or titrant was recorded. A plot of these voltage readings (usually in the millivolt region) versus concentration gave response curves similar to those using 1/R values. The advantages of this method over the true differential method are many: the method is fast, since the operator need not vary resistance readings to regain a null reading; this method permits feeding a signal to a recorder from the meter output terminals of the VTVM and is therefore especially convenient for recording a titration using an automatic buret; in cases where the response of a probe at low solution concentrations is desired, less data scatter are obtained than with the resistance box null procedure. Although the linearity of this method depends upon the specifications of the VTVM, which for the Heath VTVM is ±5% of full scale, the linearity was never observed to deviate from 2%; finally, this method responds to the total impedance changes occurring in the solution, and as will be seen, produces a more linear response versus solution concentration than does the previously described differential method using the resistance box; this occurs because capacitive contributions to the total solution impedance appear as output changes on the VTVM. The use of this method, however, requires that the gain of all amplifiers used be very stable.

d. Miscellaneous Procedures.

i. Use of a Series Capacitor. It has been mentioned that the receiver toroid circuit was used as a parallel resonant circuit (naturally or with added parallel capacitance) to produce the highest voltage output to the VTVM. If the transmitter toroid circuit is made to be a series resonant circuit by addition of the correct series capacitor (for a given frequency) between toroid and signal generator, the maximum current obtainable from the signal generator can be made to flow in the primary toroid. This capacitor, whose value is equal to $1/4\pi^2f^2L_p$, where L_p is the primary inductance in henries, should be of the low leakage variety (mica or polystyrene) so that a high circuit Q is maintained and consequently maximum current can flow.

ii. Use of FET Amplifier. It was found necessary to employ the FET amplifier (Section II J, p. 29) when solutions of low conductance were analyzed. Since constructional details of amplifiers used in the literature[22-24,27,32] are lacking, the simple design previously described was built. Its use will be denoted as "FET".

iii. Temperature. Except for the temperature study experiment, all experiments were performed at ambient temperature. For periods of 1 hour the room temperature drift was normally less than 1°C.

iv. Method of Stirring. To eliminate the induction of signals into the probe by the spinning rotor of a magnetic stirrer, a Sargent Synchronous overhead stirrer* (Catalog No. S-76425) with propeller blade shaft was used.

v. Conductance Tables. In Appendix B a table providing conversions from KCl concentration to specific conductance is available. In Appendix C a similar table for low level NaCl solutions is presented.

4. Preliminary Investigations

As in Sections III B and C, direct response curves were first obtained before attempting differential techniques, in order to gain a qualitative insight into the method of using the probes.

a. Volume Effect. As a test of the effectiveness of the electrostatic shields of Probe A (Table III, p. 34) the following experiment was performed. At the resonant frequency of Probe A, 585 kHz, the VTVM reading was noted when the probe was 3/4 covered with water (core of probe just full of water); upon adding sufficient water to completely cover the probe, the corresponding VTVM reading changed only 0.6%.

---

*E. H. Sargent and Co., Chicago, Illinois.

b. Response to Dielectric Changes. Changing the dielectric constant of the medium from 78.3 for water to 20.7 for acetone resulted in a VTVM change of 0.8%. The response of the shielded probes should therefore depend almost entirely on resistance changes occurring in the solution.

c. Direct Response of Probe A. Response curves for Probe A at its resonant frequency were determined for solutions of HCl, NaOH, and NaCl, and are shown in Figure 37. Except for the lowest concentration values, the responses are linear.

d. Effect of Solution Loop Variables.

i. Effect of Core Volume on Response. The parameter most closely analogous to the cell constant used in low frequency conductance work is the volume of the "core" of the probe.[45] The core is a cylinder whose diameter and height are dimensions C and A respectively in Table III, Section II L (p. 34).

The response of Probe A to core volume changes was investigated to verify the above statement. Two responses were obtained, one using the inherent core volume of Probe A and a second one after a glass plug had been inserted in the core to reduce its volume. The results are shown in Figure 38.

---

[45] R. Rosenthal (ed.), "Solution Conductivity Handbook," Beckman Instrument Bulletin 4090, 1969, p. 8.

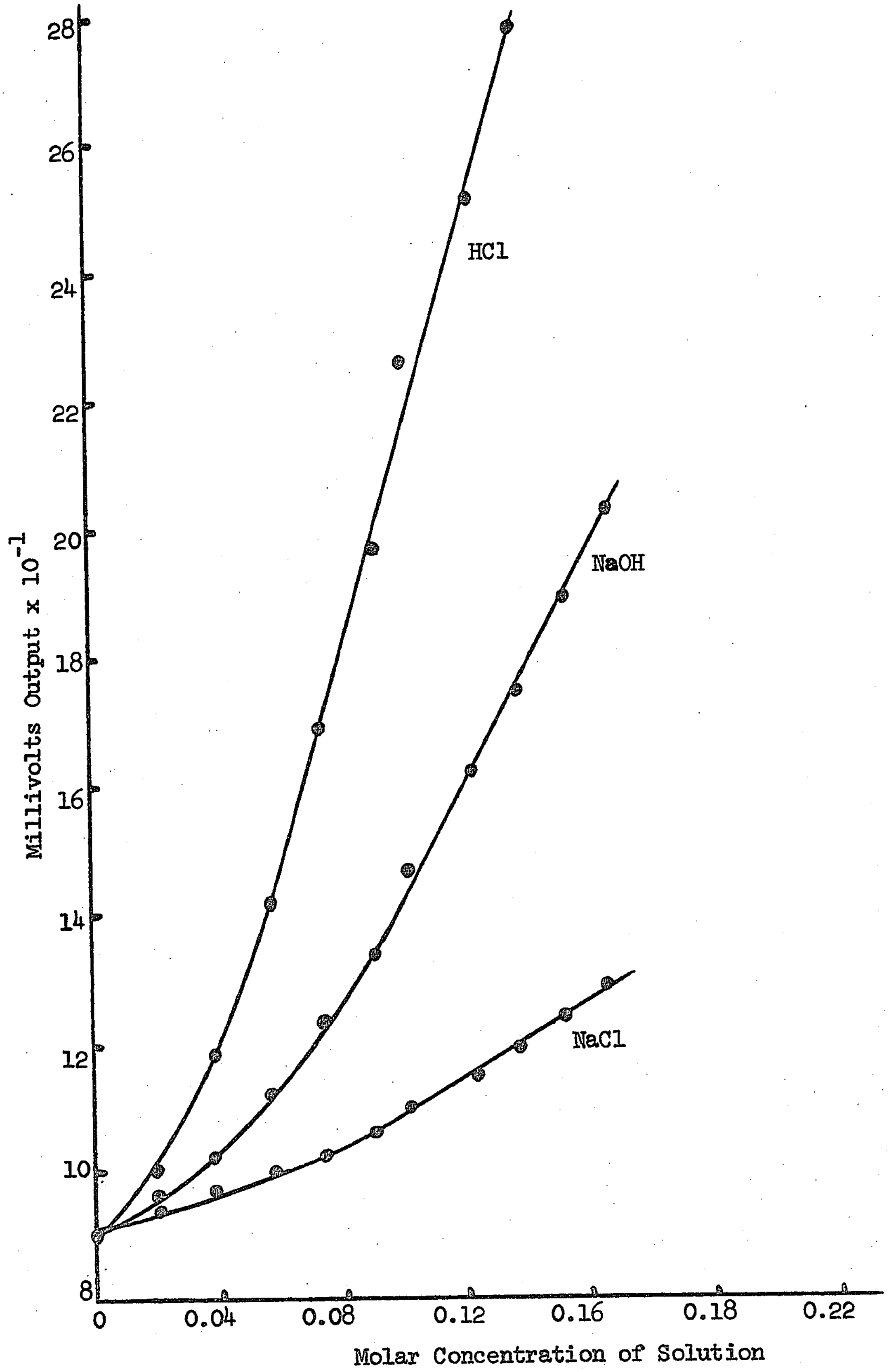

Figure 37. Direct Response of Probe A

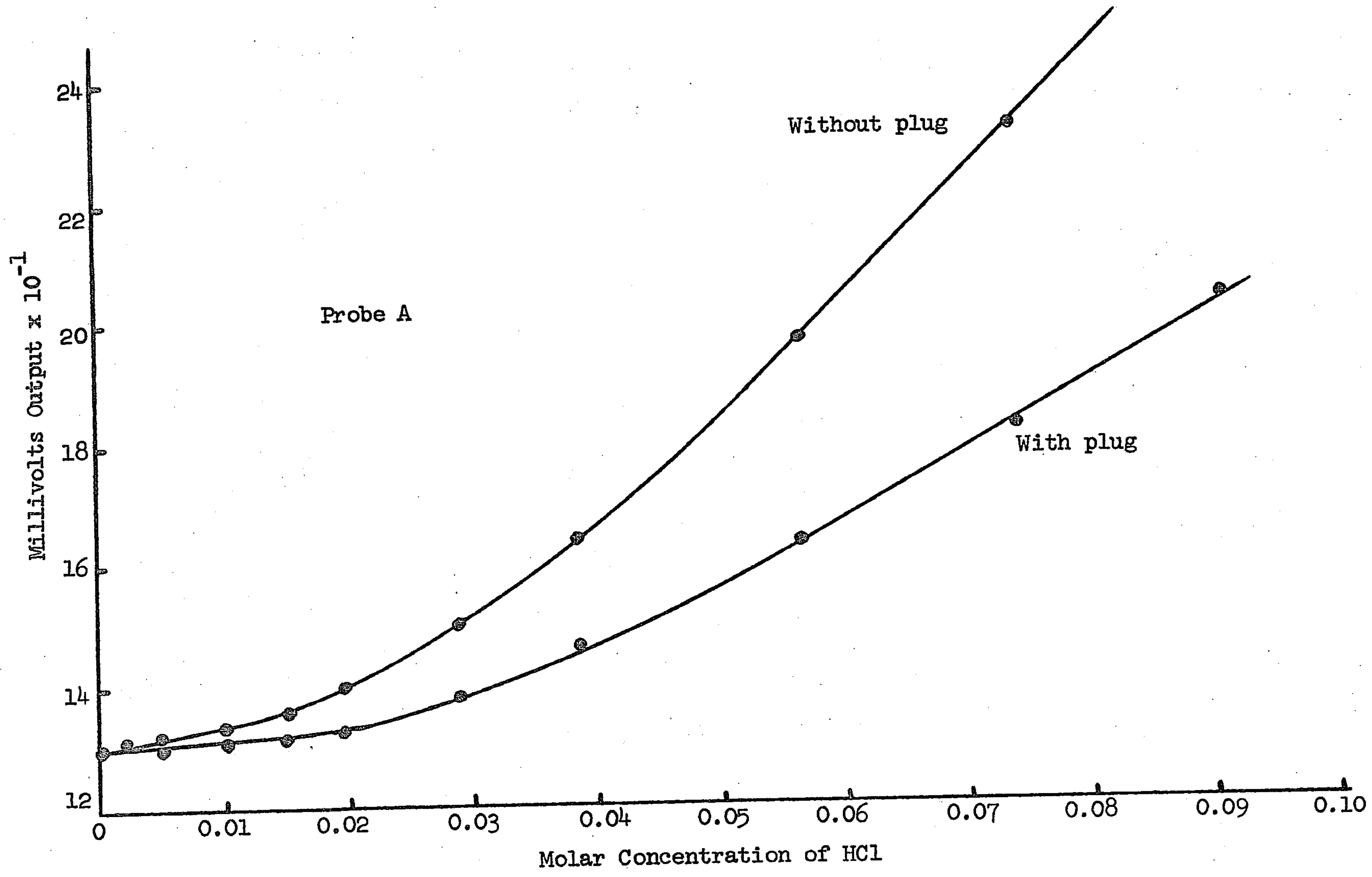

Figure 38. Effect of Varying Core Volume

Using the equation for the volume of a cylinder, the inherent volume of Probe A was calculated to be 1950 cubic mm, whereas with the plug inserted, the volume was 1625 cubic mm. The ratio of these core volumes is 1.21:1. If the slopes for the linear regions of the two responses in Figure 38 are computed, the ratio of the slopes is 1.29:1. These two ratios differ by only 6.4%, suggesting that the effective cell constant of a probe (provided the magnetic flux lines in the solution remain unchanged) is governed largely by its core volume.

ii. Effect of Container Width Upon Response. Calvert et al.[22] have suggested that the magnetic lines of flux in solution are so numerous that they constitute a virtual "short-circuit" around the outside of the probe if the solution container width is large compared to the width of the probe. Thus the cell constant effect should be governed largely by the core volume, as was noted above.

The effect of small container widths on probe response was ascertained using a probe (developed at a later time) of physical dimensions and electrical characteristics nearly identical to Probe A. Two beakers were used whose internal diameters were 54 and 46 mm. The two responses of the probe are shown in Figure 39. The wider beaker resulted in a slightly greater probe sensitivity as measured by the slopes of the lines. This is evidence of the "short-circuit" concept of the solution flux lines, for when the beaker width increased by 16% the response increased but 3.6%.

It is evident then that for large containers, the probe response is essentially unaffected by its placement in the container. However,

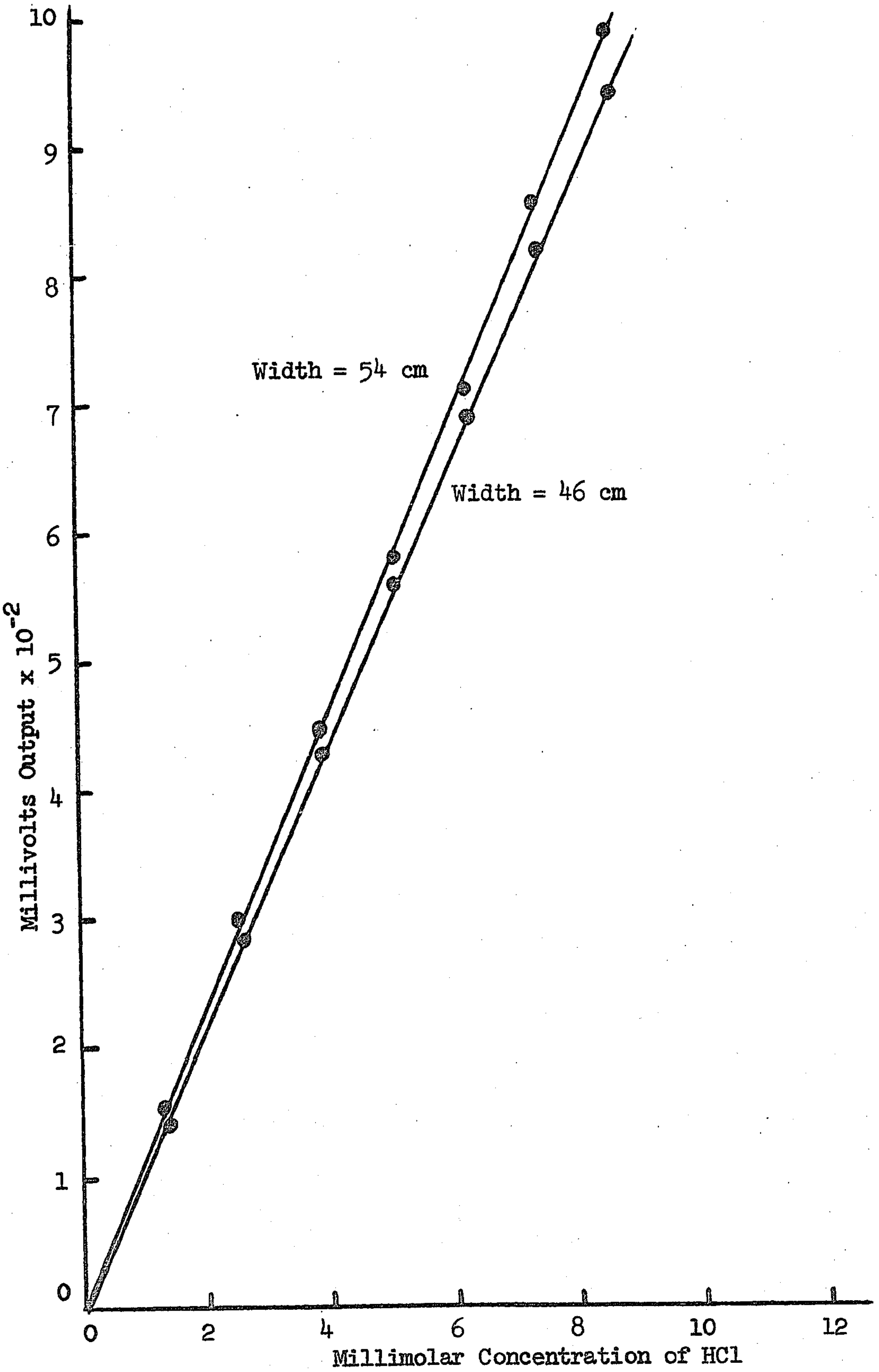

Figure 39. Effect of Container Width upon Response

for small containers, the position of the probe relative to the container must remain unchanged if reproducible results are to be obtained.

iii. Effect of Intertoroidal Distance. Using Probes B (p. 34) the effect of increasing the distance between the two toroids was investigated. As the separation was increased, the output voltage decreased, which was the expected result of lengthening the solution loop and hence increasing its resistance. However, these probes gave the undesirable type of response shown in Figure 40. With the first few additions of electrolyte, the response decreased to a minimum value before rising again to give a linear response as in Figure 37. Thus, certain VTVM readings might correspond to one of two possible concentration values.

Attempts to eliminate this double-valued response by changing the applied frequency were unsuccessful. Another pair of shielded toroids also was tried but gave the same type of response. Whenever there was an intertoroidal separation of any kind this same response occurred. This response could even be obtained on Probes A and D at certain frequencies. The effect was thought to be an anomalous capacitive effect due to the imperfect nature of the electrostatic shields, but it was not investigated further.

All subsequent probes were therefore built with the toroids close together (1 mm) in a single probe. A variation in "cell constant", if desired, could best be achieved by changing the core volume of the probe, rather than the intertoroidal distance.

5. Effect of Varying Frequency, Amperage, and Turns Ratio Upon Response

The purpose of this section is to provide confirmation that the probes which were constructed indeed obey the laws of magnetic induction

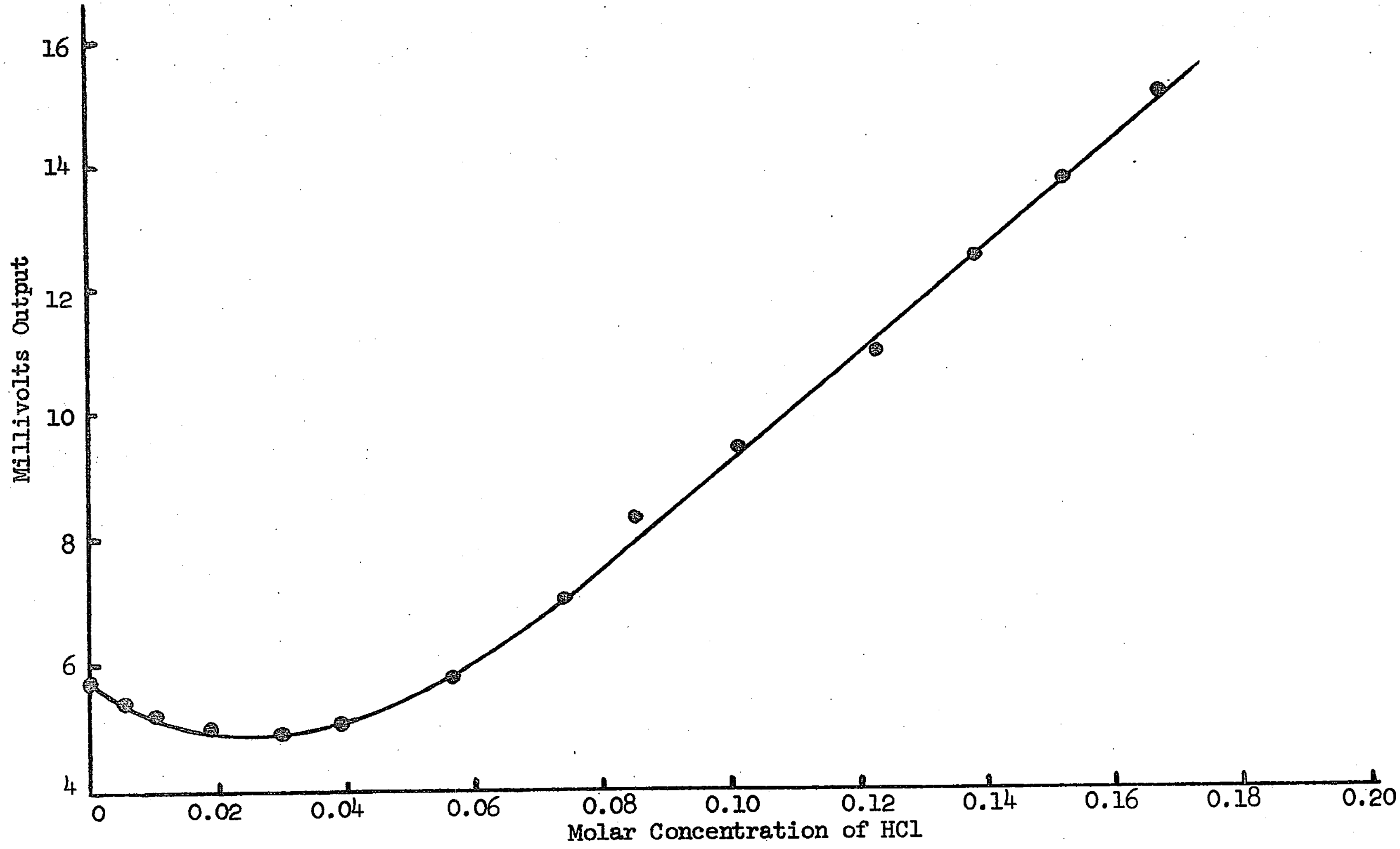

Figure 40. Response of Probes B at 1 cm Separation

as expressed by Equations 3 and 4. For these studies Probe D was used. It is identical to Probe A both electrically and in physical dimensions. The only difference is that null windings have been added so that the "Delta mv" differential technique could be employed.

a. Effect of Varying Amperage at Constant Frequency. Using the Delta mv method, the output of Probe D was measured at a frequency of 110 kHz and differing values of transmitter toroid current. Equation 4 predicts an increased output from the probe for an increase in current. The results are shown in Figure 41. The applied currents are in the ratio of 3.74:1.84:1 and the response slopes are in the ratio of 3.90:1.84:1, showing that the probe response sensitivity is a direct (1:1) function of the applied amperage.

b. Effect of Varying Frequency at Constant Amperage. Again using the Delta mv method and Probe D, the effect upon response sensitivity was recorded for three frequencies while maintaining the same transmitter toroid current (12.8 ma). The results appear in Figure 42. The frequencies used are in the the ratio of 2.82:1.77:1 while the response slopes are in the ratio of 4.40:2.18:1. It can be seen from these ratios that the response sensitivity increases in a nonlinear fashion as the frequency approaches the toroidal resonant frequency of 585 kHz.

c. Effect of Turns Ratio. For a given input current and frequency, the outputs of two probes, C and D, were compared to determine what effect an increase in the number of turns on the receiver toroid might have. Probe C is essentially identical to Probe D except that Probe C has twice the number of turns on the

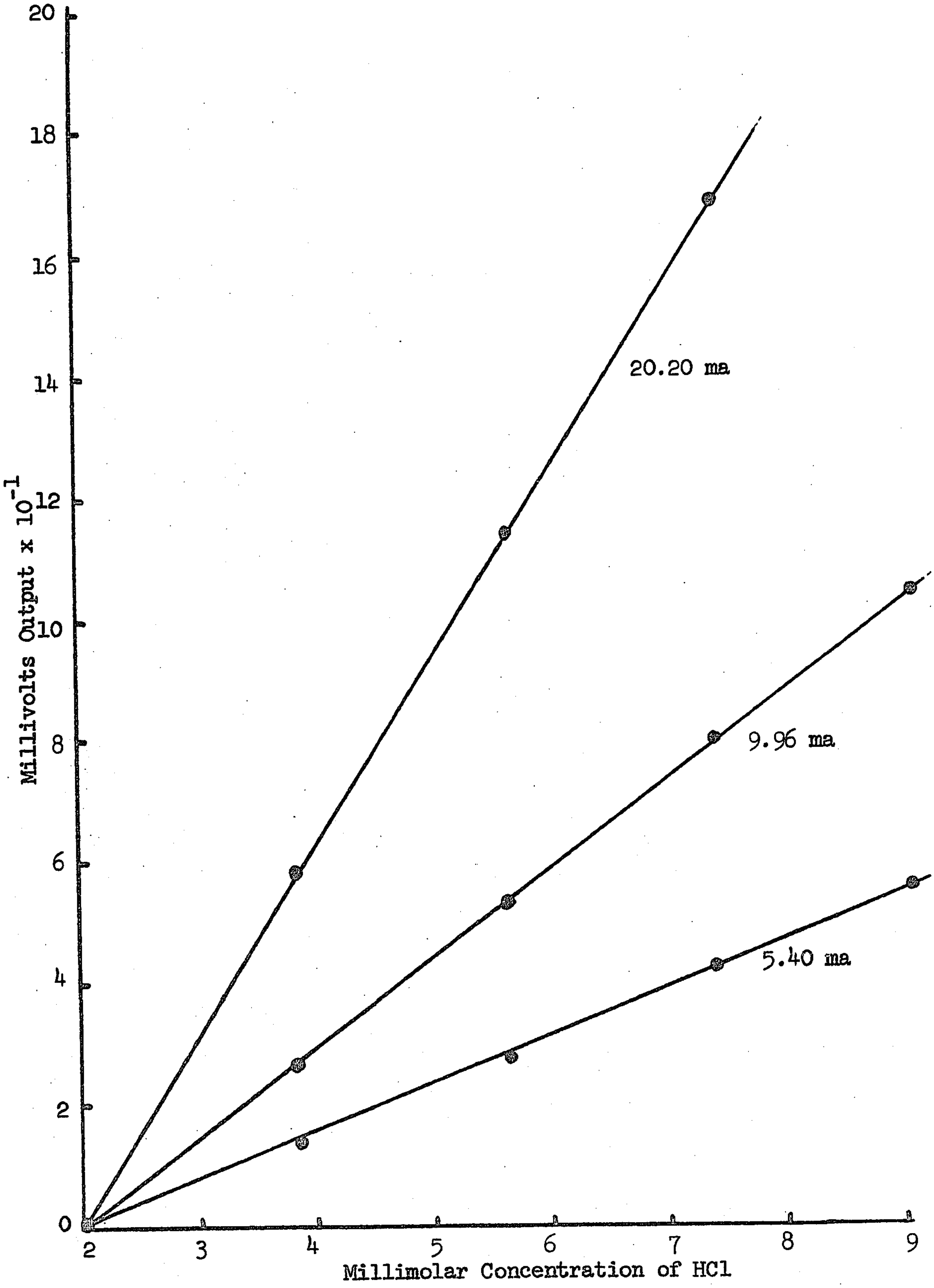

Figure 41. Effect of Varying Amperage at Constant Frequency

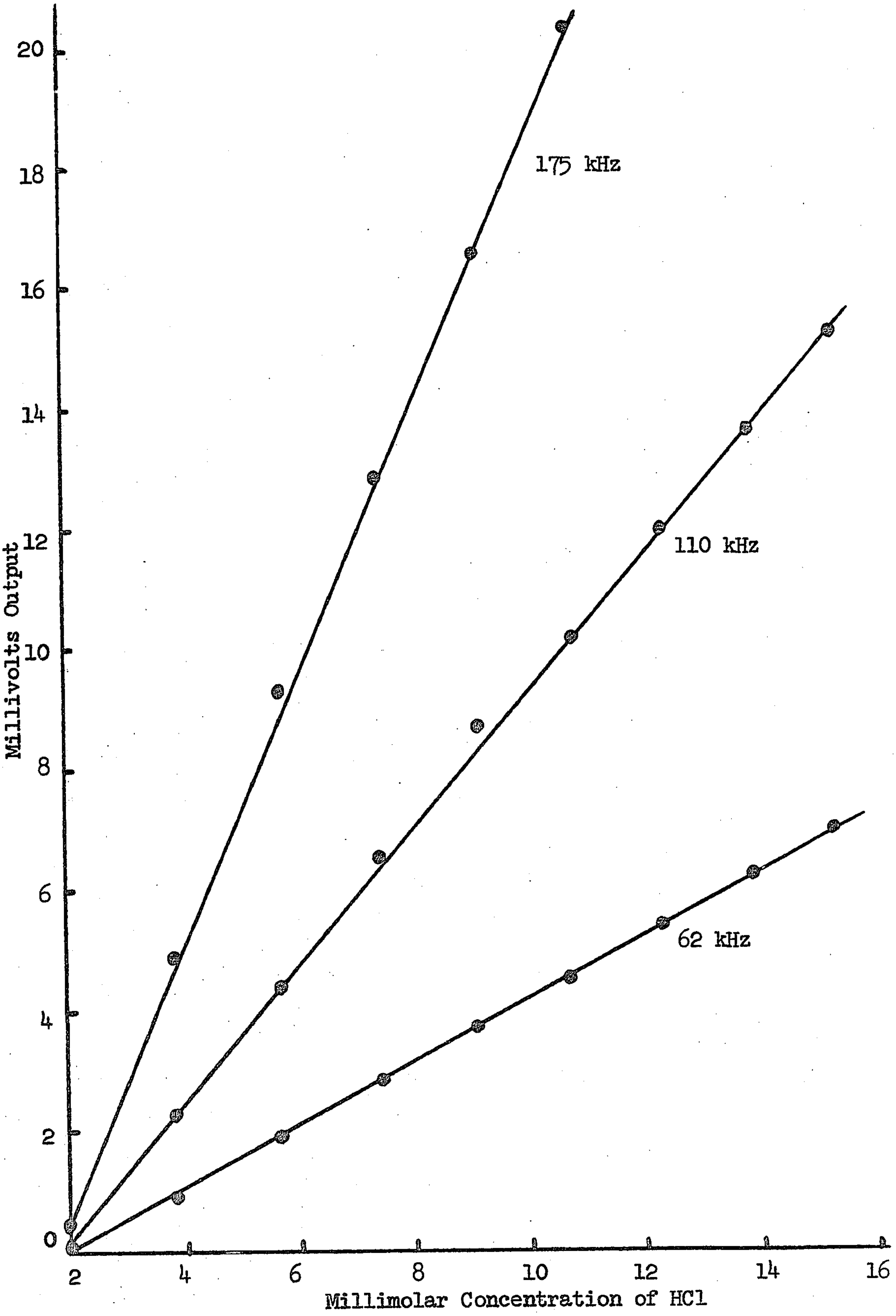

Figure 42. Effect of Varying Frequency at Constant Amperage

output toroid. The responses are shown in Figure 43 for a frequency of 110 kHz and an applied current of 16.6 ma. As predicted by Equation 4, the output of Probe C is larger. It has been stated that M, the coefficient of mutual inductance, increases with an increasing number of toroid windings. The maximum value of M possible[46] is equal to $(L_p \cdot L_s)^{1/2}$, where L_p and L_s are the inductances of primary and secondary coils. This value is only possible if every flux line from the primary coil passes through the secondary coil. For these probes, this is clearly not possible, since flux lines are undoubtedly lost in the solution loop.

Using the above equation for M, and the inductance values from Table III (p. 34, Section II), an increase in the value of M from 1 to 1.69 mh is theoretically possible when changing from Probe D to Probe C. The possible ratio for changes in M for the two probes is 1.69:1, while the experimental ratio of the slopes of Figure 43 is 1.16:1. This indicates that although the output voltage of the probe does not vary linearly with M, an increase in the secondary to primary turns ratio does increase the "voltage sensitivity" of these probes.

d. Conclusions. It is evident that these probes follow the predictions of Equations 3 and 4 concerning the laws of magnetic induction. The response sensitivity has been found to be a function of the following variables: core volume, container width, frequency, amperage, turns ratio, and the value of loop resistance being measured.

---

[46] A. Schure, "Transformers," J. F. Rider Publisher, Inc., New York, 1961, p. 19.

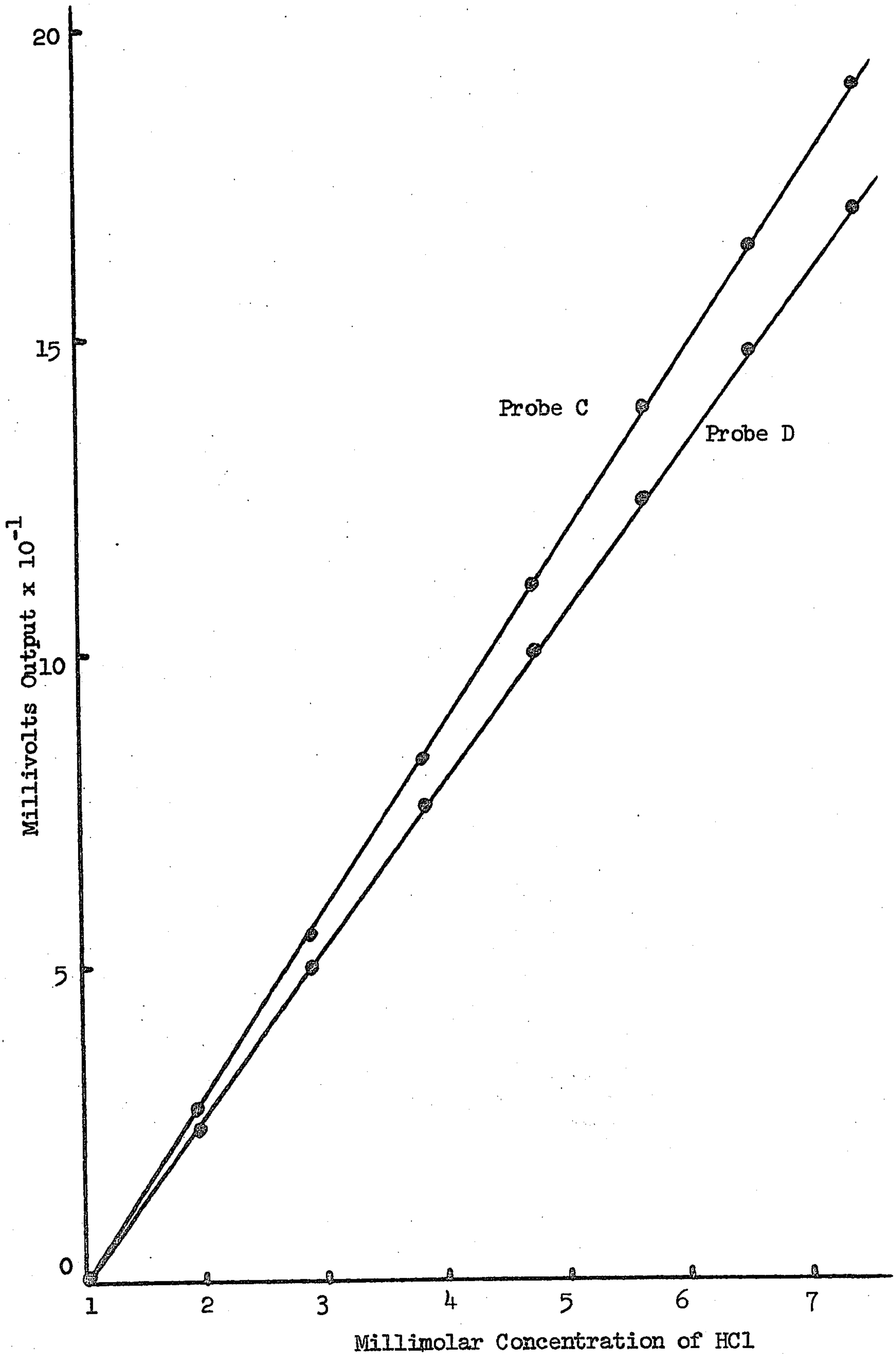

Figure 43. Effect of Turns Ratio upon Voltage Sensitivity

In general, these variables do not act independently of one another. For example, if an attempt is made to increase probe sensitivity by increasing the resonant frequency, one must decrease the number of windings per toroid (to decrease its inductance). But then M which is equal to $(L_pL_s)^{1/2}$ will decrease. Also, by increasing the frequency, the upper usable limit of the core material may be exceeded, thus increasing core losses. At the same time losses through stray capacitances increase at higher operating frequencies.

Clearly then, the interrelation of the variables governing probe sensitivity is complex. However, a method has been devised which enables one to optimize the operating conditions of a given probe in order to secure maximum response sensitivity.

6. Determination of Optimum Conditions for Probe Operation

It has been shown that the output voltage to the VTVM from the receiver toroid depends on the product of the applied frequency, the amperage flowing in the transmitter toroid circuit, and the turns ratio of the two toroids. The output voltage, E_s, per unit change in loop conductance (or per unit change in solution concentration) has served as a convenient sensitivity factor.

From the principles of parallel resonant circuits, as the self-resonant frequency of an inductor is approached, the flow of inductive current greatly decreases. Thus, maximum current does not flow at the self-resonant frequency (the highest upper usable limit of an inductor). It was anticipated, then, that at some frequency lower than resonance, conditions would exist for a given probe where the maximum i·f product (amperage times frequency) could be obtained. From Equation 4 this condition should produce the highest output voltage. In addition, this maximum i·f value, experimentally determined, automatically accounts for many other variables[1,46] such as coil Q, DC and AC winding resistance, core losses, distributed capacitance losses, shield leakage, and the coupling coefficient M.

a. Determination of i·f Maximum for Probe A. The AC current flowing into the transmitter toroid was measured from 20 kHz to 700 kHz for Probe A. Figure 44 shows a plot of the i·f product versus frequency. The frequency at the i·f maximum is 117.5 kHz. Using the formula for inductive reactance, $X_L = 2\pi fL$, and L = 0.9 mh, the reactance is calculated to be 665 ohms. The nominal output impedance of the signal generator at all frequencies is 600 ohms ± 10%. Thus the signal generator is delivering maximum energy to the transmitter toroid when the impedance of the transmitter toroid is equal to the output impedance of the generator. This is in accord with electronic theory.[1,2]

The prediction of this i·f study was then tested. Four different frequencies, above and below 117.5 kHz, were applied to the transmitter toroid; a variable capacitor was placed on the VTVM input to retune the receiver toroid to resonance at each frequency. The results for Probe A are shown in Figure 45. As predicted, the response sensitivity of Probe A is greatest at a frequency near the i·f maximum.

b. Determination of the i·f Product for Probe D. To facilitate future measurements using the Delta Millivolt method, Probe A was rebuilt with null windings and was renamed Probe D.

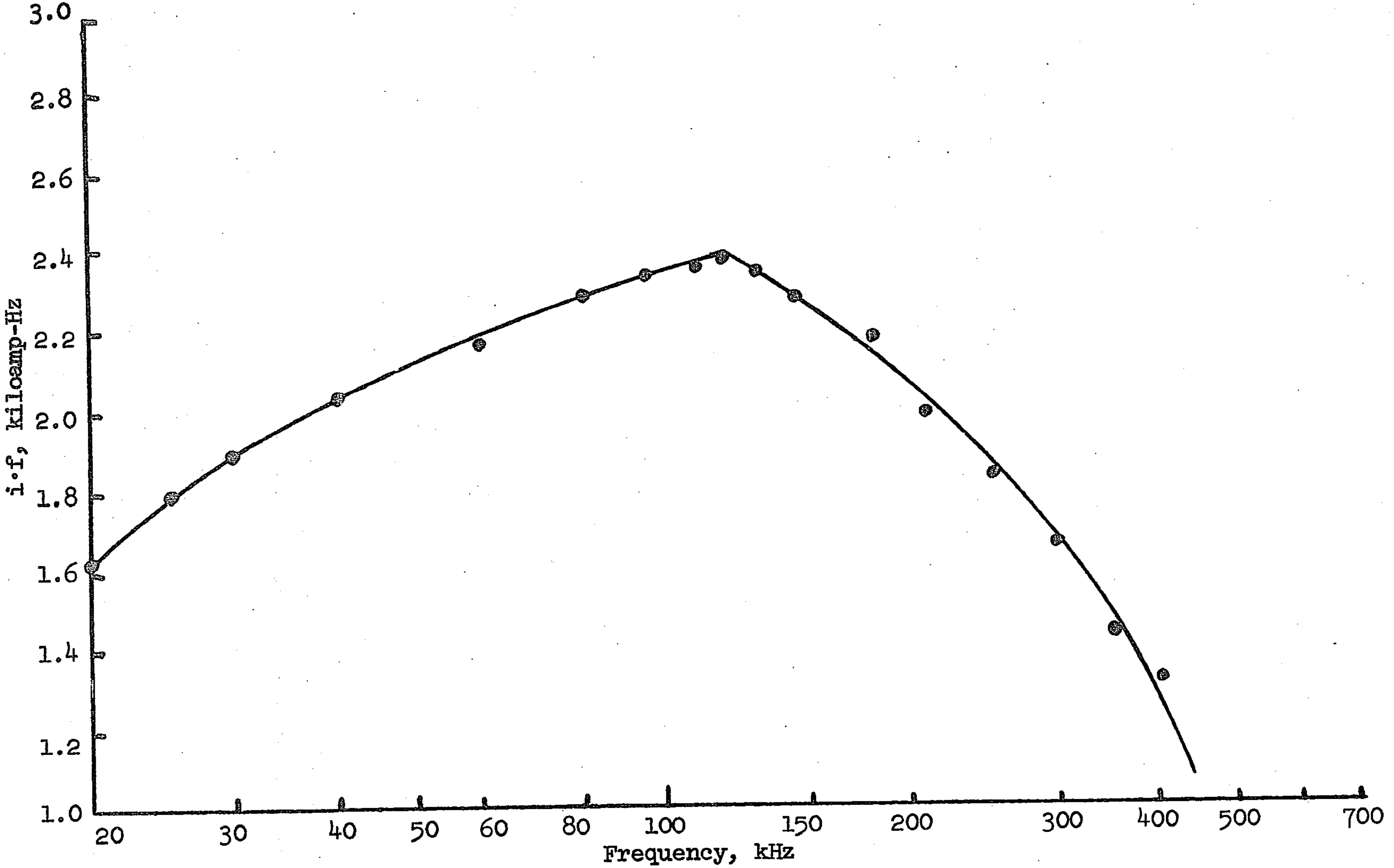

Figure 44. i·f Product Study of Probe A

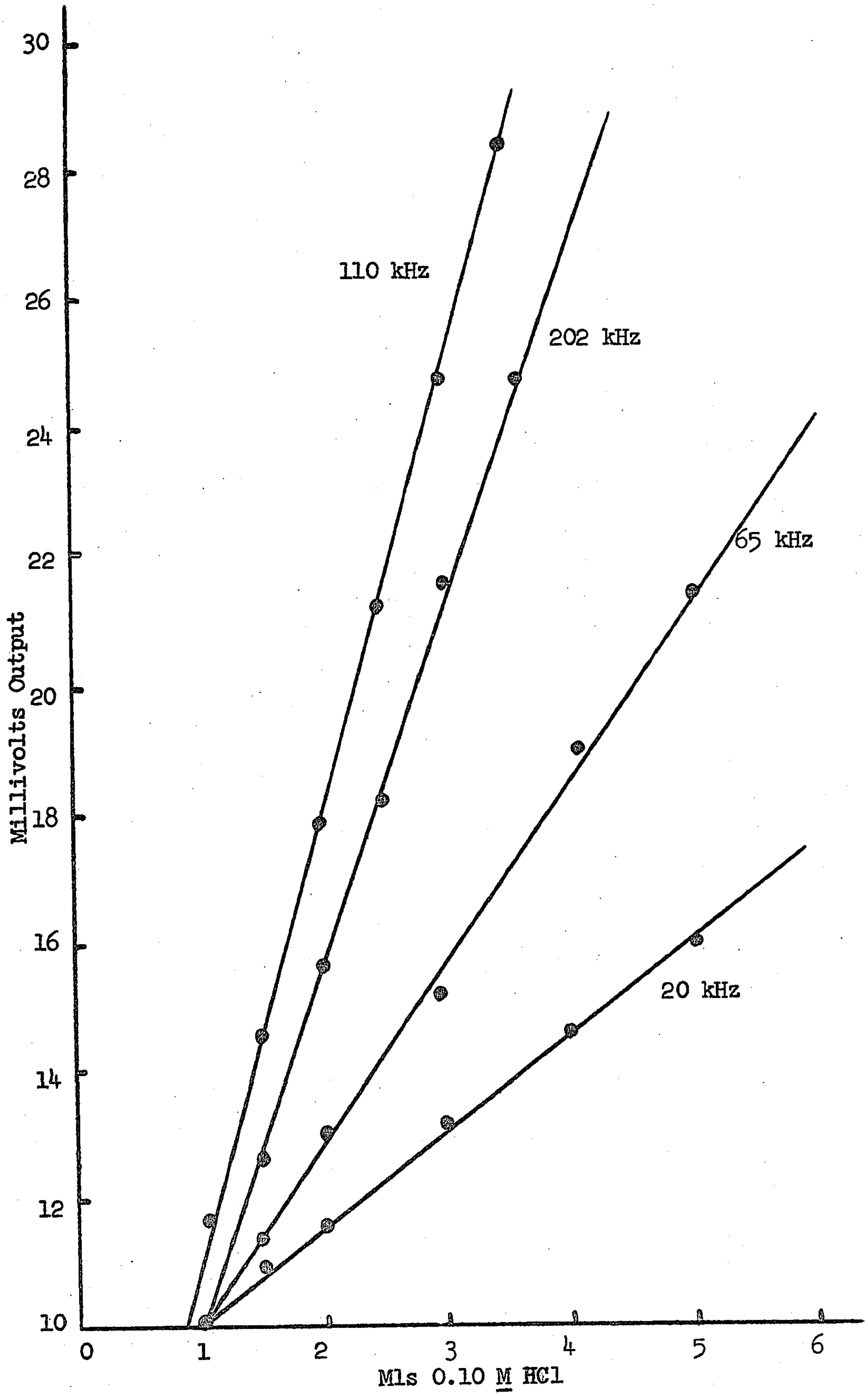

Figure 45. Response Sensitivity of Probe A

A new i·f product study using the Delta mv method was made with Probe D using a series capacitor between the transmitter toroid and the signal generator. Ideally most of the inductive reactance of the toroid could be cancelled with the capacitor; higher values of primary current would then be obtainable. The results are shown in Table V.

TABLE V

i·f Product Constants for Probe D (Series Capacitor)

f, kHz	ma, across 0.783 ohms	i·f, kiloamp-Hz
135	21.4	3.7
200	18.0	4.6
220	42.0	11.8
255	38.0	12.4
304	31.0	12.0
334	30.0	12.8 (max)
360	27.0	12.4
440	18.6	10.5

The i·f product is a maximum at 334 kHz, which is a frequency higher than could be obtained without using a series input capacitor (117.5 kHz). Also, the use of a series input capacitor has increased the i·f value from 2.37 kiloamp-Hz (Probe A, no series capacitor) to 12.8 kiloamp-Hz. Confirmation of the resultant increase in sensitivity of response is shown in Figure 46. As before, a small variable capacitor was placed across the VTVM to retune the receiver toroid to parallel resonance at each frequency. All further experiments in this section will have the receiver toroid operating at resonance for the particular frequency applied to the transmitter toroid.

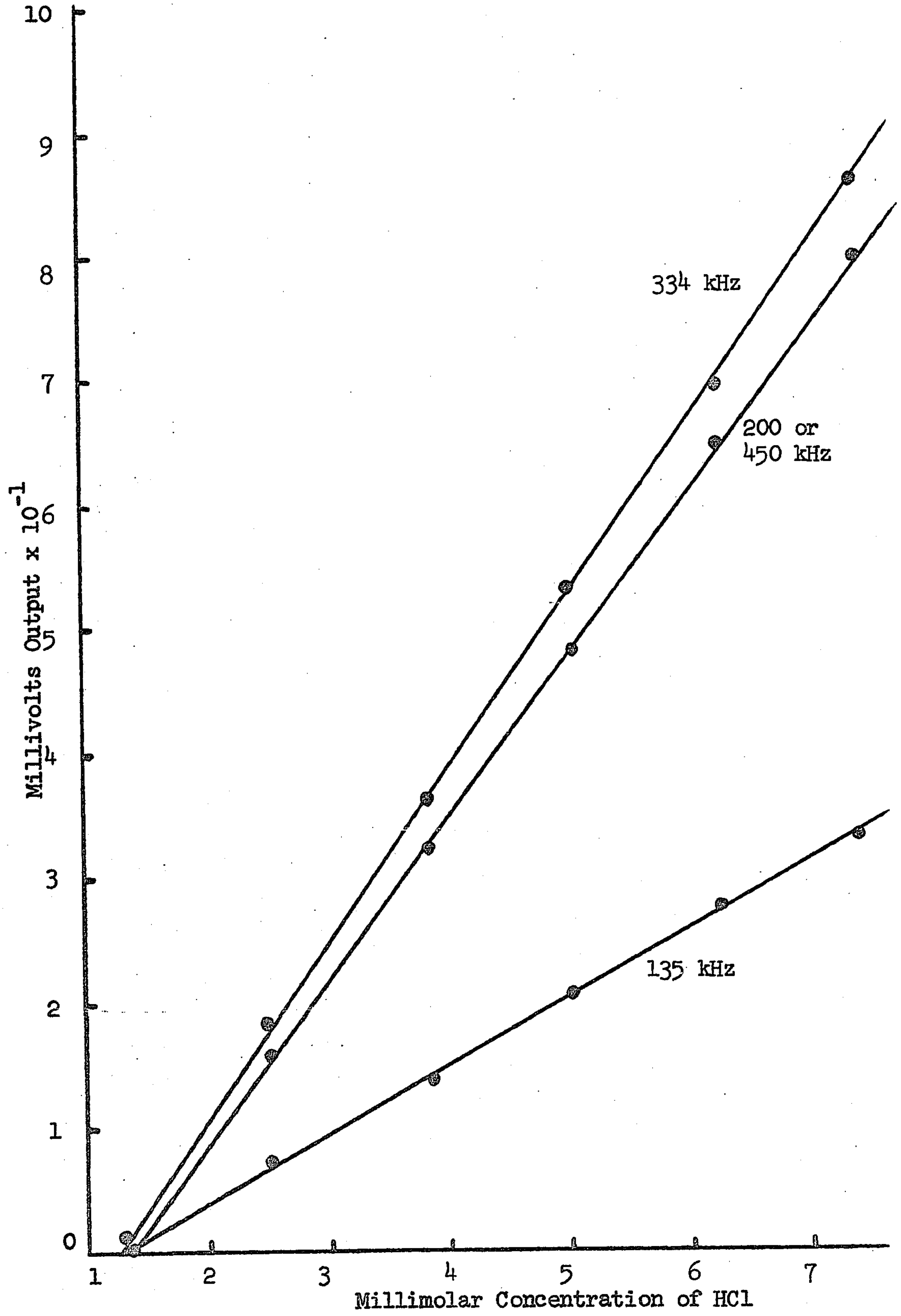

Figure 46. Response Sensitivity of Probe D

c. Conclusions. A convenient method has been developed to discover the optimum operating conditions for a given probe and related electrical equipment. The frequency at which the maximum i·f product occurs yields the greatest probe sensitivity.

7. Studies of Probe C

a. Determination of i·f Product. The self-resonant frequency of the receiver toroid was found to be 234 kHz. Using different series capacitors in the transmitter toroid circuit, optimum frequency conditions for Probe C were determined. Inspection of Table VI reveals that the maximum i·f product occurs at 196 kHz. Use of this high frequency later proved undesirable because data scatter became intolerable due to stray body capacities; operation in the 110 to 140 kHz region reduced stray noise pickup considerably without too great a sacrifice in probe sensitivity.

TABLE VI

i·f Product Constants for Probe C

f, kHz	ma across 0.783 ohms*	i·f, kiloamp-Hz
97	83.0	10.3
130	82.0	13.6
135	84.0	14.5
141	82.0	14.8
170	79.0	17.1
180	82.0	18.9
196	85.0	21.3 (max)
211	48.5	13.1
220	31.0	8.7

*These high currents resulted from a "loading effect" of Probe C upon the Knight Signal Generator. The internal feedback loop of the generator is taken from the output terminals; the inductive load of Probe C apparently causes the output of the generator to exceed its normal output capacity under the prevailing reactive load conditions.

b. Response of Probe C.

i. Null Response to Pure Resistance. After placing a piece of wire through the core of Probe C, various 1% precision resistors were attached to the ends of the wire. The Heath Resistance Box was connected to the two differential winding leads of the probe; a small variable capacitor was then wired in parallel with the resistance box. Null readings were read from the resistance box with each change in precision loop resistor. The variable capacitor required readjustment each time, especially at high loop resistance values.

Figure 47 shows the null response (hereafter called the R_{box} response) of Probe C at 120 kHz and 100 ma to various values of loop resistance. Deviation from a linear response begins at 8×10^{-4} mhos (12,500 ohms). A useful nonlinear response is maintained to 2×10^{-5} mhos.

Additional experiments were performed over each decade range of conductance values from 10^{-4} to 10^{-1} mhos loop resistance. Linearity of response was maintained within 1% from 8×10^{-4} to 6×10^{-2} mhos. At conductance values higher than 6×10^{-2} mhos, the response slope actually increased in sensitivity.

ii. Null (R_{box}) Response to Solutions. Using KCl solutions, the total R_{box} response of Probe C was obtained as a function of solution conductance. Specific conductivities were also obtained using low frequency conductance measurements (Appendix B). Figure 48 shows this response of Probe C.

Deviation from linearity begins at 3×10^{-3} mhos/cm specific conductance. It will be shown later that the cell constant for

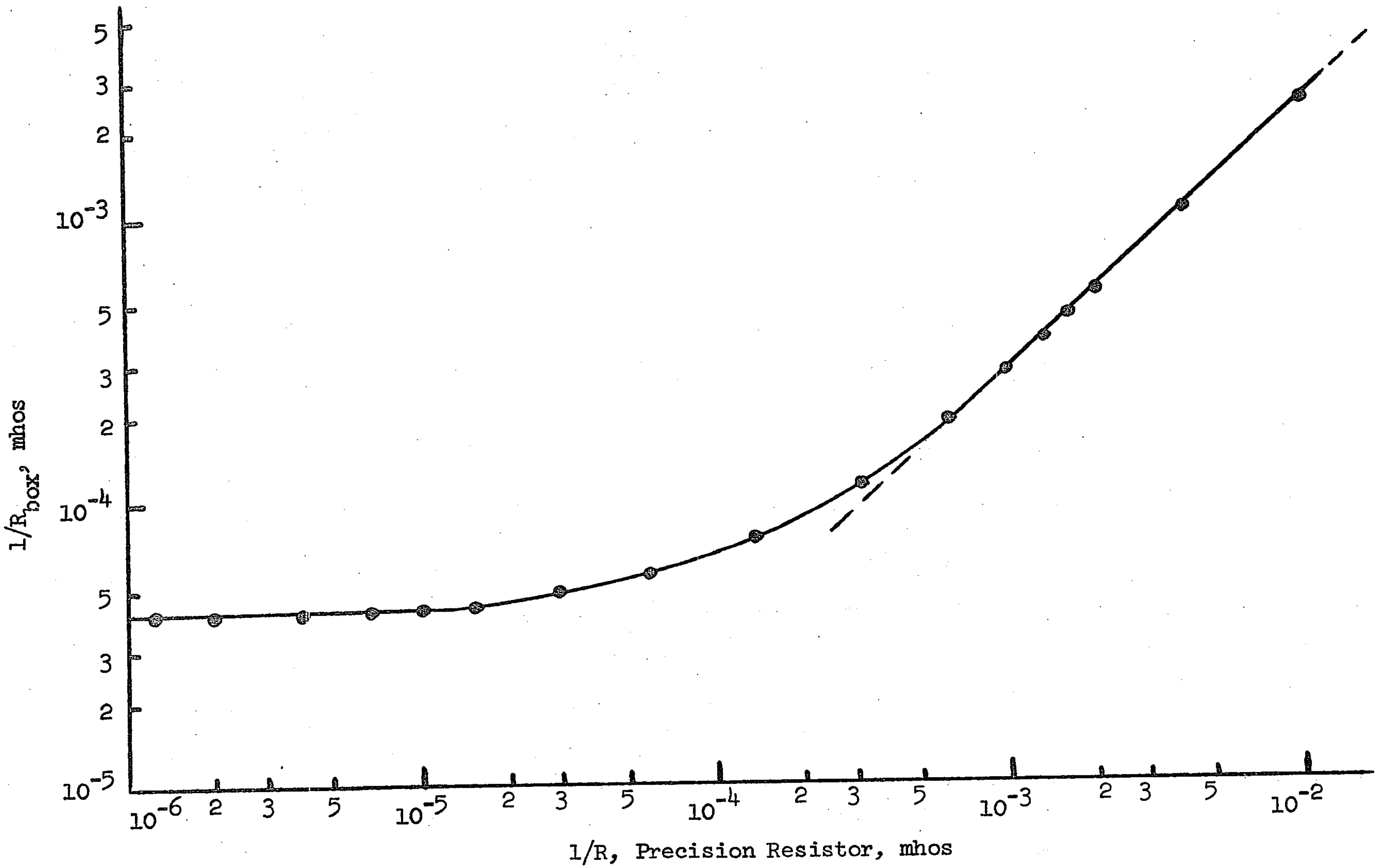

Figure 47. Response of Probe C to Pure Resistances

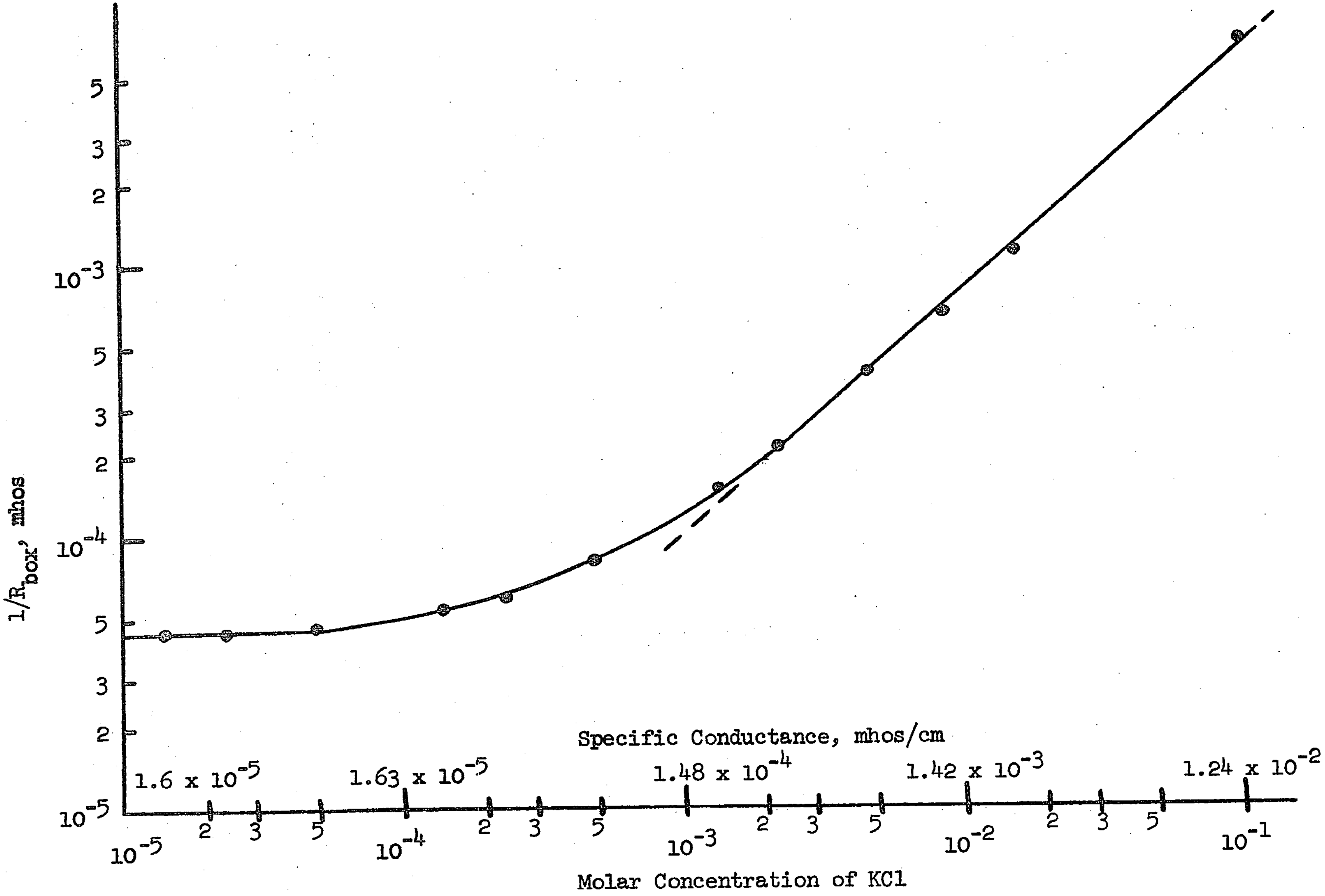

Figure 48. Response of Probe C to KCl Solutions

Probe C is 4.16 cm^{-1}. Recalling (p. 10 that $1/R = G = k/\theta$, then, 3×10^{-3} mhos $cm^{-1}/4.16\ cm^{-1} = 7.2 \times 10^{-4}$ mhos. The deviation from linearity using 1% resistors (Figure 47) began at 8×10^{-4} mhos loop resistance; the two values then are in good agreement. Thus when the cell constant is used, the values of specific conductance on the linear response portion of Figure 48 (using KCl solutions) correlate very well with the 1/R(G) values of Figure 47 which were obtained with 1% resistors rather than solutions. For example, choosing a specific conductance value from Figure 48 equal to 1.24×10^{-2} mhos/cm (0.10 M KCl), the $1/R_{box}$ value is 7.95×10^{-4} mhos. Turning to Figure 47, the value of conductance at the same $1/R_{box} = 7.95 \times 10^{-4}$ mhos is 2.9×10^{-3} mhos. Multiplying this latter value by the cell constant for Probe C (4.16 cm^{-1}), one obtains a specific conductance value of 1.21×10^{-2} mhos/cm, in good agreement (2.4%) with the originally chosen value of 1.24×10^{-2} mhos/cm from Figure 48.

iii. Delta Millivolt Response to Pure Resistance. For this method the same conditions of frequency, amperage, and resistor loop values were used as before. The results for the highest R values are shown in Figure 49. The probe does not begin to deviate from linearity until 5×10^{-6} mhos compared to 8×10^{-4} mhos for the R_{box} method (Figure 47).

When the Delta mv method is used, the variable capacitor on the resistance box remains untouched after obtaining an initial null (at infinite loop resistance). Therefore, the output VTVM senses all impedance changes associated with the probe (including any capacitive changes) and not just the resistive components of impedance. Apparently the output of the transmitter toroid contains different amounts of

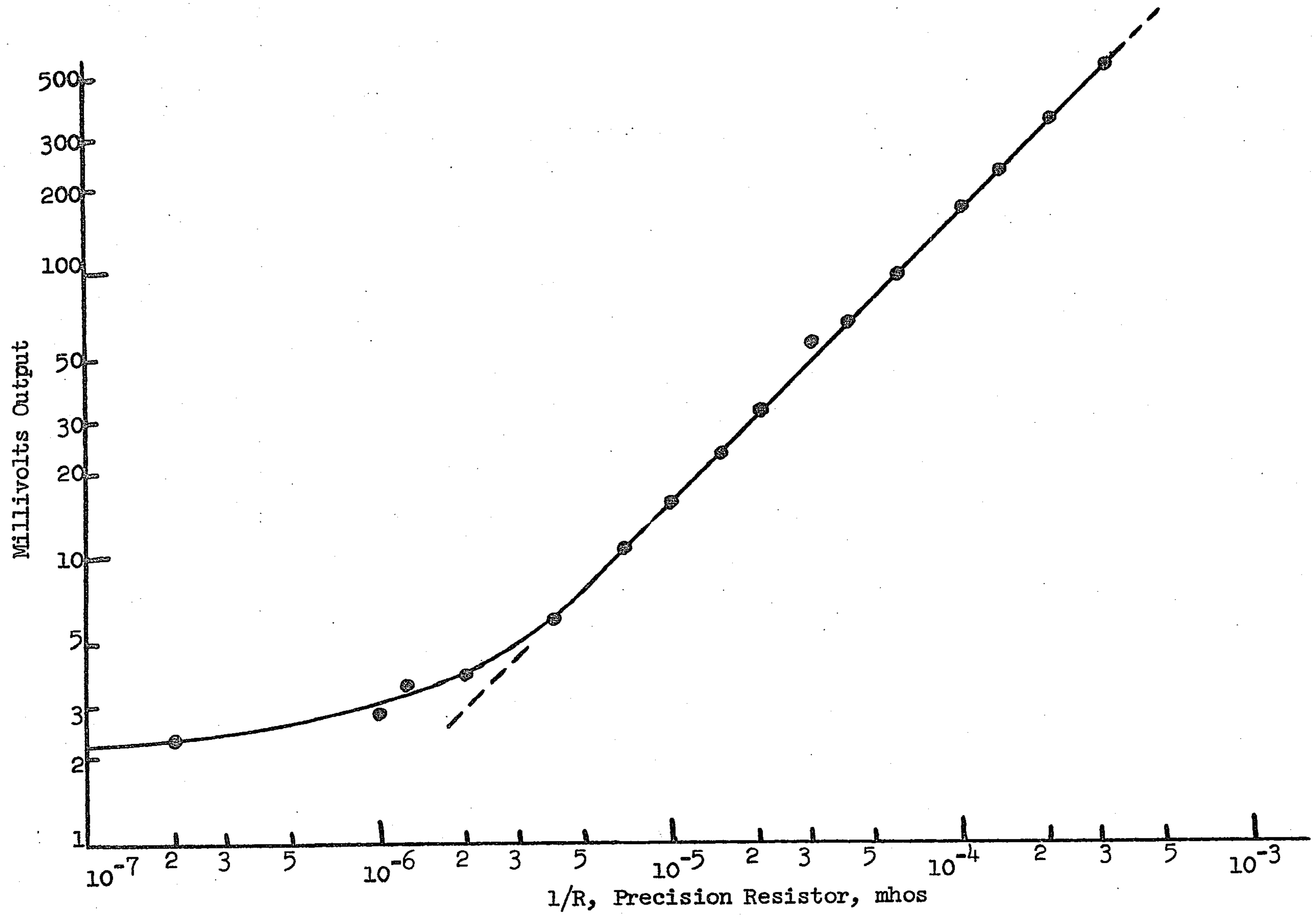

Figure 49. Response of Probe C to Pure Resistances

capacitive contribution depending upon the particular loop resistance used. In the R_{box} method, however, the variable capacitor value must be changed with each new value of loop resistance, hence shunting some signal away from the VTVM at low conductance values. Therefore, linear response is not available to as low loop resistance values using the R_{box} method as it is using the Delta mv method.

iv. Delta Millivolt Response to Solutions. Using the same KCl solutions as used in Figure 48, the response was linear to 25×10^{-6} mhos/cm. Dividing by the cell constant, 4.16 cm^{-1}, the resulting G value for deviation from linearity with pure resistances should be 6×10^{-6} mhos/cm. The actual deviation (see Figure 49) begins at 5×10^{-6} mhos/cm.

v. Conclusions. It has been shown that the response of Probe C is the same whether one employs pure loop resistances or measures the resistances of known solutions. The Delta mv method allows a linear measurement of solution conductance to 25×10^{-6} mhos/cm. The R_{box} method allows such linearity to only 2.8×10^{-4} mhos/cm. The greatest possible precision of the Delta method, however, is only 0.5% which is the maximum readability of the VTVM. Although this method permits lower conductance values to be read than does the R_{box} method, the latter has greater precision at moderate to high conductance values.

The Delta mv method does allow, however, sufficient precision for titrational applications and frees the operator from tedious null balancing; in addition, linear titrations to lower concentration levels are possible using the Delta mv method than when using the R_{box} method.

c. Low Level Response and Precision Using Probe C. Using NaCl as a typical electrolyte, the lowest conductance level at which Probe C could be used was determined using both the R_{box} and Delta mv procedures. The responses of Probe C (120 kHz, 100 ma) using millimolar solutions of NaCl are shown in Figures 50 and 51. For convenience the values of specific conductance have also been included.

It is immediately evident that less data scatter (more precision) is obtainable at low conductances with the Delta mv method (Figure 51); the calculated error in reproducing a given solution conductance value by the R_{box} procedure is ± 3.7% at 60 micromhos/cm, whereas, the precision for the Delta mv method is ± 2.6%. Figures 50 and 51 also establish the lower usable specific conductance limit of Probe C as 25 micromhos/cm.

d. Signal to Noise Ratio at Different Conductance Levels. Using Probe C at 120 kHz and 100 ma, and the FET amplifier at full gain, signal to noise (S/N) ratios were calculated for various values of pure loop resistances using the Delta mv method. The findings are presented in Table VII. A further increase in the values of loop conductance results in a proportionate increase in the S/N ratio, and a consequent decrease in the per cent noise in the signal.

e. Precision and Accuracy Obtainable. The most crucial test of the precision and accuracy obtainable using Probe C was considered to be its performance in chemical analyses. These titrations will be presented in a later section.

f. Determination of the Cell Constant of Probe C. The differential R_{box} method was used to determine the cell constant. A KCl solution (7.419 g/kg solution) whose specific conductance[41] is

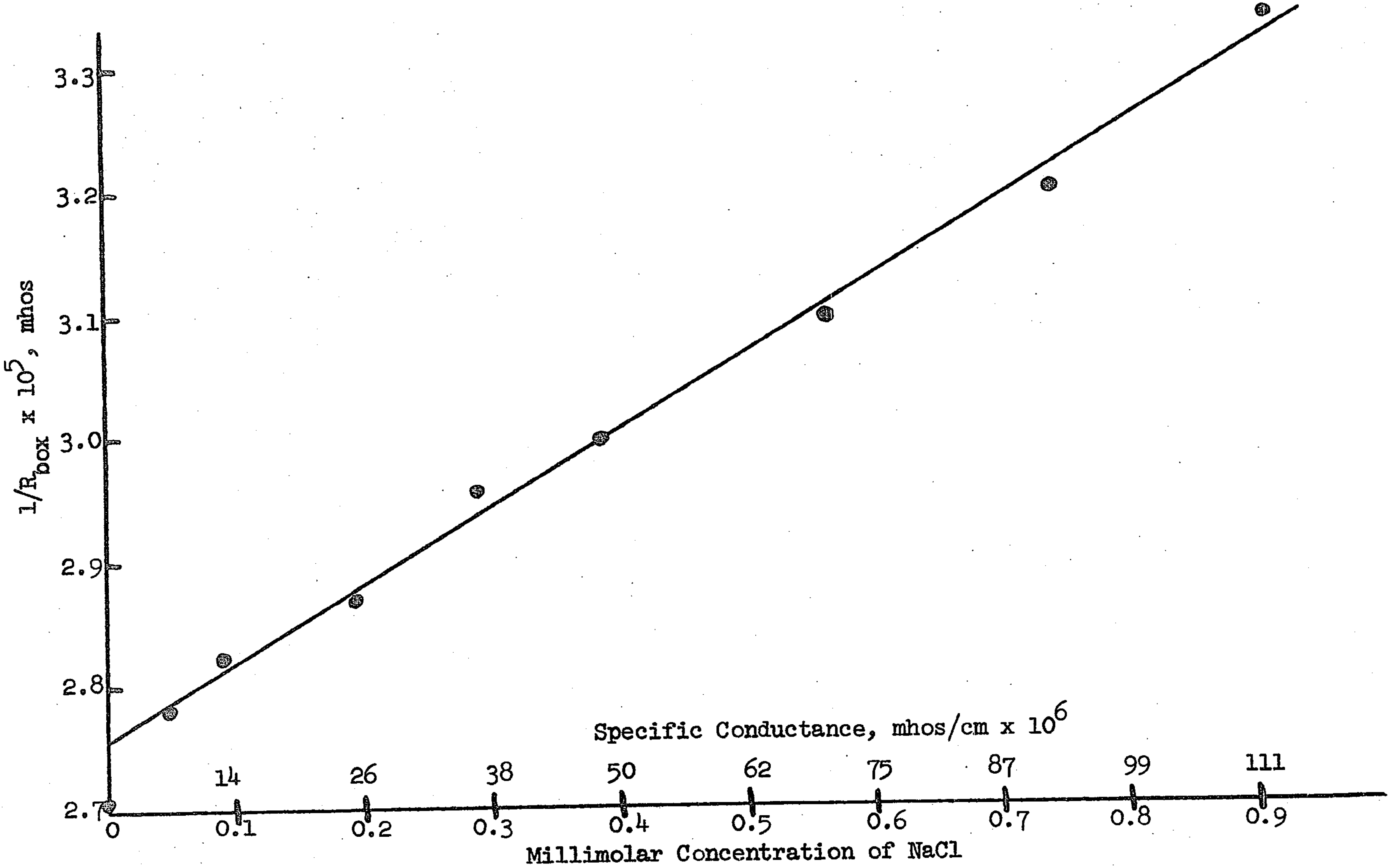

Figure 50. Precision of Probe C at Low Conductance Levels

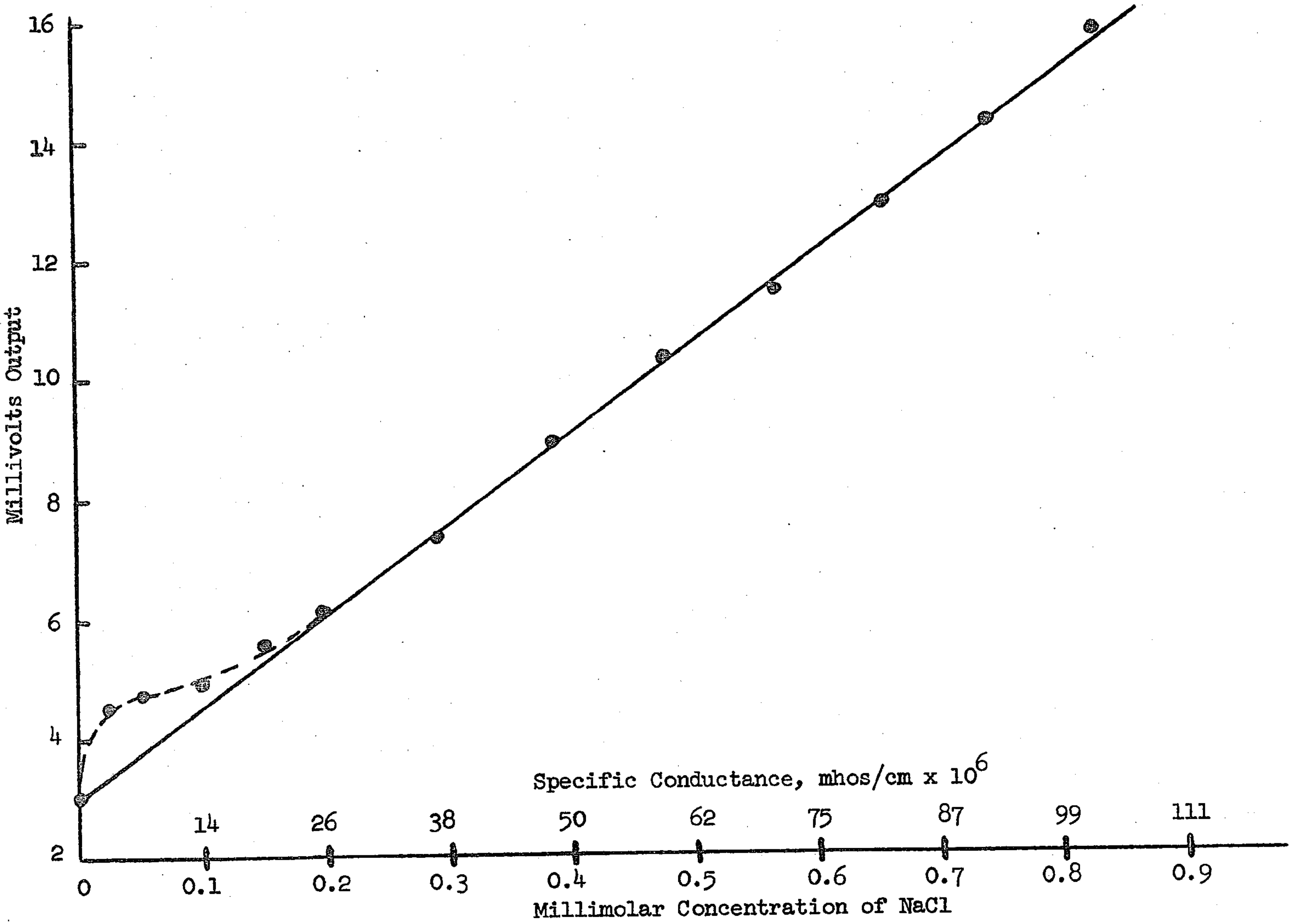

Figure 51. Precision of Probe C at Low Conductance Levels

0.01286 mhos/cm at 25°C was employed for the purpose. At 120 kHz, 100 ma and using the FET, the R_{box} null for this KCl solution was 1,218 ohms.

Probe C was then removed from the KCl solution, rinsed and dried. A wire was threaded through the core and its ends connected to a second Heath Decade Resistance Box, and the resistance on this decade box was varied until the VTVM indicated a null. The value of the loop resistance on the second decade box was 324 ohms. During this procedure, the setting on the R_{box} attached to the null windings of Probe C remained unchanged from the value obtained with the KCl solution.

The specific conductance of the standard KCl solution is 12,860 micromhos/cm; the value of (wire) loop resistance was 324 ohms. Then, since $k = \theta/R$, the value of the cell constant $\theta = 12{,}860 \times 10^{-6}$ mhos/cm $\times$ 324 ohms = 4.16 cm^{-1} for Probe C; this particular cell constant is valid only when the above operating conditions (120 kHz, 100 ma, and FET) are used.

TABLE VII

Signal to Noise Ratios for Probe C

Loop conductance 1/R = G, mhos	Output from VTVM, mv	S/N	N/S,%
0	2.3 (noise)	-	
2.0×10^{-7}	2.3	0	
1.0×10^{-6}	2.8	0.22	± 450
4.0×10^{-6}	6.20	1.7	± 59
1.0×10^{-5}	16.0	6.0	± 17
4.0×10^{-5}	65.5	27.5	± 3.4
1.0×10^{-4}	170	73	± 1.4
6.33×10^{-4}	1100	478	± 0.20
1.0×10^{-3}	1780	773	± .13
4.0×10^{-3}	4750	2060	± .05

g. Effect of the Number of Null Windings. Calvert and coworkers[22] describe the relationship of the resistance in the solution loop (a 1 turn loop) to that read on the null resistance box by the equation

$$1/R_{unk} = N_s n_s (1/R_{std}). \tag{5}$$

In terms which are used in this work,

$$G_{loop} = N_s n_s G_{R_{box}}, \tag{6}$$

where N_s is the number of null windings on the transmitter toroid and n_s is the number of null windings on the receiver toroid.

From Equation 6 it may be seen that to measure low resistance (high conductance) solutions to many significant digits on a standard decade box, the product of $N_s \times n_s$ should be made large; e.g., if the loop conductance were 0.01 mho (100 ohms), using 10 null turns on each toroid would permit the R_{box} reading ($G_{R_{box}}$) to be 100 times that of the solution, i.e., 1 mho (R_{box}= 10 kΩ); hence, rather than needing decade resistances below 1 ohm if $N_s \times n_s$ were 1, ordinary decade box resistors can be used by manipulating the $N_s \times n_s$ product.

Conversely, to measure high resistances ($> 10^4$ ohms), a low $N_s \times n_s$ product is desired to permit using resistance values available on a standard decade box. In this work, two null turns were placed on each toroid in each probe; hence, $N_s \times n_s$ should equal 4. To test this, a solution of KCl (71.135 gms/kg solution, K = 0.111 mhos/cm) gave a value of R_{loop} = 41.8 ohms; R_{box} = 165.5 ohms; thus $R_{box}/R_{loop} = G_{loop}/G_{box} = N_s \times n_s = 165.5/41.8 = 3.96$.

h. Solution Heating Effect of Probe C. To determine the quantity of energy dissipated in a solution by Probe C, the following experiment was performed at 120 kHz and 100 ma. Precision 1% tolerance resistors were used in place of the normal solution loop. Using the differential method, the R_{box} was nulled for each of 6 values of loop resistance. The voltage drop across the loop resistor was measured with the Eico VTVM. Knowing this voltage drop, the wattage dissipated by the resistor is E^2/R. This wattage would also be dissipated in a solution loop of electrolyte having the same resistance. The results are shown in Table VIII.

TABLE VIII

Watts Dissipated by the Solution Loop of Probe C

R_{loop} (1%), ohms	E, volts	E^2/R, watts
10^6	0.345	1.190×10^{-7}
10^5	0.346	1.197×10^{-6}
10^4	0.345	1.190×10^{-5}
10^3	0.344	1.182×10^{-4}
10^2	0.344	1.182×10^{-3}
10^1	0.332	1.102×10^{-2}

The resistance of the primary toroid of Probe C was found to be 0.566 ohms; under normal operating conditions (100 ma) the primary coil would dissipate I^2R watts, in this case 5.66×10^{-3} watts. Thus, the total wattage dissipated by Probe C (which heats the solution) is the sum of these two wattages.

It is known[47] that 1 joule/sec equals 4.184 gm-calories/sec which equals 1 watt. Also, the average heat capacity is $C_{avg} = q/T_2-T_1$, where T_1 is the initial temperature, T_2 is the final temperature, and q is the heat absorbed by the system.[48] For this calculation, 100 gms of water (C_{avg} = 1 gm cal/deg) was used. Assuming that an electrolyte loop of 100 ohms (from Table VIII) is being measured, and that this electrolyte does not change the specific heat of water, then

---

[47] N. A. Lange (ed.), "Handbook of Chemistry," 10th ed., McGraw-Hill Book Co., Inc., New York, 1961, p. 1820.

$$T_2 - T_1 = \Delta T = \frac{q}{C_{avg}} = \frac{1.182 \times 10^{-3} + 5.66 \times 10^{-3} \text{ watts}}{1 \text{ cal/deg} \cdot 100 \text{ gms}}$$

$$= \frac{6.84 \times 10^{-3} \text{ watts} \times 4.184 \text{ gm-cal/watt-sec}}{100 \text{ gm-cal/deg}}$$

$$= 2.86 \times 10^{-4} \text{ deg/sec}$$

Thus the heating effect of Probe C on a solution under typical operating conditions is completely negligible.

i. Effect of Temperature on the Response of Probe C. A 100 ml thermostated cell of local design was used in place of the usual beaker. Water from a 1 liter reservoir was made to flow through the jacket of this special cell by means of a Ministaltic Pump.* The temperature was varied by the addition of warm water to the liter reservoir; usually 5 minutes were required for the solution to come to a steady temperature.

The solution, whose temperature coefficient of conductance was studied, was 0.010 M KCl. According to Lange[49] the temperature coefficient for this solution is 1.91%/deg C at 25°C.

---

*Manostat Corporation, New York, New York.

[48] F. Daniels and R. A. Alberty, "Physical Chemistry," 2nd ed., John Wiley and Sons, Inc., New York, 1961, p. 45.

[49] Lange, p. 1211.

The standard R_{box} differential measuring technique was used, and the results are presented in Figure 52. The slope of the line gives a temperature coefficient of 1.33%/deg C rather than 1.91%/deg C.

One possible explanation for this discrepancy is that at 0.01 M KCl (see Figure 48, p. 109) the response of Probe C is just beginning to deviate from linearity (the response per unit concentration change is becoming less).

No attempts were made to rerun the above experiment at higher concentration levels; the primary purpose was to ascertain the linearity of response (or lack thereof) which occurred with a change in temperature in the vicinity of ambient temperature (25°C).

8. Studies of Probe F

Probe F was constructed to overcome some of the faults of Probe C. Among these faults were: a high i·f product frequency of 120 kHz, the use of which permitted a large amount of capacitive leakage through the shields; evidence for this leakage may be seen by comparing the different ranges of response linearity shown in Figures 47 and 49: Probe C also had a high cell constant factor, whereas a lower θ (larger core) would enable lower values of solution conductance to be measured.

By using cores of higher permeability (μ_o), a greater inductance, and hence mutual inductance could be secured for Probe F than was possible with Probe C. Also a lower self-resonant frequency would result, meaning less capacitive leakage through the shields.

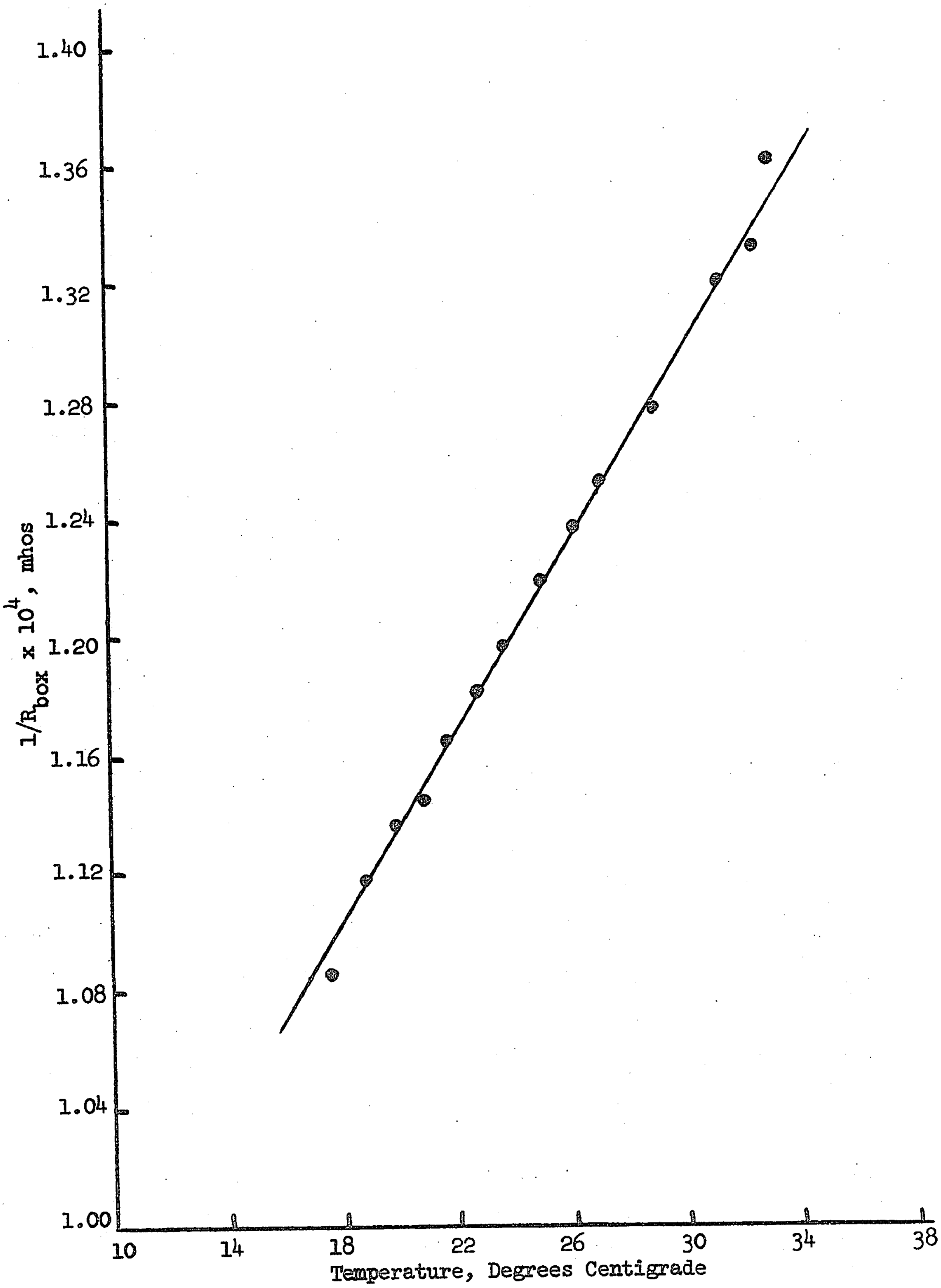

Figure 52. Effect of Temperature on Response of Probe C

The study of Probe F will be reported in a manner similar to that used for Probe C. Hence, for details in procedure, reference must be made to the detailed method descriptions given for Probe C.

a. Determination of i·f Product. The natural self-resonant frequency of Probe F was found to be 56.4 kHz. Using a series capacitor to the input (transmitter) toroid, an i·f product study was made, and the results are shown in Table IX.

TABLE IX

i·f Product Constants for Probe F

Frequency, kHz	Milliamperes	i·f, kiloamp-Hertz
62.5	1.15	0.0719
60.0	1.37	0.0822
55.0	1.80	0.099
50	2.44	0.122
45	3.12	0.140
40	3.83	0.153
35	4.34	0.152
30	5.36	0.161 (max)
25	6.41	0.160
20	7.53	0.151
18.5	7.79	0.144
14.8	9.07	0.134

From this study a frequency of 30 kHz was chosen for all future studies. Although the magnitude of the i·f product is less than that found for Probe C, the sensitivity of response for Probe F was found to be almost identical in terms of unit output change per unit conductance change; the slopes of Figures 49 (p. 111) and 55 (p. 127) are nearly equal.

Responses were obtained at frequencies above and below 30 kHz to prove that the maximum i·f product frequency was the most sensitive to changes in solution conductance.

b. Response of Probe F.

i. Null Response to Pure Resistance. In a manner identical to that used with Probe C, the R_{box} differential procedure was used to determine the response of Probe F to a pure resistance loop (1% precision resistors). The response (f = 30 kHz, ma = 4.3, FET) is shown in Figure 53. Deviation from linearity at the low end of conductance values begins at 6×10^{-5} mhos (Probe C began at 8×10^{-4} mhos). This demonstrates that even with a reduction of the magnitude of the i·f product, an increase in usable response (to 2×10^{-6} mhos) can be obtained by using a lower frequency if high permeability core materials are used.

By investigating each decade of loop resistance values in detail, it was found that linearity extends from 6×10^{-5} mhos to 1×10^{-1} mhos; above the latter value the response decreases, a response opposite to that found using Probe C.

ii. Null (R_{box}) Response to Solutions. The KCl solutions used for Probe C were again used here. The results appear in Figure 54. Deviation from linearity begins at 6×10^{-5} mhos/cm. The cell constant of Probe F is known to be 1.04 cm^{-1}. The correlation of the values using pure resistances versus using KCl solutions is thus very good: 6.24×10^{-5} mhos/cm for pure R vs. 6.0×10^{-5} mhos/cm for KCl. Other specific conductance values of Figures 53 and 54 agree to a precision of ± 2%.

iii. Delta Millivolt Response to Pure Resistance. Using the same operating conditions as before, the response of Probe F employing the Delta mv technique was determined. The response is

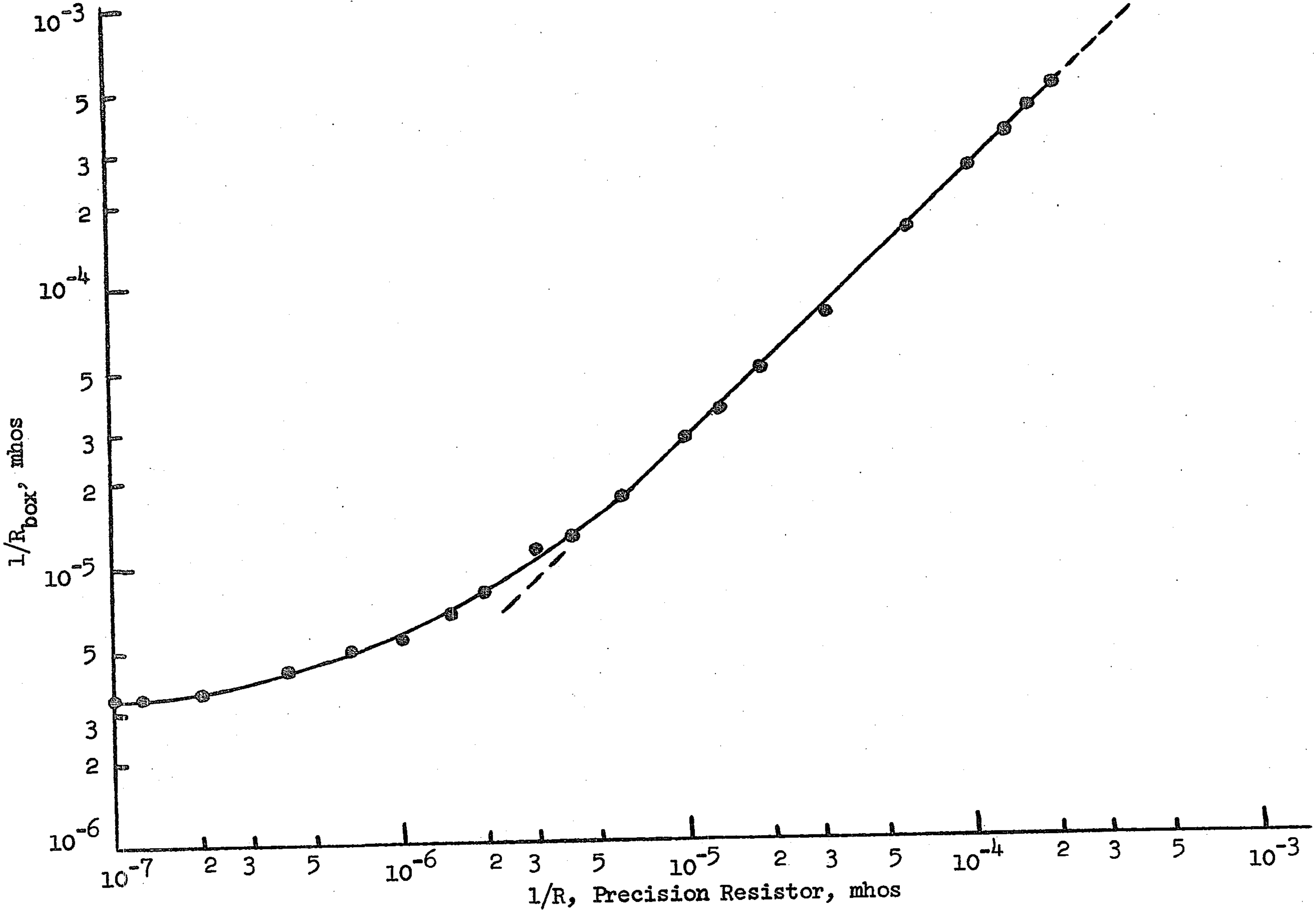

Figure 53. Response of Probe F to Pure Resistances

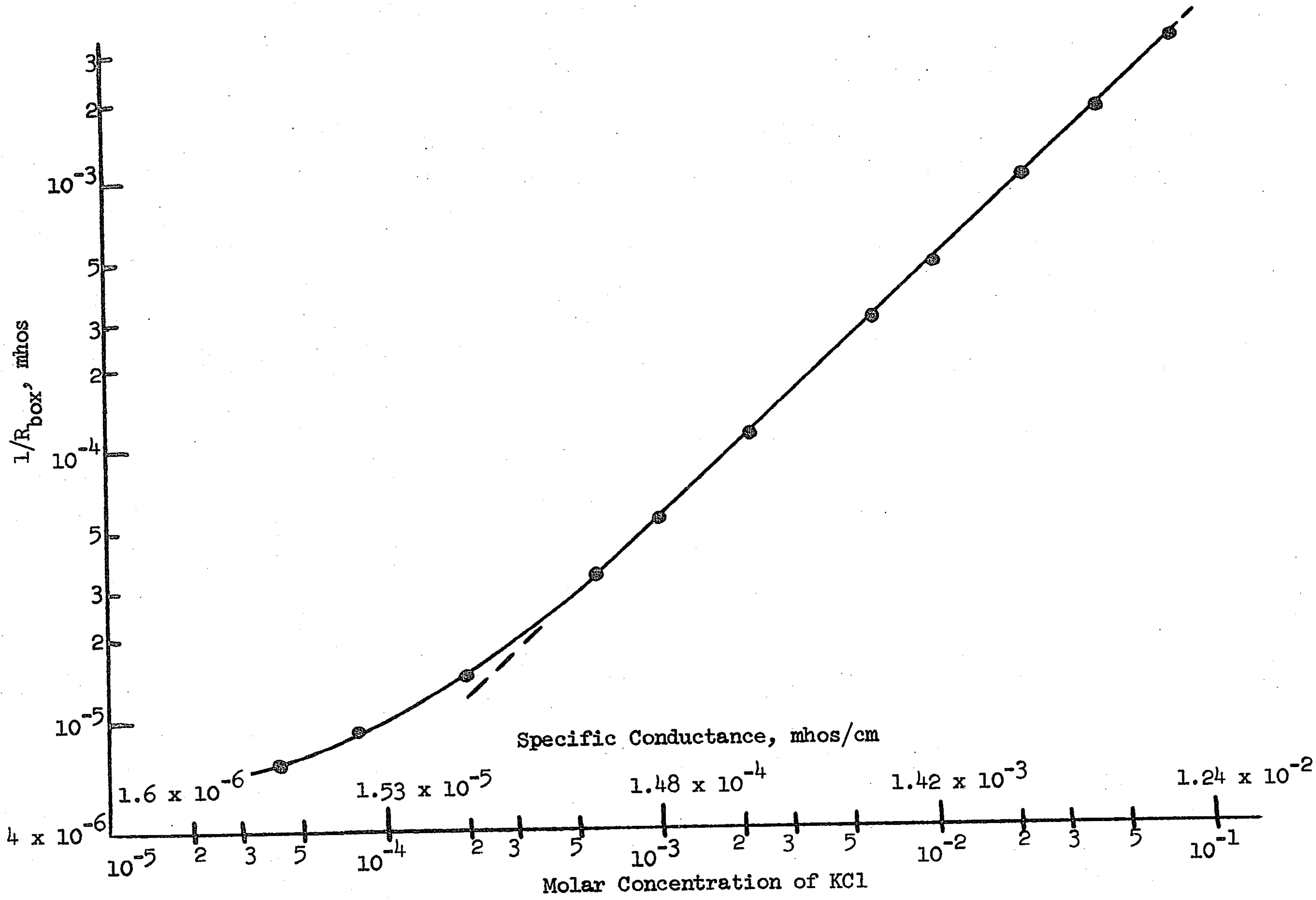

Figure 54. Response of Probe F to KCl Solutions

shown in Figure 55. The response begins to deviate from linearity at 2×10^{-6} mhos.

iv. Delta Millivolt Response to Solutions. Using KCl solutions, and the same operating conditions as before, deviation from linearity began at approximately 2×10^{-6} mhos/cm, in good agreement with the value for a pure resistance loop.

v. Conclusions. Using lower frequencies (30 kHz vs. 120 kHz), better shielding (copper vs. Al foil), higher permeability toroidal cores, and a smaller cell constant, linear conductance measurements are possible to 2×10^{-6} mhos/cm using Probe F; Probe C allowed linear conductance measurements to only 25×10^{-6} mhos/cm.

c. Low Level Response and Precision Using Probe F. Again using NaCl as a typical electrolyte, the response of Probe F at micromolar solution levels was investigated. Figure 56 shows the response of Probe F at 30 kHz and 4.3 ma. From evaluation of the point scatter by drawing "worst case" slopes as was done with Probe C, the precision of measurement at 3.0×10^{-6} mhos/cm using the Delta mv method was considered to be ± 3%. The precision for the R_{box} method was not determined because the shunt switch capacitances to ground in the Heath Decade Box made such a determination extremely unreliable.

d. Signal to Noise Ratio at Different Conductance Levels. For various values of pure loop resistances, the S/N ratio was evaluated for Probe F (30 kHz, 4.3 ma and FET) using the Delta mv technique. The results appear in Table X.

For identical loop resistances, the S/N ratio for Probe F is lower than that for Probe C (see Table VII, p. 116).

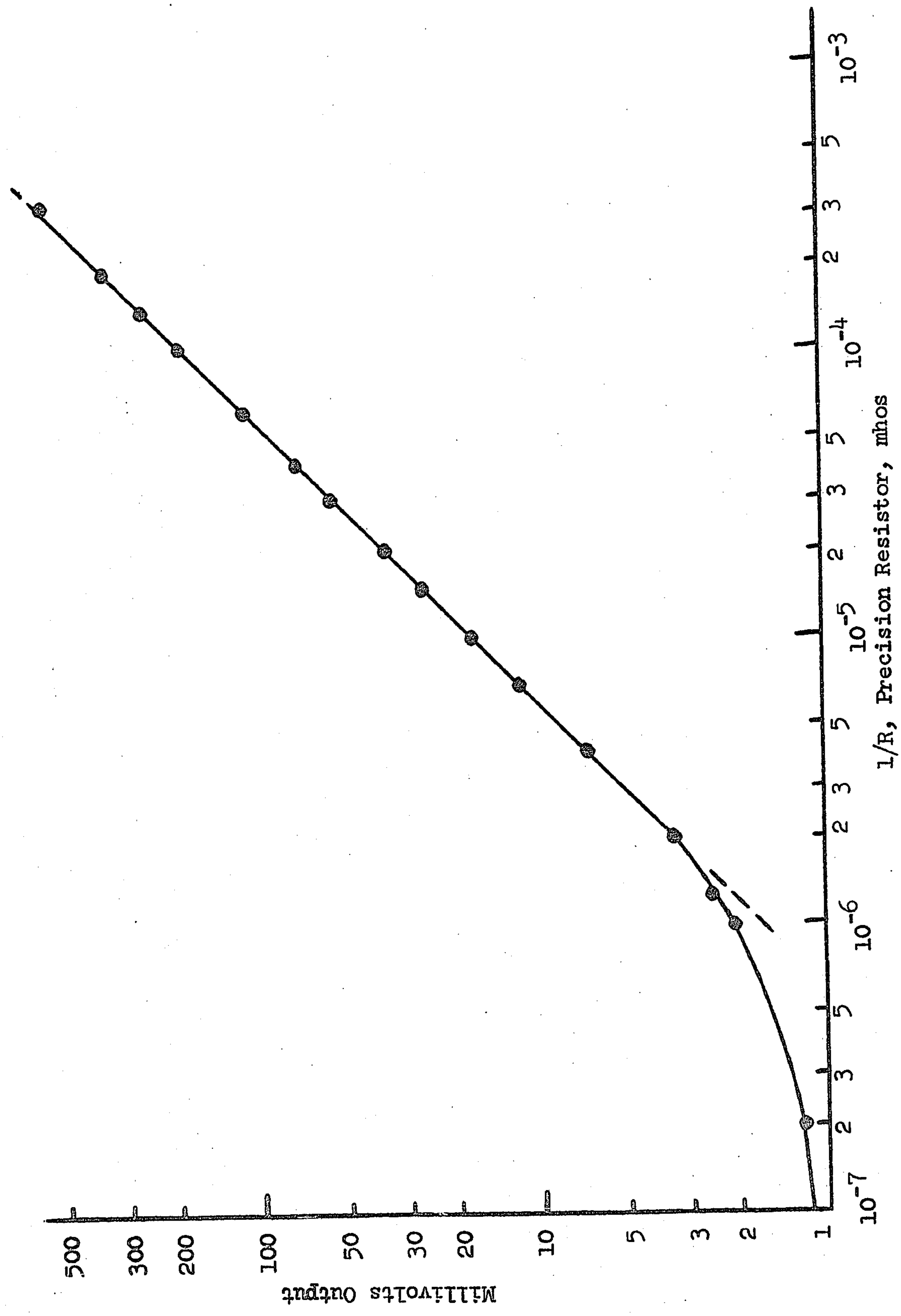

Figure 55. Response of Probe F to Pure Resistances

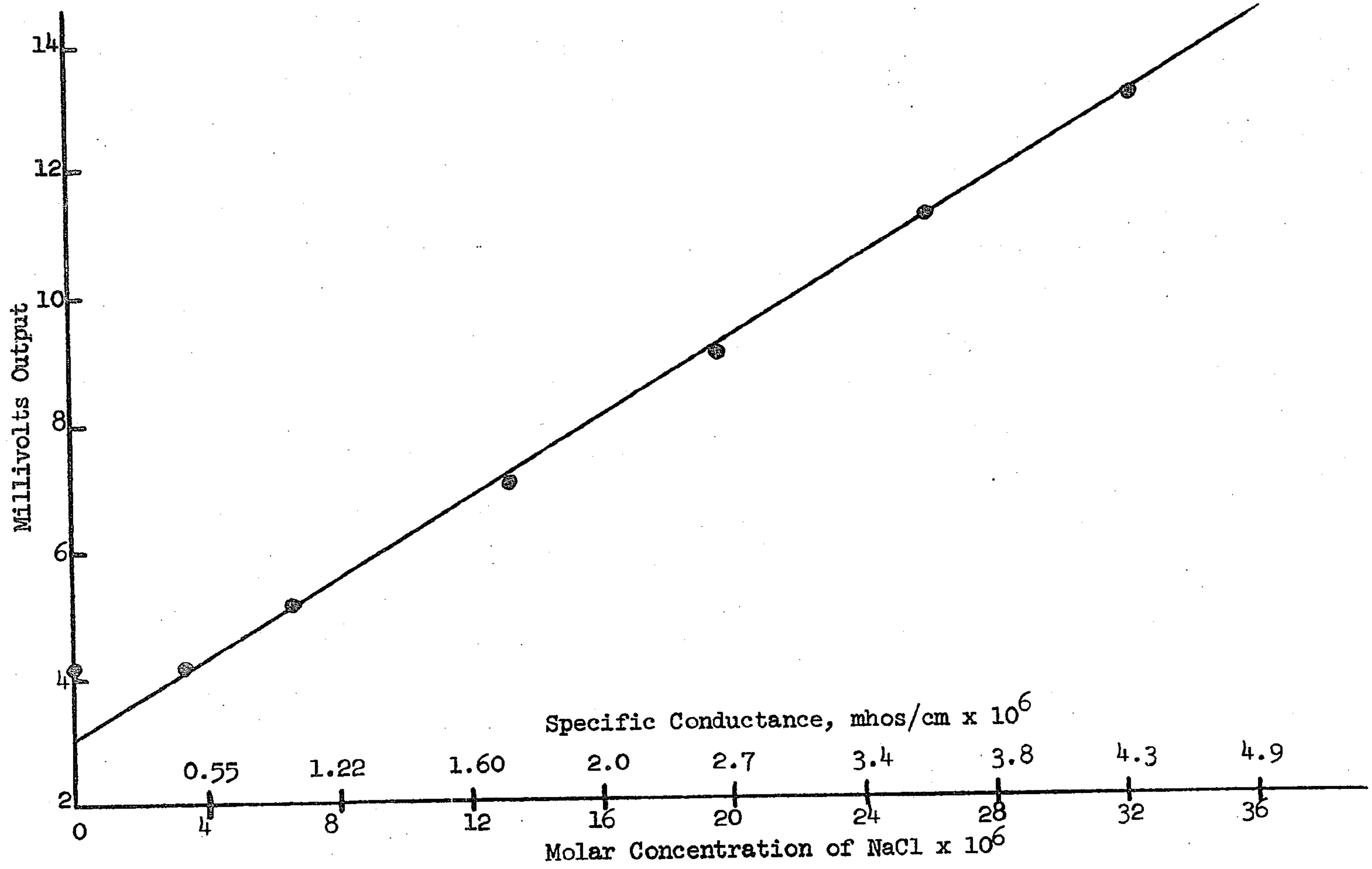

Figure 56. Precision of Probe F at Low Conductance Levels

TABLE X

S/N Ratios for Probe F

Loop conductance 1/R = G, mhos	Output from VTVM, mv	S/N	N/S, %
0	1.4 (noise)	-	-
2×10^{-7}	1.4	0	-
1×10^{-6}	2.1	0.50	200
4×10^{-6}	6.9	3.92	25.5
1×10^{-5}	17.8	11.7	8.55
4×10^{-5}	74.3	52.0	1.92
1×10^{-4}	189	134	.75
6.18×10^{-4}	1225	374	.11

e. Precision and Accuracy Obtainable. As mentioned before, the most crucial test of the accuracy and precision that can be obtained will be the performance of Probe F in analytical determinations. This will be described shortly in Section 10.

f. Determination of the Cell Constant of Probe F. The differential R_{box} procedure used for Probe C was also used for Probe F. Using 0.010 M KCl, the value of R loop (30 kHz, 4.3 ma, FET) was 738.5 ohms. The specific conductance[9] of 0.010 M KCl is 0.001409 mhos/cm at 25°C. Therefore $\theta = 0.001409 \times 738.5 = 1.04\ cm^{-1}$.

g. Determination of $N_s \times n_s$ Product. Using 0.010 M KCl, the value of R_{box} was 2,940 ohms when the solution loop resistance was 738.5 ohms. Therefore $R_{box}/R_{loop} = N_s \times n_s = 2{,}940/738.5 = 3.98$, which is in good agreement with the expected product of 4.0.

h. Solution Heating Effect of Probe F. A procedure identical to that for Probe C was used. The values of R_{loop}, voltage, and watts are presented in Table XI for Probe F (30 kHz, 4.3 ma, FET).

TABLE XI

Watts Dissipated by the Solution Loop of Probe F

R_{loop} (1%), ohms	E, volts	E^2/R, watts
10^5	0.232	5.39×10^{-7}
10^4	0.231	5.34×10^{-6}
10^3	0.230	5.29×10^{-5}
10^2	0.228	5.20×10^{-4}

The resistance of the primary toroid of Probe F was found to be 0.269 ohms; under normal operating conditions (4.3 ma) the primary coil would dissipate 4.98×10^{-6} watts. Using 150 mls of a solution whose loop resistance is 100 ohms and whose specific heat is 1.0, the heating rate is 1.47×10^{-5} deg/sec, which again is entirely negligible.

9. Limitations and Sources of Error

The basic limitation of the Magnetic Induction Method is the small induced voltage at low conductance levels; hence some degree of amplification is necessary to obtain a useful response.

A second limitation is the signal leakage through the imperfect shields to ground; this results in a loss of the induced signal as well as bothersome stray capacitance effects. It should be noted that this leakage is the primary reason for using fairly low operating frequencies; at frequencies greater than 100 kHz, capacitive leakage destroys response linearity at low solution conductivities; this has been evidenced by the responses of Probe C. Thus the operating frequency cannot be extended indefinitely to gain more probe sensitivity.

An increase in core volume of the probe allows measurements to be made at lower solution conductivities because of a decrease in cell constant; however, the increase in core volume may increase the size of the probe to the point of requiring wasteful volumes of solution for analysis.

Finally, the voltages and currents available from the signal generator are fixed; more current (to secure greater probe sensitivity) would require more elaborate signal sources.

Sources of error in a true differential measurement technique could include the signal generator frequency drift (0.03%/hour), and the tolerance of the R_{box} resistors (0.5%). In the Delta mv technique, the gain stability of the VTVM and FET amplifiers as well as the voltage output stability of the signal generator also become sources of error; then too, the accuracy, linearity and readability of the output VTVM determine the accuracy of this quasi-null method.

The final test of the possible accuracy and precision of these probes is their performance in a chemical analysis, the subject of the following section.

10. Chemical Applications

a. Introduction. Many titrations were performed in the areas of acid-base, precipitation, complexation, and redox titrimetry. One was performed in the presence of a 200-fold excess of foreign electrolyte. The major advantage of these probes over the conventional low frequency dipping conductance electrodes is their ability to null out the conductance contributions from foreign electrolytes and respond primarily to conductance changes involving the species under investigation.

Some analyses were performed using the true differential R_{box} procedure, while others used the simpler Delta mv method. As in conventional conductance analyses, interpretation of the "titration breaks" in terms of limiting equivalent ionic conductances is possible for most of the titrations performed; however, in the presence of high concentrations of electrolyte such interpretations become dubious. For all titrations studied, the end point break occurred at titrant concentrations proportional to the amount of substance being determined.

In some of the analyses, particularly those involving low concentrations of silver halides, output VTVM readings taken at definite time intervals after titrant addition greatly increased the accuracy and precision obtained.

b. Probe C - Titrations at Low Solution Conductances. Normal operating conditions in all the following experiments involved the operation of Probe C at 110 kHz and 85 ma. Use of the FET amplifier (narrow band, C_3 out of circuit) will be specified.

i. Acid-Base Titrations.

(a) Strong Acid. Since precise and accurate titration results at all higher concentrations of acid and base are easily obtained, a titration at a low level was performed. The following conditions were used:

Mode: Delta mv, FET.

Sample: 100 mls of 5.00×10^{-4} $\underline{M}$ HCl (0.05 meq).

Titrant: 0.0500 $\underline{M}$ NaOH.

Reaction: $HCl + NaOH \rightarrow NaCl + H_2O$.

Initial Solution Conductance: 220×10^{-6} mhos/cm.

Graph: Figure 57.

Calculated End Point: 1.000 mls.

Experimental End Point: 0.995 mls.

Per Cent Error: -0.5%.

(b) Weak Acid.

Mode: R_{box} differential, no FET.

Sample: 50.0 mls of 0.0207 $\underline{M}$ HOAc (1.035 meq).

Titrant: 1.000 $\underline{M}$ NaOH.

Reaction: $HOAc + NaOH \rightarrow NaAc + H_2O$.

Initial Solution Conductance: 250×10^{-6} mhos/cm.

Graph: Figure 58.

Calculated End Point: 1.035 mls.

Experimental End Point: 1.042 mls.

Per Cent Error: + 0.7%.

ii. Precipitation Titrations. Although a 20 millimolar solution of $AgNO_3$ was also titrated with equal accuracy, only the following 6 millimolar titration is described in detail.

Mode: R_{box} differential, no FET.

Sample: 0.300 meq $AgNO_3$.

Titrant: 0.500 $\underline{M}$ NaCl.

Reaction: $AgNO_3 + NaCl \rightarrow \underline{AgCl} + NaNO_3$.

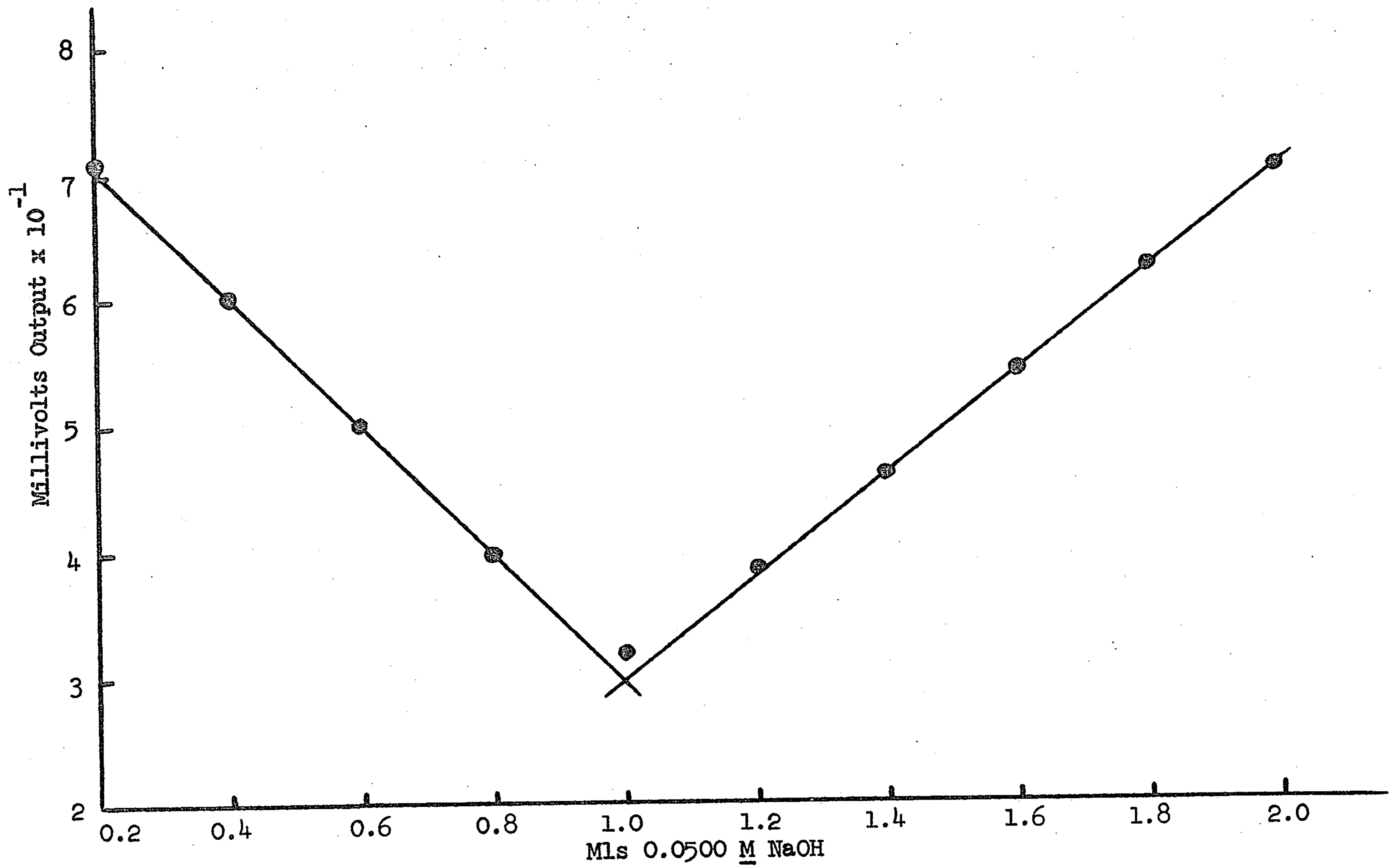

Figure 57. Strong Acid - Strong Base Titration

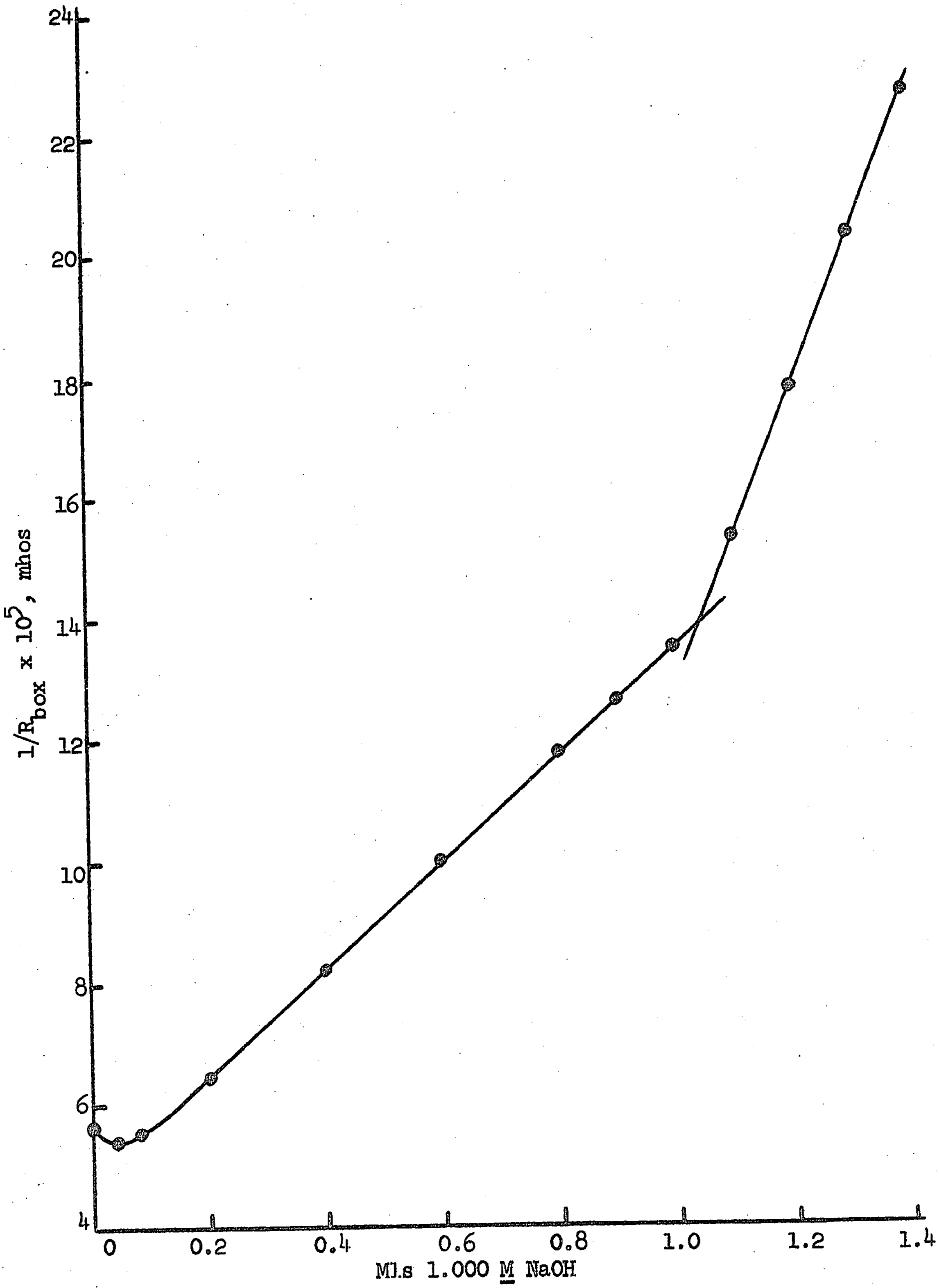

Figure 58. Weak Acid - Strong Base Titration

Initial Solution Conductance: 800×10^{-6} mhos/cm.

Graph: Figure 59.

Calculated End Point: 0.600 mls.

Experimental End Point: 0.592 mls.

Per Cent Error: -1.3%.

iii. Compleximetric Titration. Copper (II) with EDTA in 1 M NH_3.

Mode: R_{box} differential, no FET.

Sample: 0.100 meq Cu(II).

Titrant: 0.100 M EDTA.

Reaction: Cu(II) + EDTA → Cu·EDTA.

Initial Solution Conductance: 1200×10^{-6} mhos/cm.

Graph: Figure 60.

Calculated End Point: 1.000 mls.

Experimental End Point: 0.988 mls.

Per Cent Error: -1.2%.

iv. Conclusions. Several titrations have been performed with Probe C in concentration ranges normally used with conventional low frequency conductance techniques. The shape of the titration breaks are exactly analogous to those found using a conventional Wheatstone bridge and platinized electrodes. The accuracy is also comparable to that found using classical techniques. Analyses where conventional conductance techniques are unsuited will now be examined.

c. Probe C - Titrations in the Presence of Foreign Electrolytes. All but one of the following titrations used the Delta mv differential method. For some of the redox titrations it was found advantageous to make up the titrant in an inert electrolyte solution; thus, most of the

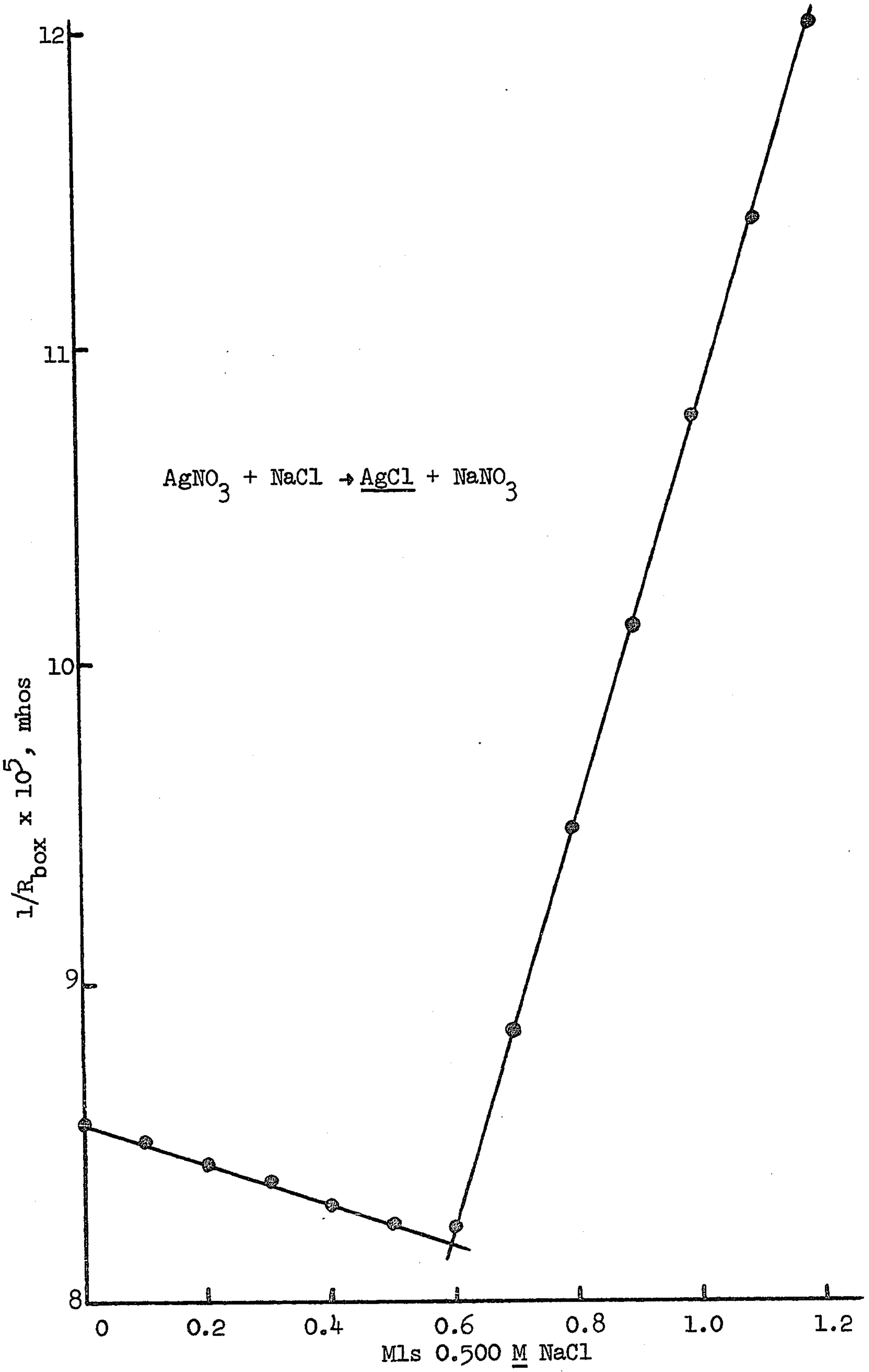

Figure 59. Precipitation Titration

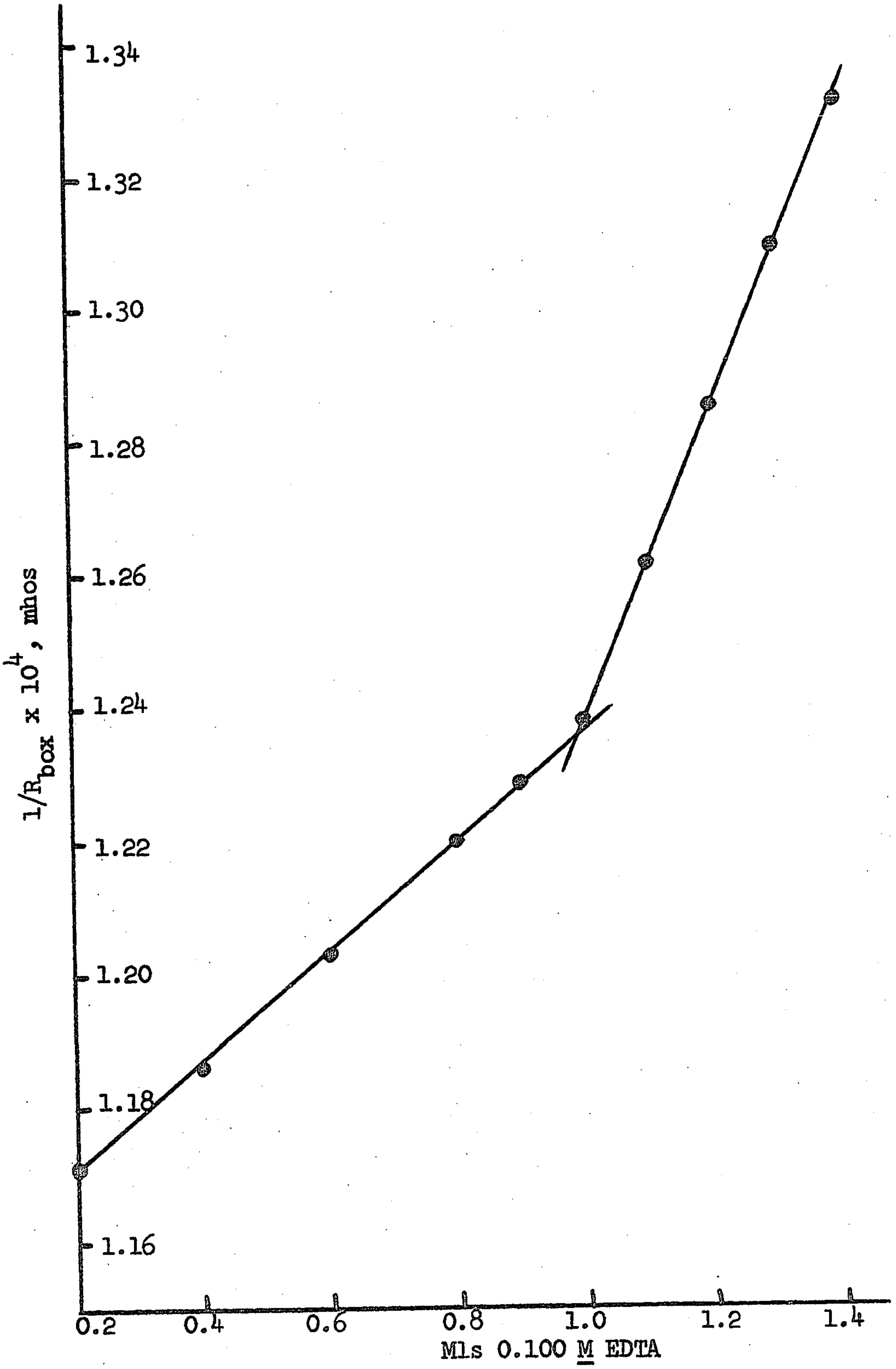

Figure 60. Compleximetric Titration of Copper(II)

conductance changes occurring from addition of titrant would not be due to the dilution of the solution, but rather to the reaction of the desired species.[14]

i. Acid-Base Titration.

Solution: 100 mls of 0.10 M NaCl.

Sample: 0.100 meq HCl (100 mls of 1 mM HCl in the above 100 mls of 0.10 M NaCl).

Titrant: 0.100 M NaOH.

Reaction: $HCl + NaOH \rightarrow NaCl + H_2O$.

Initial Solution Conductance: 0.011 mhos/cm.

Graph: Figure 61.

Calculated End Point: 1.000 mls.

Experimental End Point: 1.005 mls.

Per Cent Error: +0.5%.

ii. Precipitation Titration.

Solution: 100 mls of 0.10 M $NaNO_3$.

Sample: 0.100 meq $AgNO_3$.

Titrant: 0.100 M NaCl.

Reaction: $AgNO_3 + NaCl \rightarrow \underline{AgCl} + NaNO_3$.

Initial Solution Conductance: 0.0122 mhos/cm.

Graph: Figure 62.

Calculated End Point: 1.000 mls.

Experimental End Point: 1.015 mls.

Per Cent Error: +1.5%.

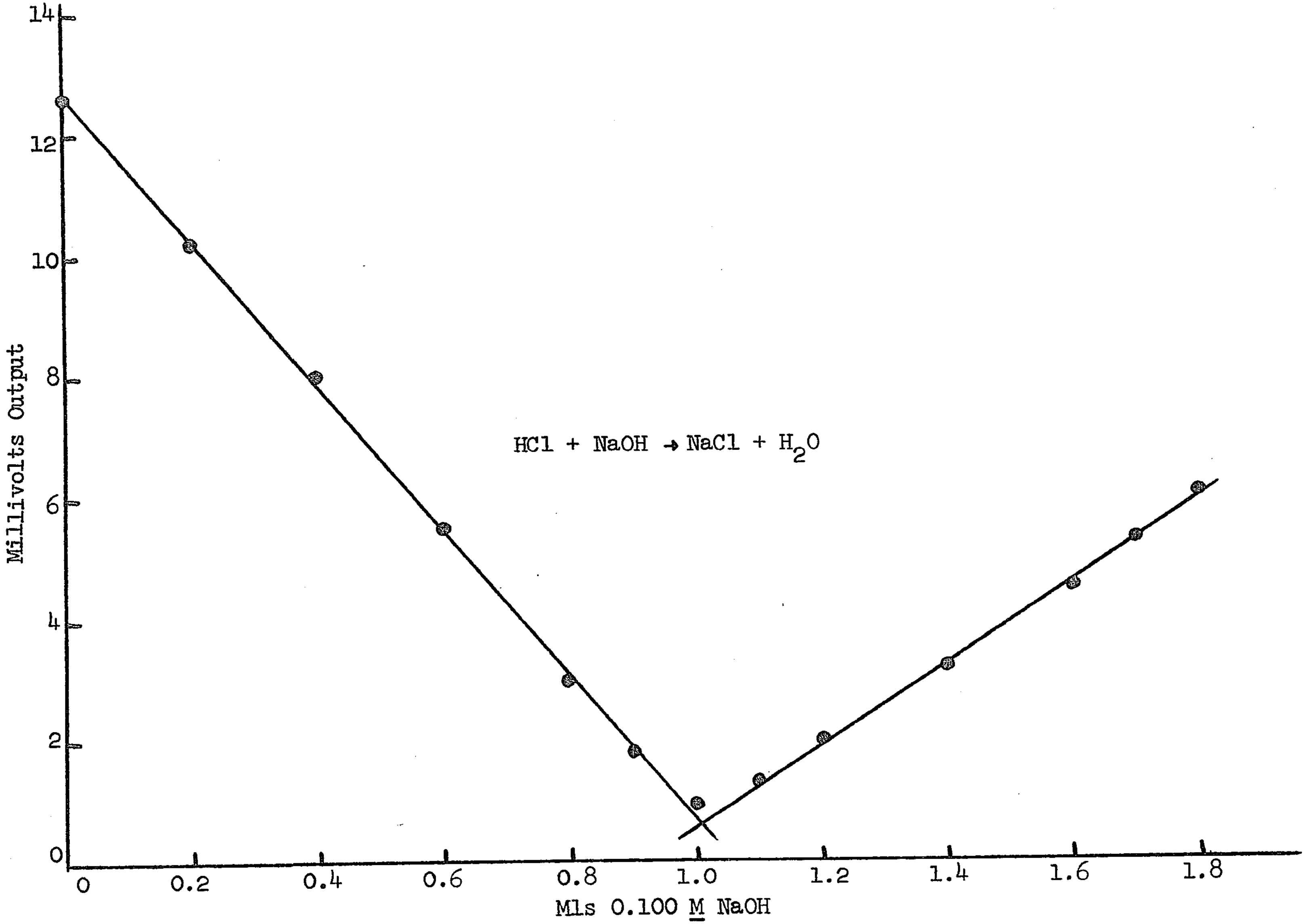

Figure 61. Acid-Base Titration in 0.10 M NaCl

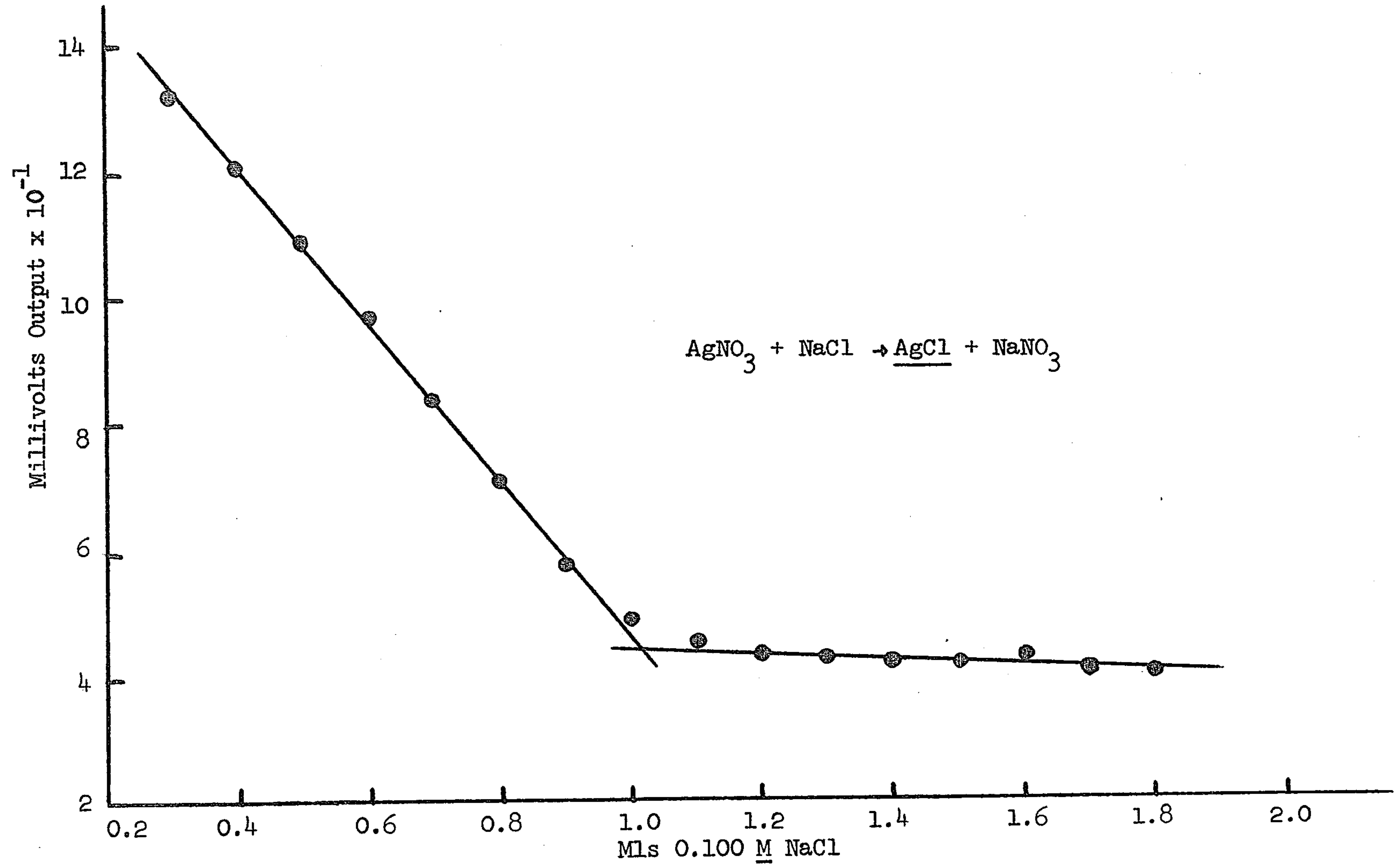

Figure 62. Precipitation Titration in 0.10 M $NaNO_3$

iii. Compleximetric Titrations.

(a) Zn(II) with EDTA.

Mode: R_{box} differential, FET.

Solution: 125 mls, 0.176 M in NH_3 and 0.032 M in NH_4Cl.

Sample: 0.420 meq $Zn(NO_3)_2$.

Titrant: 0.0999 M EDTA.

Reaction: Zn(II) + EDTA → Zn·EDTA.

Initial Solution Conductance: 0.0046 mhos/cm.

Graph: Figure 63.

Calculated End Point: 4.204 mls.

Experimental End Point: 4.235 mls.

Per Cent Error: +0.7%.

This titration was used by Johnson and Enke[50] to demonstrate a new bipolar pulse conductance technique which is capable of measuring small changes in conductance in a highly conducting solution. In the vicinity of the end point, the EDTA titration of Zn^{2+} in the highly buffered medium represents a conductance change of 40 micromhos out of 40,000 total.[50] These authors were able to locate the end point only if the titration was automatically recorded using an automatic buret for titrant delivery.

A titration using Probe C was performed using their "worst case" conditions, i.e., their highest buffer concentration. Their conductometric end point correlated within 0.2% with an Eriochrome Black T titration on the same solution. The end point obtained in this work agreed within 0.7% of that using the same visual indicator.

---

[50] D. E. Johnson and C. G. Enke, Anal. Chem. 42, 329 (1970).

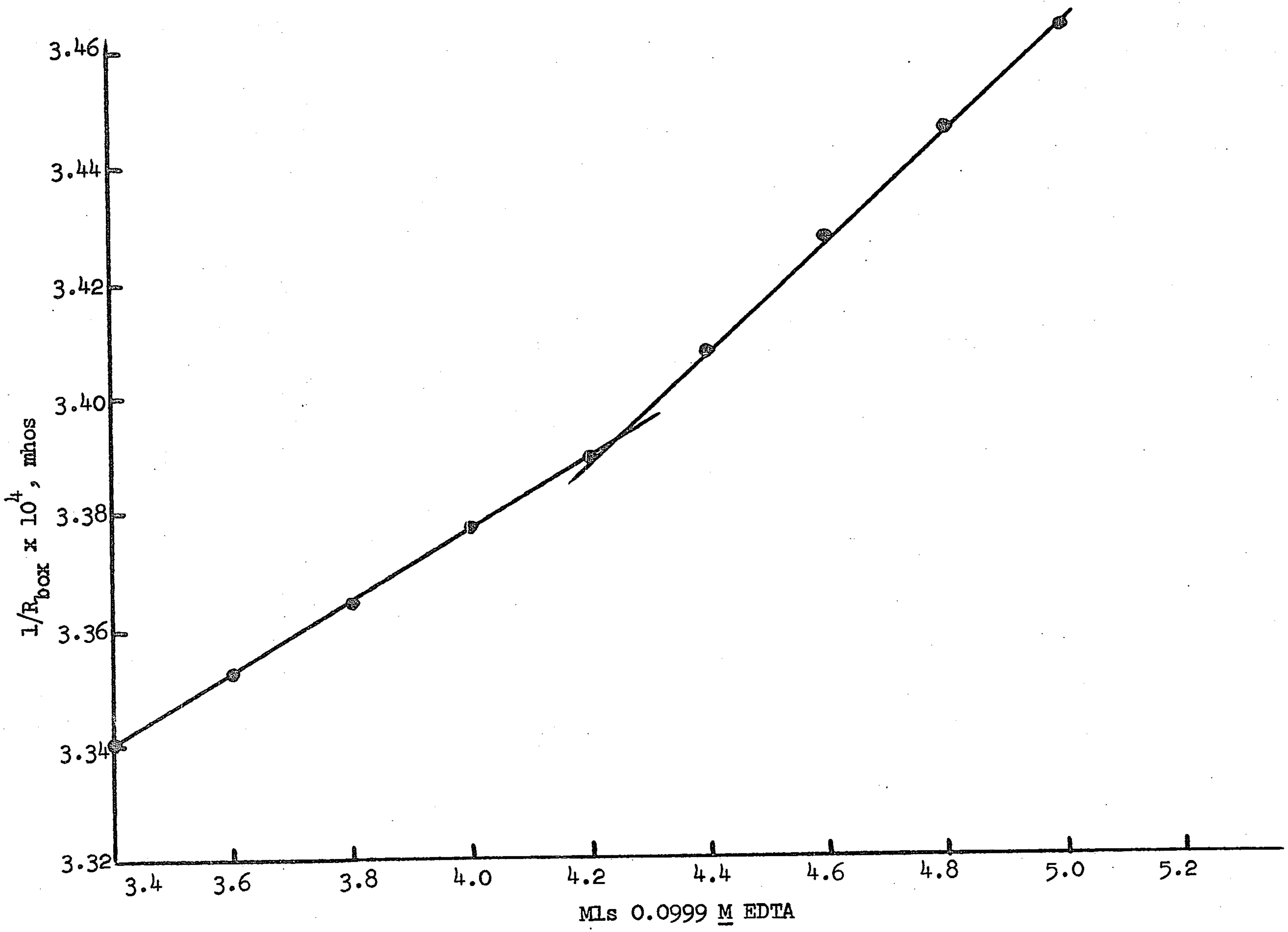

Figure 63. Compleximetric Titration of Zn(II)

However, the end point using Probe C could be obtained using manual plotting methods; the location of the end point using Probe C is also much less ambiguous than that using the bipolar pulse technique (which uses conventional platinum electrodes).

(b) TiO^{2+} with EDTA. This titration[41] involves the determination of the titanium-hydrogen peroxide complex by adding an excess of EDTA, and back titrating the excess EDTA with standard Fe^{3+} using salicylic acid as the visual indicator for comparison with the conductometric end point.

Mode: Delta mv, FET.

Solution: 15 mls CH_3OH, 2 mls 1.0 M H_2SO_4, 75 mls H_2O, 0.5 ml of 3% H_2O_2, 1 ml of 2% salicylic acid in CH_3OH; sufficient sodium acetate was added to bring the pH of the solution to 2.55.

Sample: approximately 0.05 meq TiO^{2+}.

Titrants: 0.0999 M EDTA and 0.101 M Fe^{3+}.

Reaction: EDTA (excess) + Fe(III) → Fe(III)·EDTA.

Initial Solution Conductance: 0.0081 mhos/cm.

Graph: Figure 64.

Visual End Point: 0.513 mls (average of 3 analyses); standard deviation of a single determination (s) for the 3 analyses was ± 0.2%.

Conductometric End Point: 0.517 mls (average of 3 analyses); s = ± 1.0%.

Per Cent Error (from visual end point): +0.8%.

Titer of Sample (average of visual and conductometric analyses): 0.0481 M TiO^{2+}.

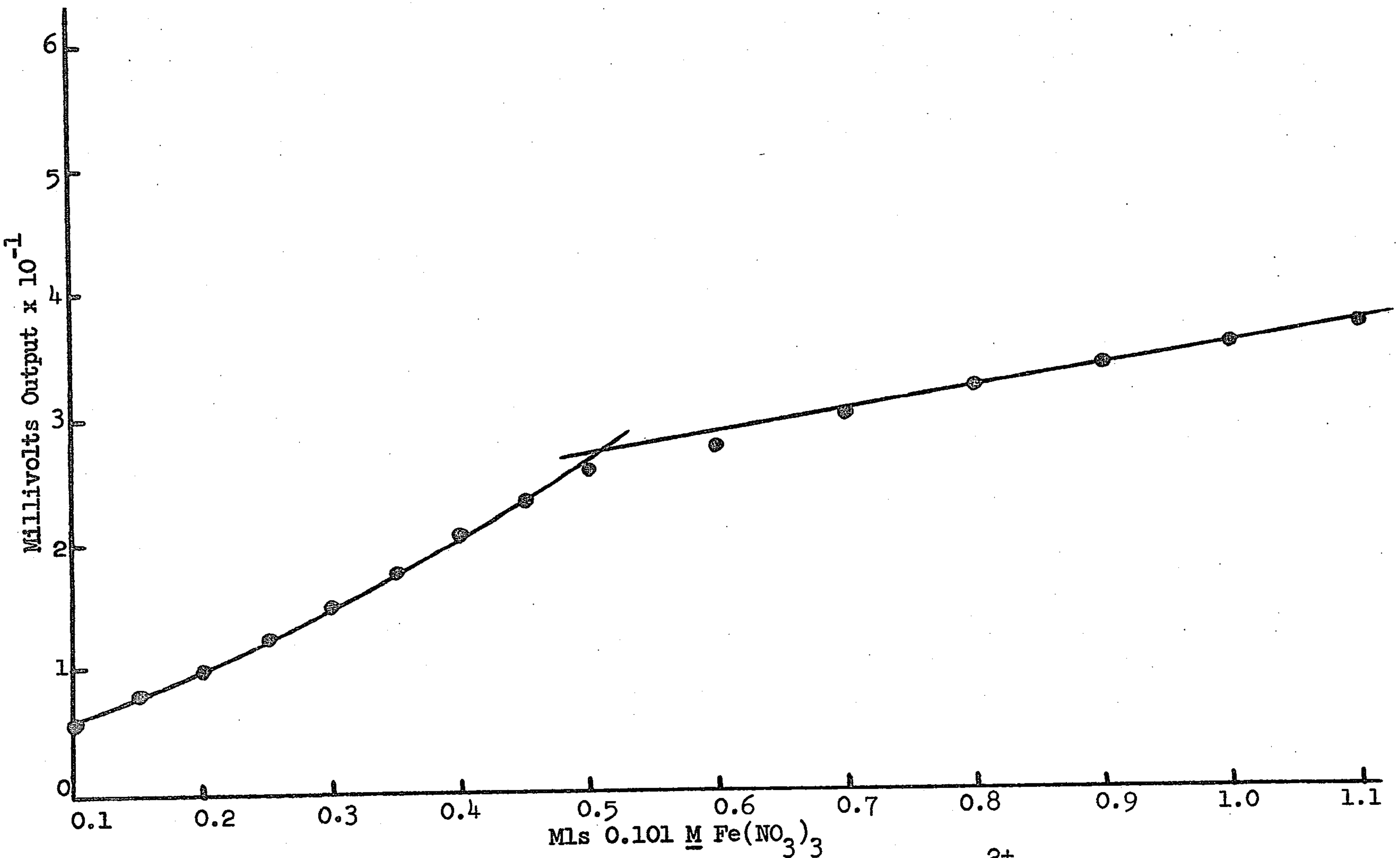

Figure 64. Compleximetric Titration of TiO^{2+}

iv. Redox Titrations. Because these magnetic induction probes can "null out" conductance contributions from foreign electrolytes and respond only to the small conductance change of interest, attention was focused on the possibility of detecting end points in redox titrimetry. Many redox titrations involve a decrease in hydrogen-ion concentration, although the relative changes in a highly acid solution are small. Because removal of H_3O^+ gives a sharp decrease in conductance, the end point using a probe should be well defined since the conductance contribution from the bulk acid can be eliminated.

In general, the titrations to be reported are performed according to classical procedures[51] except that the titrants (or samples) may be made up in an inert electrolyte solution. Usually the samples were smaller than the ones used in classical redox analyses.

In each titration the accuracy and precision of the end point determined by conductometric means was judged by the end point found using a visual indicator present in the same solution. When it was found necessary, indicator blank corrections were made.

(a) Titration of Ferrous Iron with Permanganate.

Mode: Delta mv, no FET.

Solution: 100 mls of 0.10 M H_2SO_4.

Sample: 0.51 meq $FeSO_4(NH_4)_2SO_4 \cdot 6H_2O$.

Titrant: 0.10 N $KMnO_4$.

---

[51] I. M. Kolthoff et al., "Quantitative Chemical Analysis," 4th ed., The Macmillan Co. Ltd., London, 1969.

Reaction: $MnO_4^- + 5Fe^{2+} + 8H^+ \rightarrow Mn^{2+} + 5Fe^{3+} + 4H_2O$.

Initial Solution Conductance: 0.045 mhos/cm.

Graph: Figure 65.

Visual End Point: 5.00 mls.

Conductometric End Point: 5.04 mls.

Per Cent Error: +0.8%.

(b) Standardization of HCl Using KIO_3.

Mode: Delta mv, no FET.

Solution: 100 mls H_2O, 3 gms (18.0 m Moles) KI, 3.2 gms (20.2 m Moles) $Na_2S_2O_3$, 2 drops of 0.1% methyl orange indicator.

Sample: 5.00 meq KIO_3.

Titrant: approx. 1.00 N HCl.

Reactions: $IO_3^- + 5I^- + 6H^+ \rightarrow 3I_2 + 3H_2O$;

$2Na_2S_2O_3 + I_2 \rightarrow Na_2S_4O_6 + 2NaI$.

Initial Solution Conductance: 0.048 mhos/cm.

Graph: Figure 66.

Visual End Point: 4.99 mls.

Conductometric End Point: 4.98 mls.

Per Cent Error: -0.2%.

(c) Standardization of $Na_2S_2O_3$ with KIO_3.

Mode: Delta mv, no FET.

Solution: 100 mls 0.10 M H_2SO_4, 2 gms (12 meq) KI, 5 mls starch solution (added near the end point).

Sample: 2.500 meq KIO_3.

Titrant: approx. 0.100 N $Na_2S_2O_3$ in 1 M KCl.

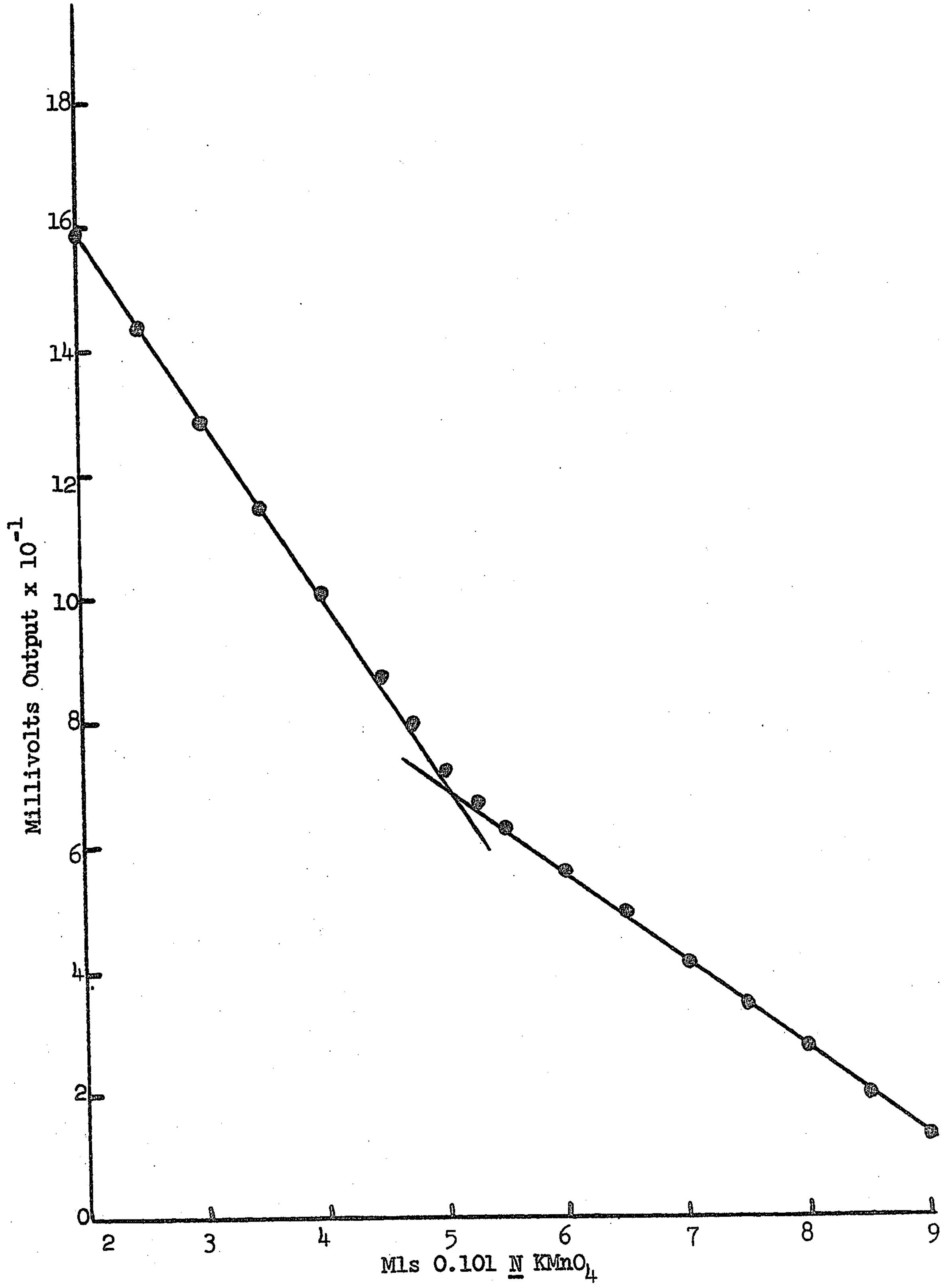

Figure 65. Titration of Iron(II) with Permanganate

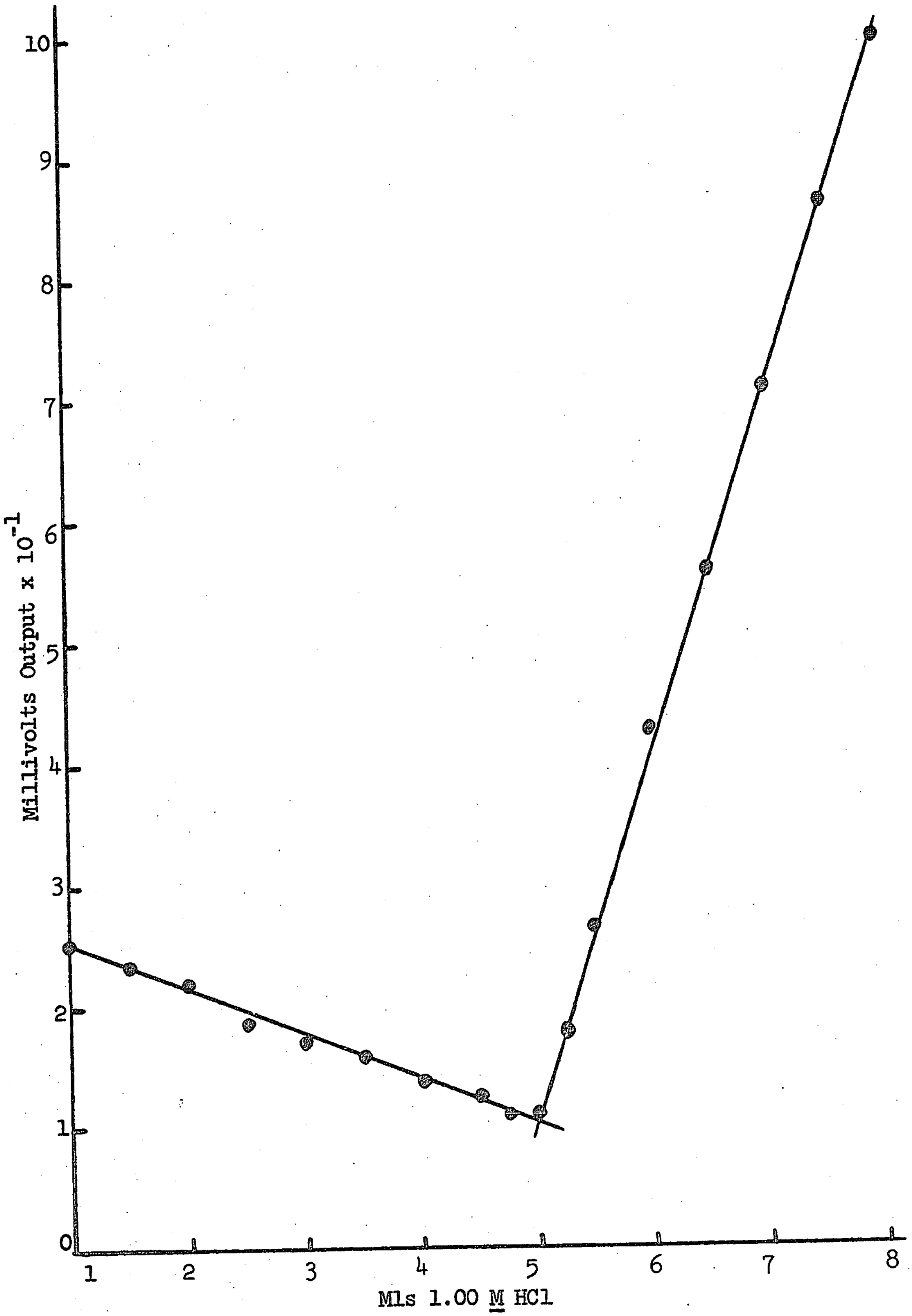

Figure 66. Standardization of HCl with KIO_3

Reactions: $IO_3^- + 5I^- + 6H^+ \rightarrow 3I_2 + 2H_2O$;

$2Na_2S_2O_3 + I_2 \rightarrow Na_2S_4O_6 + 2NaI$.

Initial Solution Conductance: 0.070 mhos/cm.

Graph: Figure 67.

Visual End Point: 25.52 mls.

Conductometric End Point: 25.12 mls.

Per Cent Error: -1.6%.

(d) Titration of $Na_2S_2O_3$ with I_2 in KI.

Mode: Delta mv, no FET.

Solution: 100 mls H_2O, 4 gms KI, 5 mls starch solution.

Sample: 1.00 meq $Na_2S_2O_3$.

Titrant: 0.200 N I_2 in KI.

Reaction: $2Na_2S_2O_3 + I_2 \rightarrow Na_2S_4O_6 + 2NaI$.

Initial Solution Conductance: .028 mhos/cm.

Graph: Figure 68.

Visual End Point: 5.03 mls.

Conductometric End Point: 5.02 mls.

Per Cent Error: -0.2%.

(e) Standardization of I_2 with As_2O_3.

Mode: Delta mv, no FET.

Solution: 85 mls of 0.025 M phosphate buffer, pH = 6.85 (0.025 M in KH_2PO_4 and Na_2HPO_4), 5 mls starch solution, 4 gms KI.

Sample: 1.00 meq As_2O_3.

Titrant: 0.200 N I_2 in KI.

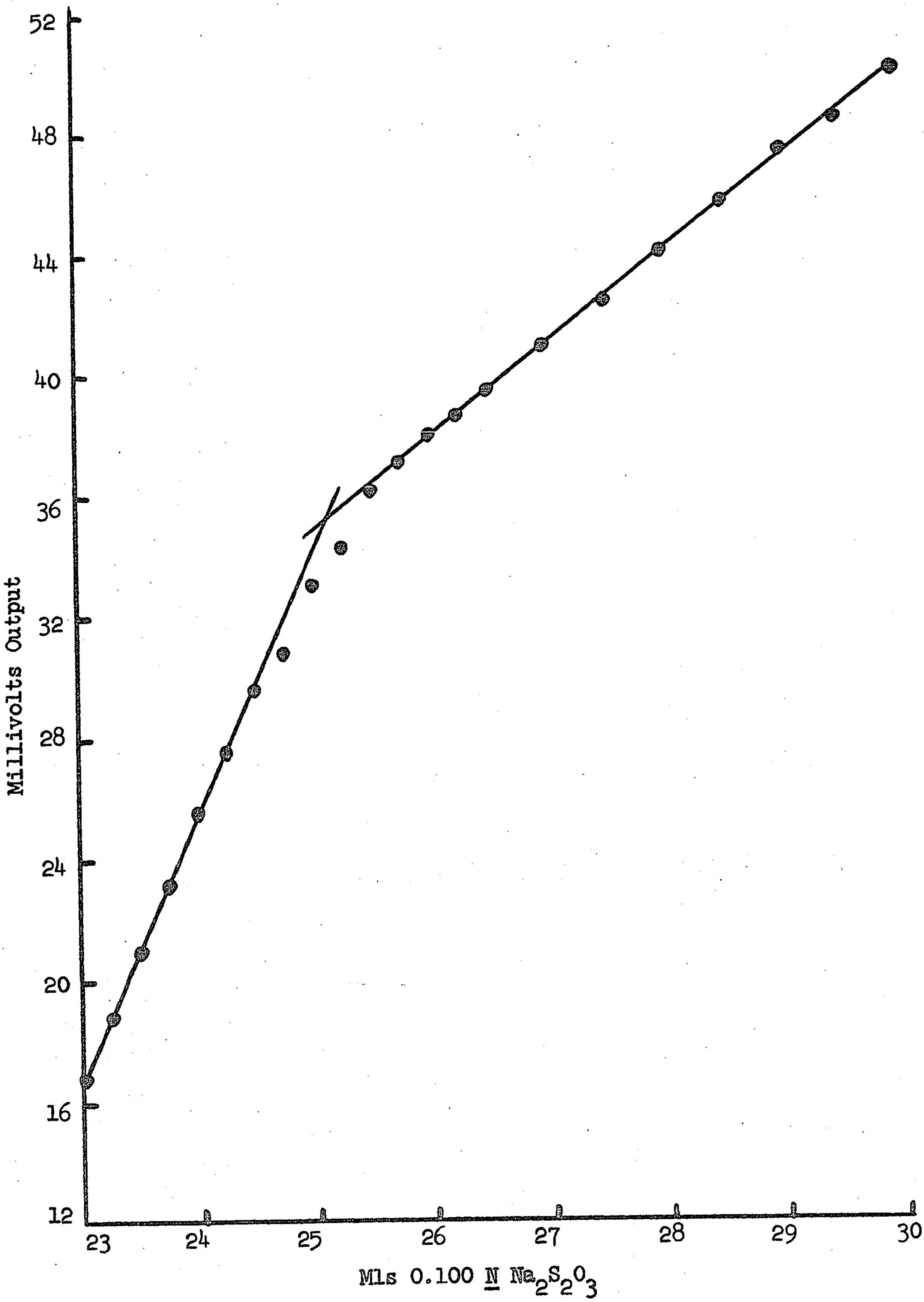

Figure 67. Standardization of $Na_2S_2O_3$ with KIO_3

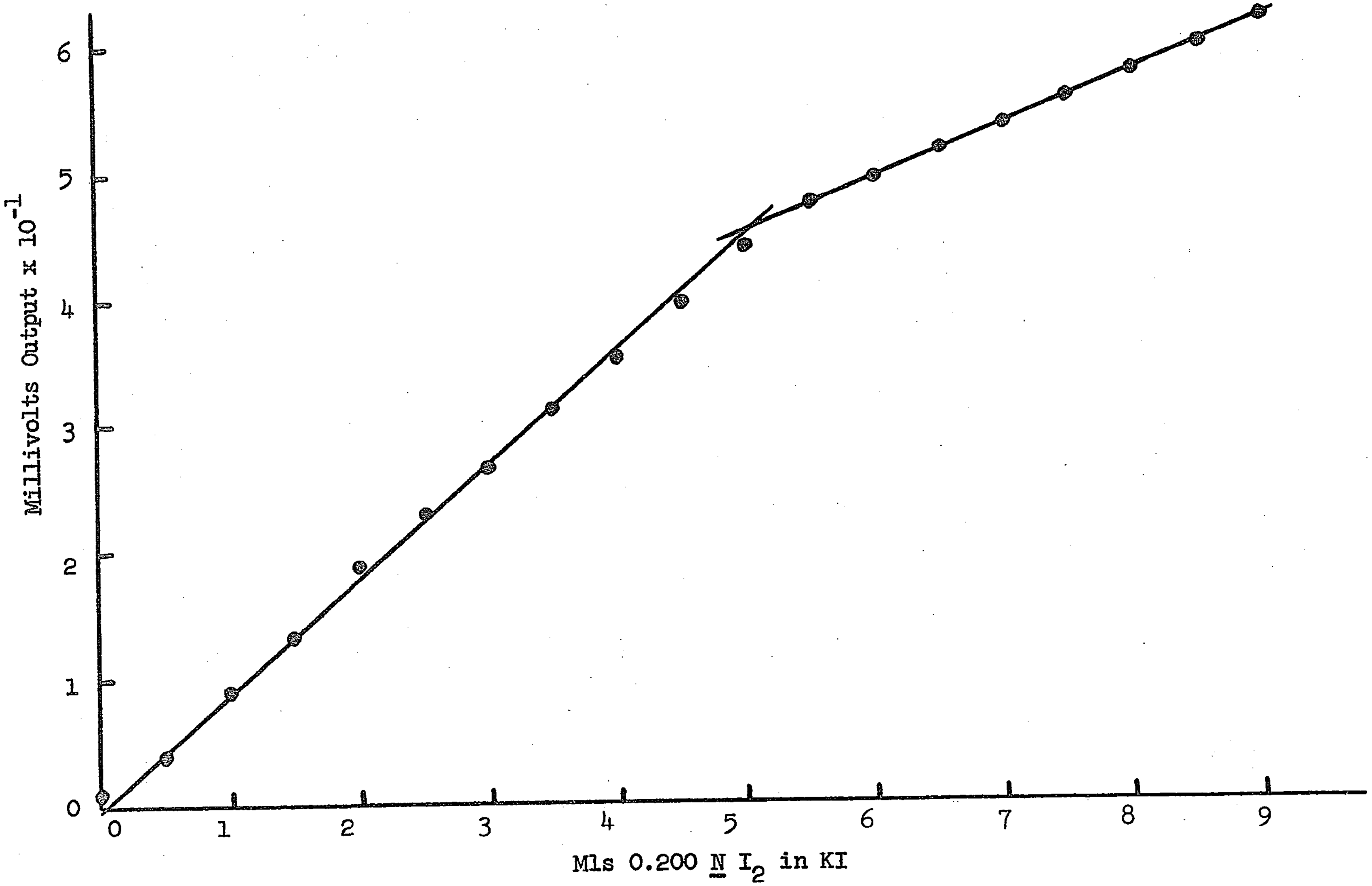

Figure 68. Titration of $Na_2S_2O_3$ with Iodine

Reaction: $As_2O_3 + 2I_2 + 5H_2O \rightarrow 2HAsO_4^{2-} + 4I^- + 8H^+$.

Initial Solution Conductance: 0.031 mhos/cm.

Graph: Figure 69.

Visual End Point: 5.00 mls.

Conductometric End Point: 5.06 mls.

Per Cent Error: +1.2%.

(f) Assay of Potassium Ferrocyanide Using Cerate. This reaction was selected to estimate the precision which would be possible in an analysis using a magnetic induction probe. The concentration ratio of foreign electrolyte (1 M H_2SO_4) to sample species (5.0 mM $K_4Fe(CN)_6$) was 200:1. However, the specific conductance of a 5mM solution of $K_4Fe(CN)_6$ in water was approximately 1.35×10^{-2} mhos/cm. The specific conductance of 1 M sulfuric acid[52] at 25°C is approximately 0.4 mhos/cm; therefore the ratio of foreign electrolyte conductance to sample conductance was near 30:1.

Commercial hydrated $K_4Fe(CN)_6$ was dried for 4 hours at 110°C and stored over CaO in a desiccator.

Mode: Delta mv, no FET.

Solution: 100 mls of 1.0 M H_2SO_4, 1 drop of 0.025 M ferrous-phenanthroline indicator.

Sample: 0.500 meq $K_4Fe(CN)_6$.

Titrant: 0.100 N $Ce(SO_4)_3^{2-}$.

Reaction: $Fe(CN)_6^{4-} + Ce(SO_4)_3^{2-} \rightarrow Fe(CN)_6^{3-} + Ce^{3+} + 3SO_4^{2-}$.

Initial Solution Conductance: 0.4 mhos/cm.

Graph: Figure 70.

Results: Table XII.

---

[52] Lange, p. 1207.

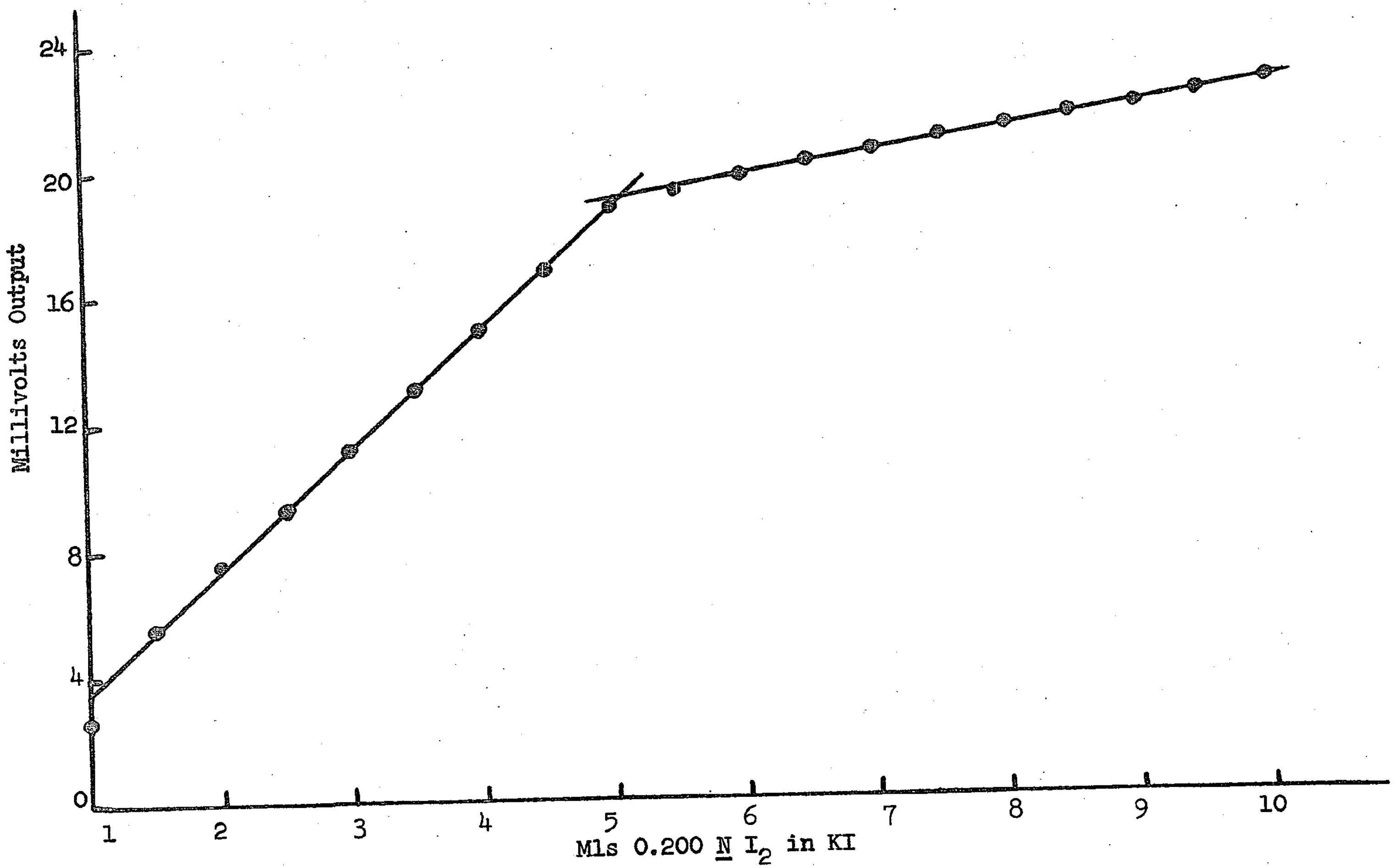

Figure 69. Standardization of I_2 with Arsenious Oxide

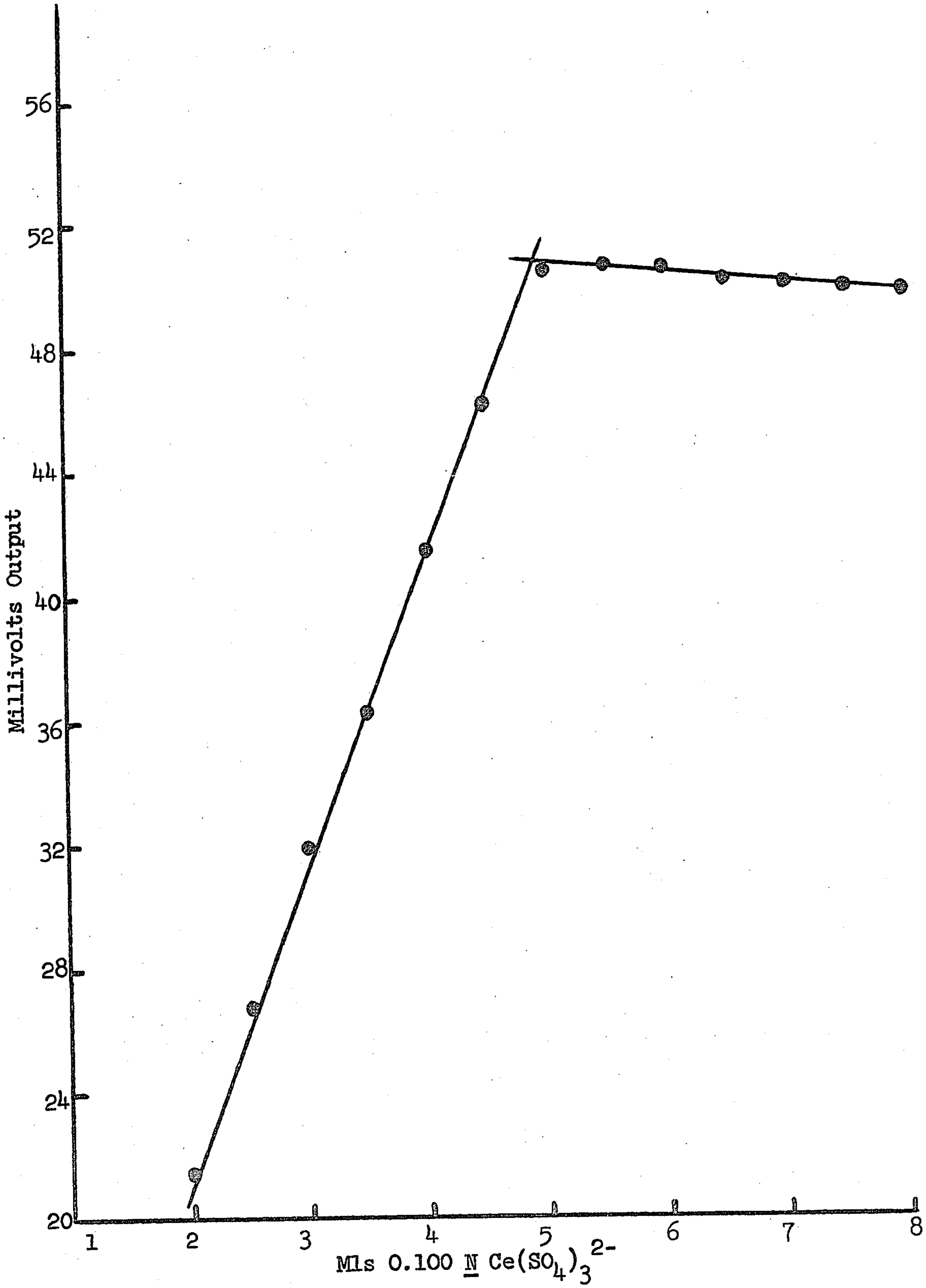

Figure 70. Assay of Ferrocyanide with Cerate

TABLE XII

Accuracy and Precision of Ferrocyanide Assay

Visual Indicator Method

Sample	Meq taken	Meq found	Assay, %	Difference from mean, %
1	0.5131	0.523	98.1	0.0
2	0.5084	0.516	98.5	+0.4
3	0.5212	0.532	98.0	-0.1
4	0.5231	0.536	97.7	-0.4
Mean			98.1	
Std. dev.				s = ± 0.3%

Conductometric (Probe C) Method

Sample	Meq taken	Meq found	Assay, %	Difference from mean, %
1	0.498	0.487	97.8	-0.1
2	0.512	0.502	98.0	+0.1
3	0.489	0.480	98.2	+0.3
4	0.502	0.494	98.4	+0.5
5	0.547	0.532	97.3	-0.6
Mean			97.9	
Std. dev.				s = ± 0.4%

The precision of the results is expressed as the standard deviation of a single measurement. The precision of the assay is 3 ppt for the visual method of end point detection and 4 ppt for the conductometric method. These values of precision not only agree well with one another, but also compare favorably with the precision limits expected using classical redox procedures. It should be noted too that the sample size of $K_4Fe(CN)_6$ used was 7 to 8 times smaller than that normally used for a typical macromolar redox titration.

The true assay value of the ferrocyanide was taken as 98.1%, since this value was also found using a potentiometric readout system in which the potential break at the end point was followed using platinum and saturated calomel electrodes. Thus, the assay by Probe C agrees within 0.2% of that found by conventional techniques.

d. Probe F - Titrations at Very Low Solution Conductances. Probe F was developed to extend the usable response of the Magnetic Induction Method to the micromolar concentration range. Although this was the primary purpose of Probe F, it may, of course, be used wherever Probe C was employed.

Three silver halide precipitation titrations were selected for a study of the accuracy and precision obtainable using Probe F. Two of these studies involved a comparison with the conventional low frequency conductometric method; another study was performed using only the standard reagent titers for evaluation of the obtainable precision and accuracy.

i. Titration of $AgNO_3$ with NaCl using Probe F.

Mode: Delta mv, FET, Normal Operating Conditions = 30.0 kHz, 4.5 ma.

Solution: 150 mls H_2O, seeded with crystals of AgCl; alternately, 150 mls 67% ethanol and no seed crystals.

Sample: 25.0 microequivalents $AgNO_3$, concentration in 150 mls of $H_2O = 1.67 \times 10^{-4}$ M.

Titrant: 0.0250 M NaCl.

Reaction: $AgNO_3 + NaCl \rightarrow \underline{AgCl} + NaNO_3$.

Initial Solution Conductance: 23.5×10^{-6} mhos/cm.

Graph: Figure 71.

Results: Table XIII.

TABLE XIII

Accuracy and Precision of $AgNO_3$ Analyses

Sample	μeq taken	μeq found, Wheatstone bridge	Difference from mean, %	μeq found, Probe F	Difference from mean, %
1	25.0	23.5	-0.8	-	-
2	25.0	23.6	-0.4	23.6	+0.4
3	25.0	23.3	-1.6	23.5	0.0
4	25.0	23.6	-0.4	23.3	-0.9
5	25.0	24.3	+2.4	-	-
6	25.0	24.0	+1.2	-	-
Mean		23.7		23.5	
Std. dev.			s = ± 1.5%		s = ± 0.7%
% error		-5.2%		-6.0%	

The average values of Ag^+ found by the two conductometric methods are seen to agree well. The assay by both conductance methods

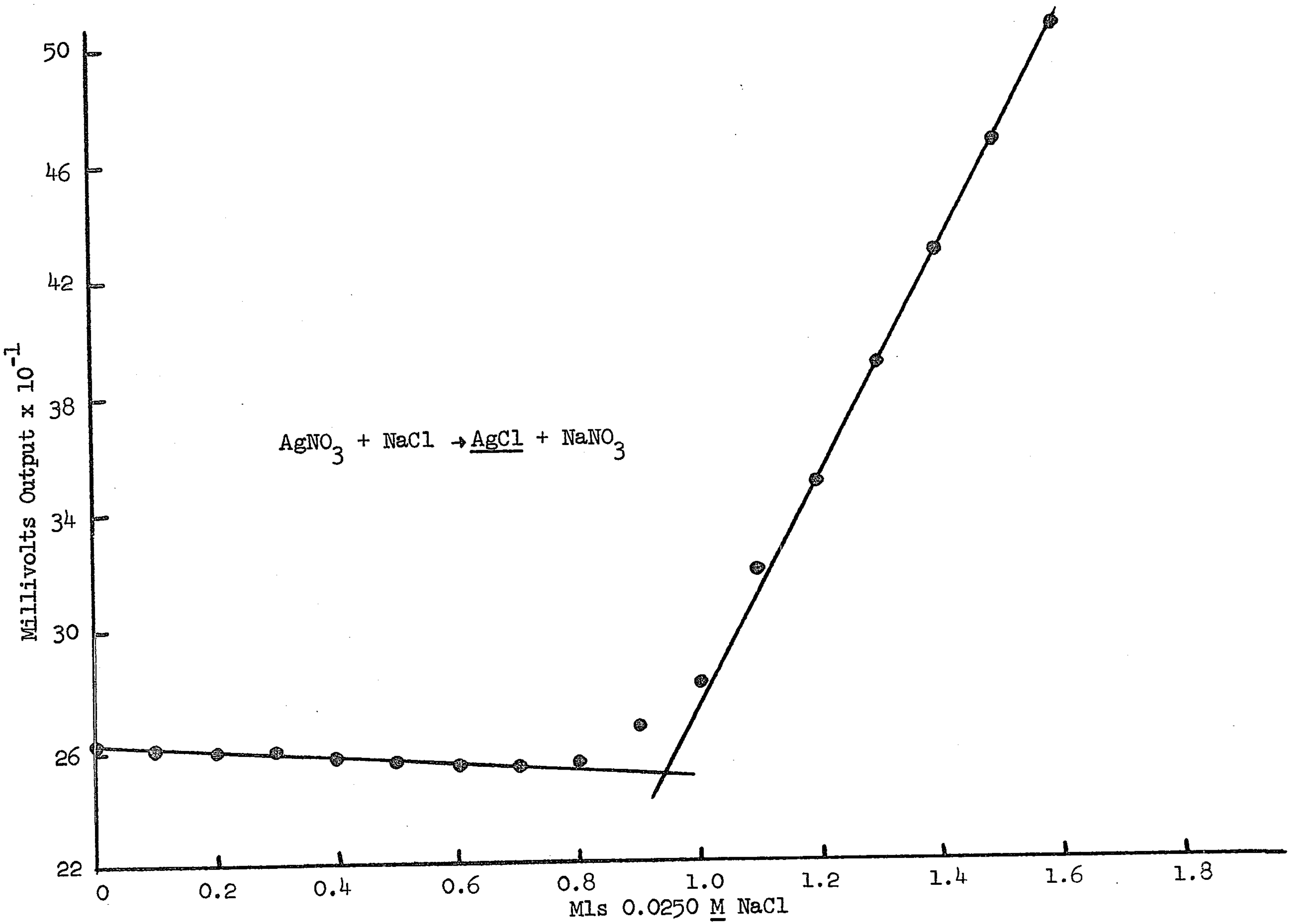

Figure 71. Precipitation Titration Using Probe F

is low by 5.6%. A correction factor can be calculated for the error introduced by the solubility of the AgCl in the vicinity of the equivalence point[14] in order to obtain the true assay value; however, since the purpose of the analysis was to compare the assay by Probe F to that found using the Wheatstone bridge, "relative" assay values sufficed. The "accuracy" of analysis by Probe F, assuming that the bridge analysis is correct, is -0.8%. The precision obtained by the classical bridge method is worse by a factor of 2, in terms of the standard deviation of a single measurement.

ii. Titration of $AgNO_3$ with KI. In order to minimize problems due to precipitate solubility, AgI, which has a lower K_{sp} value than AgCl, was made to be the product of the reaction.

Mode: Delta mv, FET.

Solution: 150 mls H_2O.

Sample: 15.0 microequivalents $AgNO_3$, concentration = 1.00×10^{-4} M.

Titrant: 0.0250 M KI.

Reaction: $AgNO_3 + KI \rightarrow \underline{AgI} + KNO_3$.

Initial Solution Conductance: 14×10^{-6} mhos/cm.

Graph: Figure 72.

Results: Table XIV.

By using AgI as the precipitate in the analysis of $AgNO_3$, the accuracy of the analysis has been increased greatly over that found using AgCl as the precipitate.

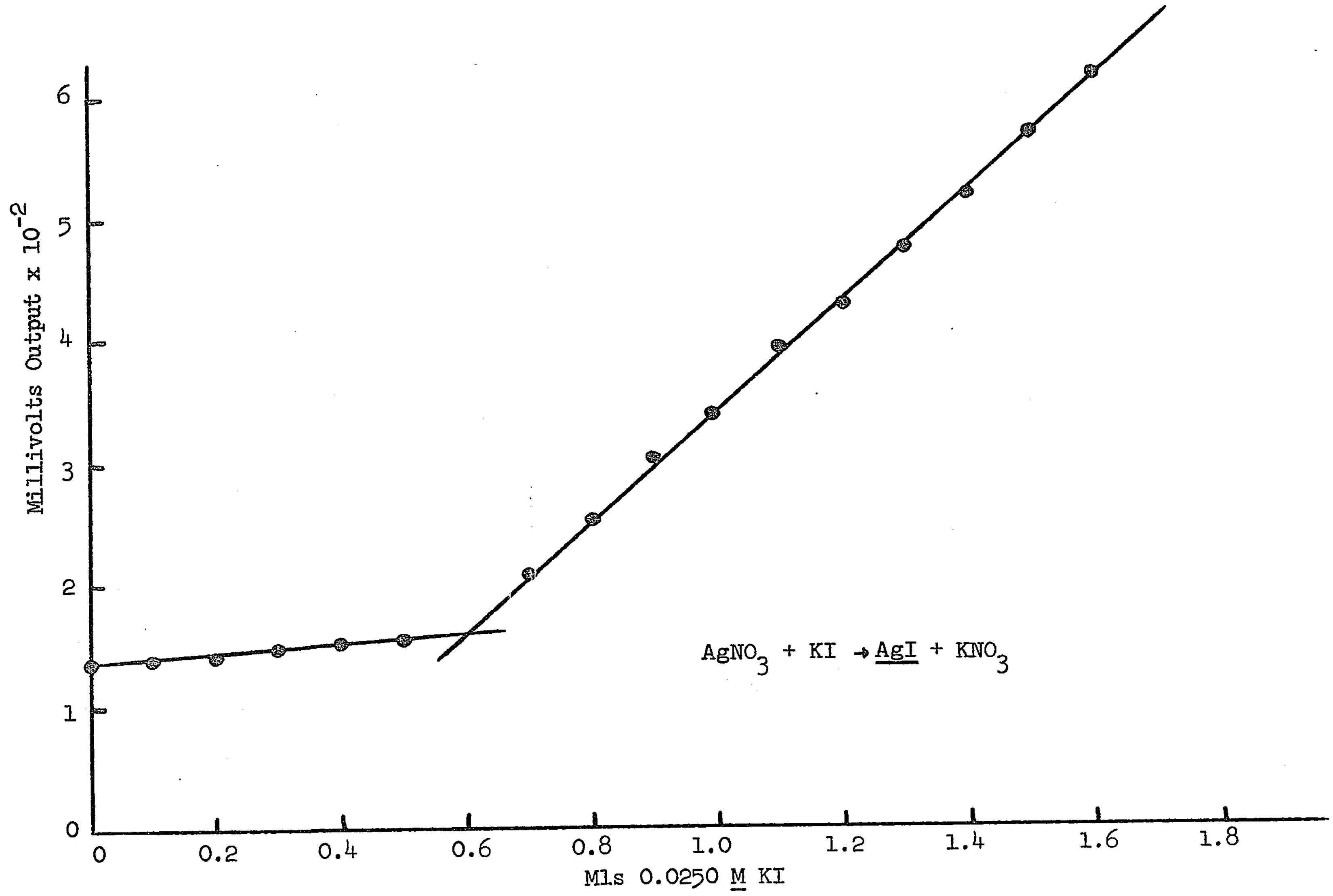

Figure 72. Precipitation Titration Using Probe F

TABLE XIV

Determination of $AgNO_3$ with KI (Probe F)

Sample	μeq taken	μeq found	Difference, %
1	15.0	15.2	+1.3
2	15.0	15.0	0.0
3	15.0	14.8	-1.3
4	15.0	15.1	+0.7
5	15.0	14.9	-0.7
Mean		15.0	
Std. dev.			s = ± 1.1%
% error		0.0%	

iii. Titration of 3.33×10^{-5} M $AgNO_3$ with KI. This analysis represents the lowest conductance level investigated (4.8×10^{-6} mhos/cm). It does not represent the lower limit of analyses possible with Probe F.

Mode: Delta mv, FET.

Solution: 150 mls H_2O.

Sample: 5.00 microequivalents $AgNO_3$, concentration = 3.33×10^{-5} M.

Titrant: 0.0100 M KI.

Reaction: $AgNO_3 + KI \rightarrow \underline{AgI} + KNO_3$.

Initial Solution Conductance: 4.8×10^{-6} mhos/cm.

Graph: Figure 73.

Results: Table XV.

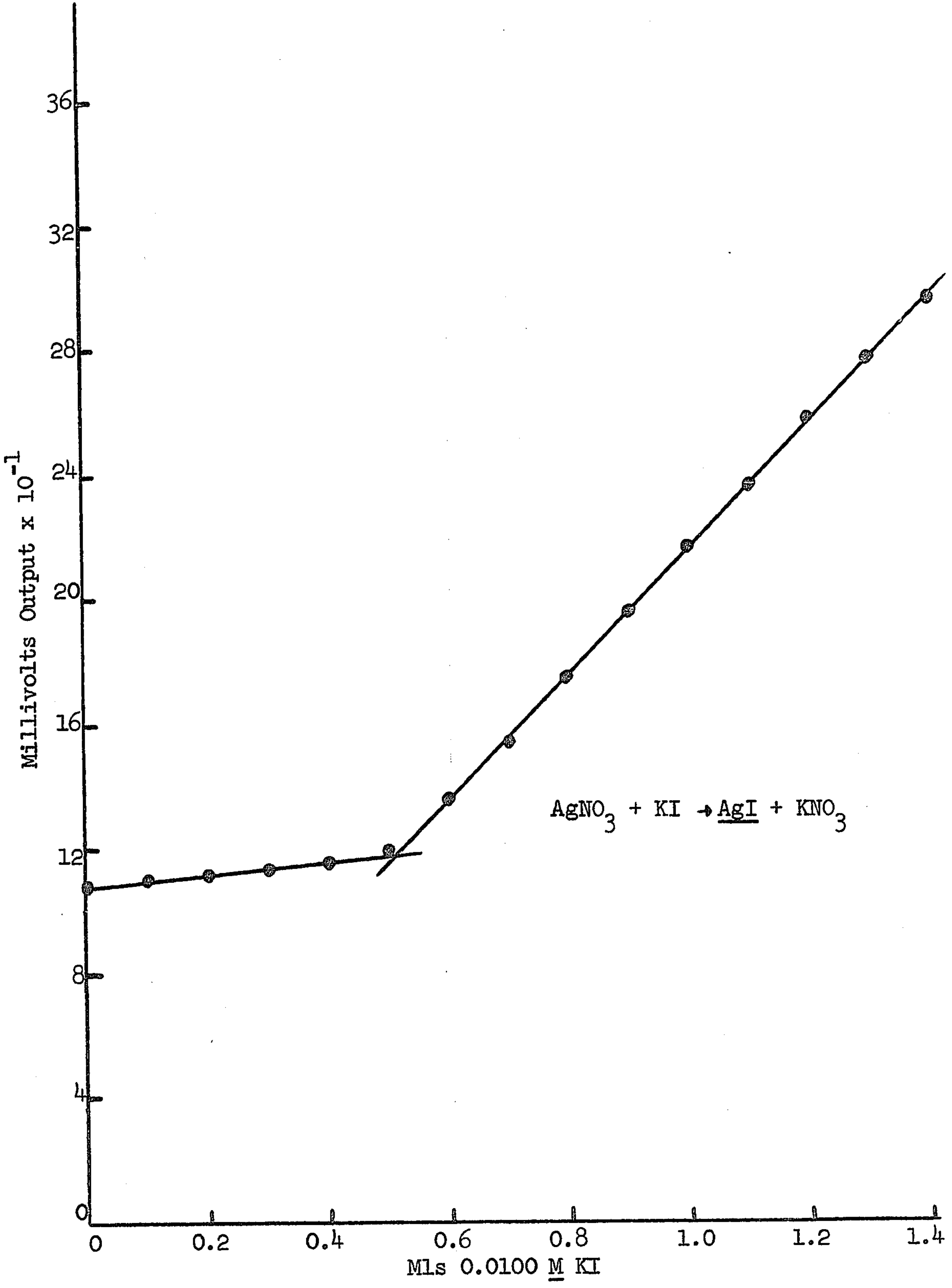

Figure 73. Precipitation Titration Using Probe F

TABLE XV

Determination of $AgNO_3$ (3.33×10^{-5} M) with KI

Sample	μeq taken	μeq found, Wheatstone bridge	Difference from mean, %	μeq found, Probe F	Difference from mean, %
1	5.00	4.86	-0.6	5.01	-1.4
2	5.00	4.83	-1.2	5.04	-0.8
3	5.00	4.99	-0.2	5.12	+0.8
4	5.00	-	-	5.17	+1.8
Mean		4.89		5.08	
Std. dev.			s = ± 1.0%		s = ± 1.5%
% error		-2.2%		+1.6%	

Even at these low concentration levels, the precision and accuracy obtained by Probe F agree extremely well with those found using the conventional bridge method.

iv. Conclusions. Using Probe F, the analysis of a solution whose specific conductance is 5 micromhos/cm can be performed with a standard deviation of ± 1.5%. An estimated lower limit for precipitation titrations would involve a solution whose specific conductance is approximately 2 micromhos/cm.

e. Probe F - Titrations in the Presence of Foreign Electrolyte.

i. Titration of $AgNO_3$ with KI. Titrations of 5.00 microequivalents (concentration = 3.33×10^{-5} M) of $AgNO_3$ with KI were performed in a 0.10 mM solution of $NaNO_3$. This excess electrolyte represents a concentration ratio of electrolyte to sample of 30:1. An extra table of data (Table XVI) has been included to compare typical data readings using magnetic induction Probe F to those using a Wheatstone bridge and platinized electrodes ($\theta = 0.306\ cm^{-1}$).

Mode: Delta mv, FET.

Solution: 150 mls 0.10 M $NaNO_3$.

Sample: 5.00 microequivalents $AgNO_3$, concentration = 3.33×10^{-5} M.

Titrant: 0.0100 M KI in H_2O.

Reaction: $AgNO_3 + KI \rightarrow \underline{AgI} + KNO_3$.

Initial Solution Conductance: 144×10^{-6} mhos/cm; conductance due to $AgNO_3 = 4.8 \times 10^{-6}$ mhos/cm.

Graphs: Figure 74 (Probe F) and Figure 75 (Wheatstone bridge).

Data: Table XVI.

Results for Probe F: Table XVII.

TABLE XVI

Comparison of Data: Probe F vs. Wheatstone bridge

Mls titrant	Mv, Probe F	Relative conductance values using Wheatstone bridge, in μmhos
0.000	8.4	472
0.100	8.3	473
0.200	8.6	473
0.300	8.8	474
0.400	8.7	475
0.500	9.1	475
0.600	11.2	479
0.700	13.7	481
0.800	16.3	484
0.900	19.0	489
1.000	21.8	492

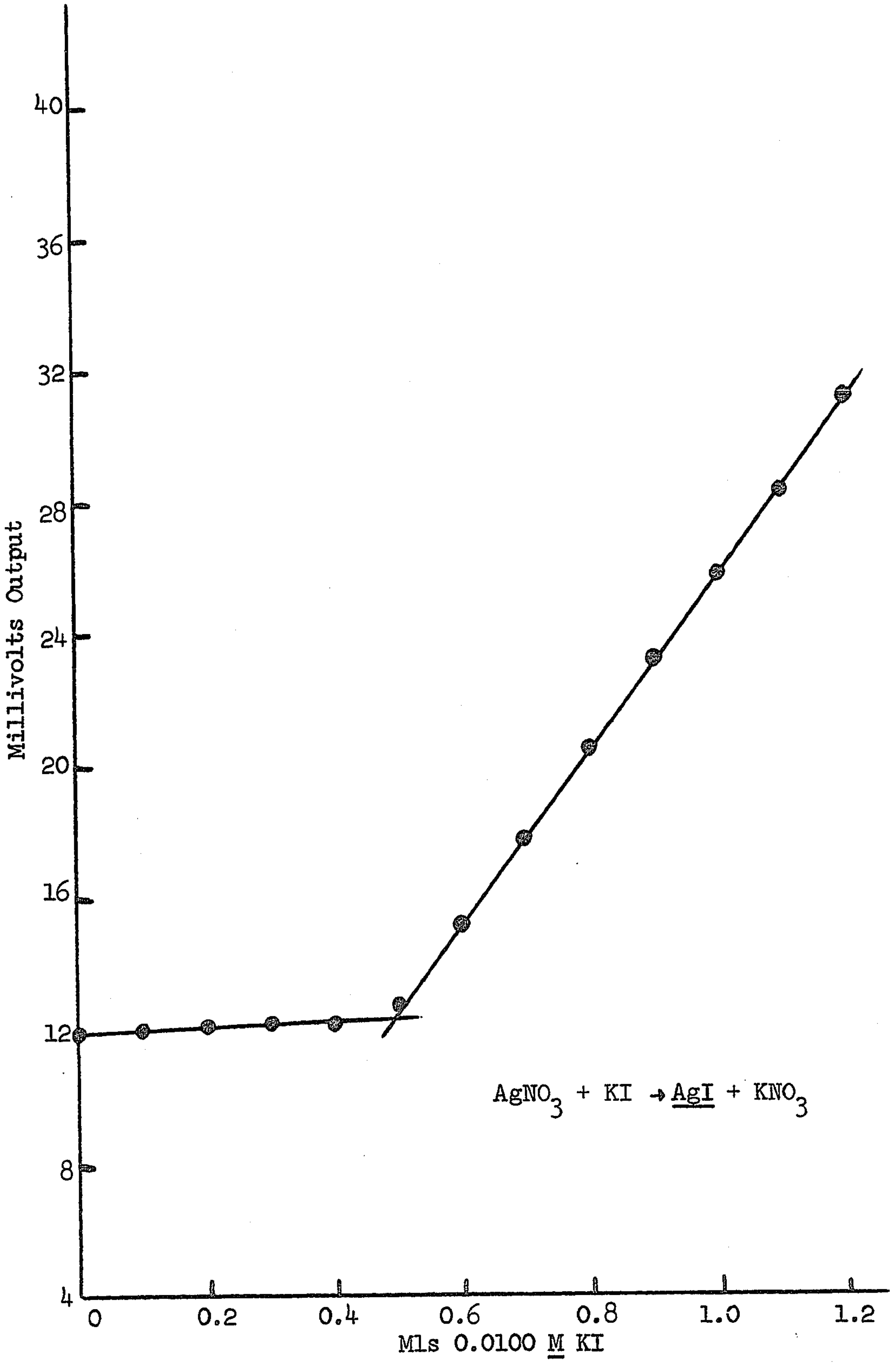

Figure 74. Precipitation Titration in 1.0 mMolar $NaNO_3$ Using Probe F

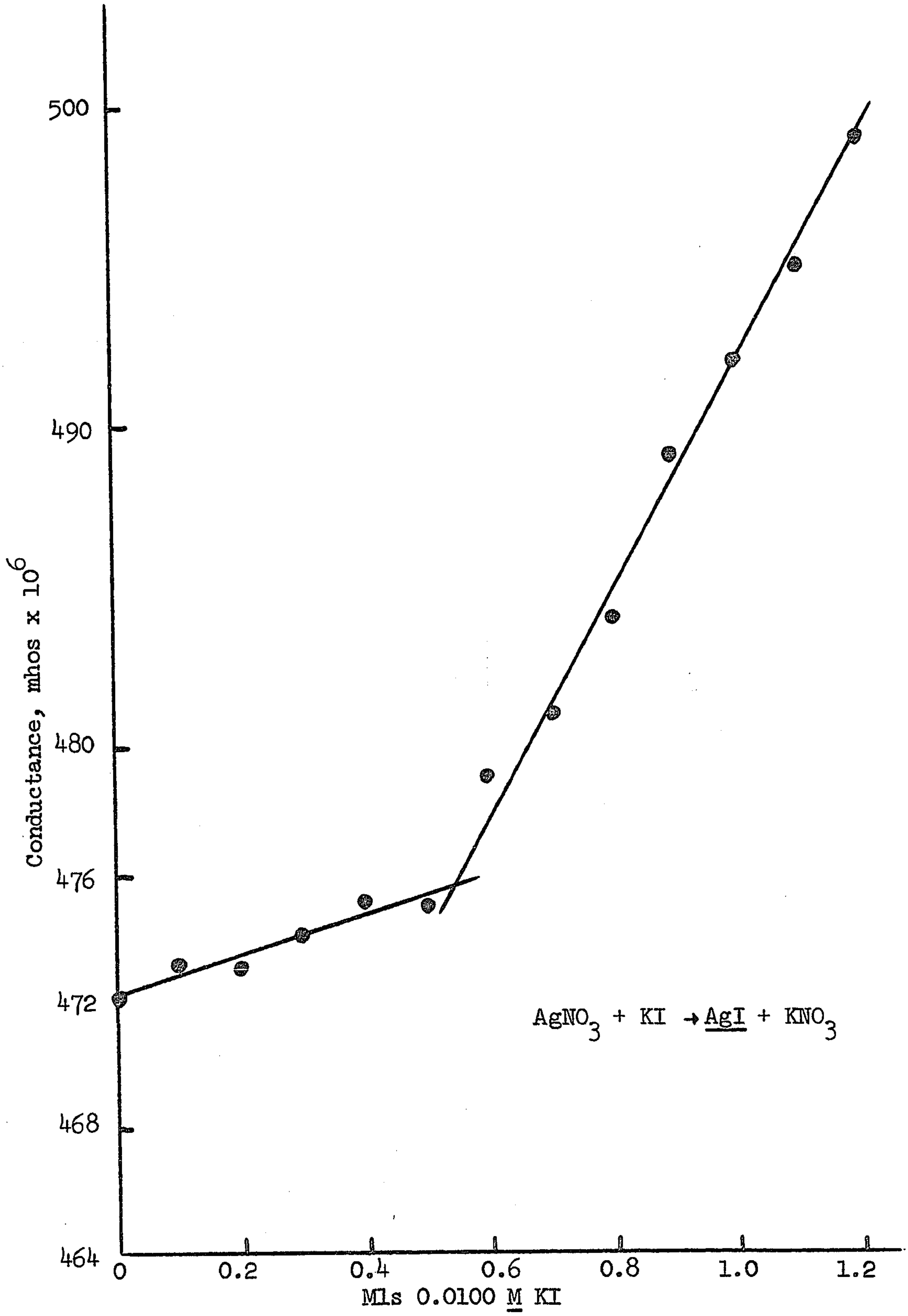

Figure 75. Precipitation Titration in 1.0 mM $NaNO_3$ Using a Wheatstone Bridge

TABLE XVII

Determination of $AgNO_3$ in 0.10 mM $NaNO_3$ Using Probe F

Sample	μeq taken	μeq found	Difference from mean, %
1	5.00	4.86	-0.6
2	5.00	4.83	-1.2
3	5.00	4.99	+1.0
Mean	5.00	4.89	
Std. dev.			s = ± 1.2%
% error		-2.2%	

ii. Conclusions. Because the titration was performed in a 100 fold excess of $NaNO_3$, Figure 75 shows a large degree of data scatter for the conventional Wheatstone bridge method. This is the expected result of reading small differences between large numbers. It should be noted that such data scatter is absent in Figure 74 using Probe F. Graphical smoothing yields an analysis error of +7% for the bridge analysis and -2.2% for Probe F.

Hall *et al.*[53] have proposed the use of a "resolving limit" in terms of concentration differences to show the superiority of one measuring system over another. Although this calculated resolving limit is arbitrary and dependent on many factors, it does represent a practical basis for determining which of two available measuring systems is better suited for a particular application. Their equation is: resolving limit = $\Delta C \times \Delta R/(\Delta \text{ dial for } \Delta C)$, where ΔC is the change in solution concentration, R is the reproducibility (precision) of a single measurement in the particular concentration range (in terms of mhos or millivolts), and Δ dial is the change in instrument reading caused by the above concentration change.

---

[53] J. L. Hall *et al.*, Anal. Chem. 26, 1539 (1954).

Thus, using the data of Table XVI, the following Table (XVIII) was constructed.

TABLE XVIII

Resolving Limits of Two Conductance Measuring Systems in a 100-fold Excess of $NaNO_3$

Method of conductance measurement	Reproducibility (precision of a single measurement)	ΔC, moles liter^{-1} of KI	Δ dial for ΔC (for values after the end point)	Resolving limit, moles liter^{-1}
Probe F	± 0.3 mv (± 1%), mv full scale = 30	1.67×10^{-5}	2.65 mv	2.0×10^{-6}
Wheatstone bridge	± 1.0 μmho (± 0.2%) at 500 μmhos, (θ = 0.306)	1.67×10^{-5}	3.3 μmhos	5.1×10^{-6}

These resolving limits represent the smallest concentration changes that can be detected by each measuring system. As might be expected, the resolving limit for Probe F is better(by a factor of about 2.5) in the 1 mM $NaNO_3$ medium. Evidence of this superiority is clearly observable by comparing the data scatter of Figures 74 and 75. Although the precision of a single conductance measurement by the classical bridge method (no foreign electrolyte) is better by a factor of 5, the bridge method cannot compete with the magnetic induction probe in solutions of high excess electrolyte.

The accuracy and precision obtained using Probe F in all the low level analyses performed were considered excellent; a change in the titrant used from KI to LiI would result in even sharper end point breaks, with a corresponding improvement in precision and accuracy.

Thus, an outstanding feature of using magnetic induction probes is that, within wide limits, the standard deviations are essentially identical whether an excess of foreign electrolyte is present (Table XVII, s = ± 1.2%) or absent (Table XV, s = ± 1.5%). Since most analyses contain contributions to the total conductance from other nontitratable ions, the Magnetic Induction Method of conductance analysis would seem to offer a considerable advantage to the analyst.

11. Literature Specifications and Applications

a. Commercial Salinometers. The Beckman Salinometer* (Model RS-7B) measures absolute conductance values by a null procedure using decade resistors. This, to the author's knowledge, is the only commercial apparatus which measures conductance in this manner; other salinometers measure only difference ratios between sample and standard sea water samples. The specifications for the Beckman Salinometer follow.[54]

---

*Beckman Instruments Co. Inc., Cedar Grove, New Jersey.

[54] Beckman Lab. Instrumentation Catalog 2500-A, June, 1967.

Ranges: 0 to 0.140 and 0 to 1.400 mhos/cm full scale.

Accuracy: ± 0.50% of full scale; i.e., on lowest scale,
± 70 micromhos/cm.

The lower limits of conductance measurement (for comparison with Probe F) are not known, since the instrument is only designed to measure moderate and highly conducting solutions with great precision.

Both Probes C and F could be designed to operate like this Salinometer at high conductivities using the Heath Decade Box if more null windings were placed on each toroid.

b. Applications. The only reported chemical analysis is that of Park et al.[33] using a commercial Salinometer.* These authors measured the total alkalinity of sea water as HCO_3^-, CO_3^{2-}, and $H_2BO_3^-$ using HCl. The concentration ratio of sea salt (assuming pure NaCl) to alkalinity was calculated to be 250:1. The reported relative standard deviation, s/mean, for six determinations was ± 0.5%.

It may be recalled that a similar titration was performed in this work (see Figure 61) in a 100-fold excess of NaCl. The error for that single determination was 0.5%.

12. Summary and Conclusions

From this study of five magnetic induction probes, the following conclusions regarding the response characteristics of these probes are warranted:

---

*Hytech Corp., Model 621, San Diego, California.

(1) The response to solution conductance obtained from each probe is linear and follows the laws of magnetic induction as expressed by Equations 3 and 4; i.e., the response sensitivity depends upon the frequency used, the amperage flowing in the primary toroid, and the turns ratio (M) between the two toroids; the value of M also depends upon the inductances of the toroids and their distance apart. In general, all of these variables are interdependent.

(2) The response sensitivity also depends upon the cell constant of the particular probe, the solution container width, and the value of solution loop conductance; to further explain this last factor, it may be recalled that the response slope becomes less sensitive and nonlinear at low values of solution conductance.

(3) Maximum probe sensitivity is achieved by operating the output (receiver) toroid as a parallel resonant circuit.

(4) The most sensitive frequency for probe operation is that frequency where the i·f product is a maximum. Contrary to certain literature reports, frequency is a primary variable in the operation of these magnetic induction probes.

(5) The Delta mv differential mode of probe operation results in greater response linearity (and hence sensitivity) at low conductance levels. This occurs because the output VTVM is sensing all impedance changes associated with a

particular probe and not just the resistive component of impedance; the true differential mode of operation senses only changes in resistance.

Two of the probes (C and F) were selected for detailed study. Probe C was best used at high solution conductances because of its large cell constant; its response sensitivity begins to fall off at specific conductance values lower than 1 x 10^{-3} mhos/cm. Probe F, with its lower cell constant, produced a linear response in the true differential mode to specific conductances of 2 x 10^{-5} mhos/cm. This lower response limit was obtainable by the use of better shields and low operating frequency (30 kHz) to reduce the capacitive losses of Probe F.

Both probes can be used with solutions one order of magnitude lower in specific conductance values than mentioned above if the Delta mv differential mode of operation is used. The precision obtainable at these low conductance levels has been evaluated.

Many chemical applications using these two probes were developed. In analyses where ordinary low frequency conductance techniques are applicable, these electrodeless probes were capable of comparable precision and accuracy. In analyses where conventional methods are unsuitable, i.e., in solutions containing large amounts of foreign salts, as in redox titrations, these probes still provide the same precision and accuracy as when all foreign salts are absent. Such chemical applications have not been previously reported.

Using Probe F and the techniques of probe operation already described, analyses of 10^{-5} M solutions whose specific conductances are 5×10^{-6} mhos/cm have been performed with a standard deviation of ± 2% (with or without the presence of inert salt). The ability to perform electrodeless conductance analyses at this concentration level was a primary goal of this work.

E. Summary

Initial attempts at electrodeless conductance measurements using toroids resulted in responses which closely resembled those obtained using classical impedimetric equipment; several experiments were performed which showed that the Immersion and Sidearm responses follow the predictions of impedimetric (high frequency analysis) theory. Optimum sensitivity for these methods was obtained at frequencies 6 to 12 db low from toroid resonance. Using frequencies under 500 kHz, both of the above methods proved applicable to solutions whose specific conductance was in the range 1 to 2500 x 10^{-6} mhos/cm.

In addition to the direct mode impedimetric response, it was found possible to operate these toroids in a differential mode; the net impedimetric response was then resolved into its resistive and capacitive components. The obtainable precision of the Immersion and Sidearm Methods when operated in a differential mode is near 1%.

Using electrostatic shields on the Sidearm Apparatus, a magnetic response to solution conductance changes was found; the total conductance (1/R) response of the Sidearm Method closely resembled that found by other investigators[16,17] who also used inductive sensing equipment to measure changes in solution impedance.

For subsequent magnetic conductance measurements, the toroidal inductors were incorporated into dipping type measuring probes. It was found that these probes followed the laws pertaining to induced magnetic effects; certain conflicting literature reports about probe operation were clarified by subsequent measurements. A method was developed whereby one could easily ascertain the optimum operating parameters for a particular probe.

The differential response of two probes was studied in detail; it was found that conductometric analyses could be performed from 5 x 10^{-6} mhos/cm specific conductance to virtually any upper concentration limit. The measurement techniques which allowed the successful application of these probes at the micromolar level were described in detail. Using these probes, the precision and accuracy of chemical analyses in the areas of acid-base, complexation, precipitation, and redox titrimetry were evaluated. Even in a 200-fold excess of sulfuric acid (1 $\underline{M}$), analyses of $K_4Fe(CN)_6$ (0.5 meq) were possible to a precision of ± 0.4%. For a 100-fold excess of foreign electrolyte, the accuracy and precision of analyses using these magnetic induction probes were identical to those obtained in the absence of excess electrolyte.

Thus this work has shown that electrodeless conductance measuring techniques using toroidal inductors give results comparable to conventional low frequency conductance techniques; in the presence of large amounts of foreign electrolytes, these probes permit precise and accurate analyses which are unobtainable using classical conductance methods.

Finally, the equipment required for these electrodeless conductance measurements is both simple and inexpensive.

APPENDIX A

SPECIFIC CONDUCTANCE VALUES OF HCl SOLUTIONS AT 25°C USED IN SECTIONS III B AND III C

Cell Constant = θ = 0.294 cm^{-1}

HCl Concentration, $\underline{M} \times 10^6$	Specific Conductance, mho $\text{cm}^{-1} \times 10^6$
5.0	1.5
12.5	4.6
24.8	8.4
37.2	13.9
49.5	18.8
73.9	27.7
98.0	36.2
146	53.4
192	68.4
238	80.5
356	123
474	177
591	250
708	269
939	361
1,168	445
1,620	619
2,163	774
2,500	935
3,850	1,510
5,200	2,020
6,980	2,670
9,200	3,520
11,400	4,600
15,700	5,800
19,960	7,210
24,100	8,690
44,000	15,800
144,000	44,000

APPENDIX B

SPECIFIC CONDUCTANCE VALUES OF KCl SOLUTIONS AT 25°C USED IN SECTION III D

Cell Constant = θ = 0.324 cm^{-1}

KCl Concentration, moles $liter^{-1}$	Specific Conductance, mhos cm^{-1} Experimental	Literature[53]
1.00×10^{-5}	1.60×10^{-6}	-
1.00×10^{-4}	1.53×10^{-5}	1.489×10^{-5}
1.00×10^{-3}	1.481×10^{-4}	1.469×10^{-4}
1.00×10^{-2}	1.415×10^{-3}	1.413×10^{-3}
1.00×10^{-1}	1.244×10^{-2}	1.289×10^{-2}
1.00	1.104×10^{-1}	1.119×10^{-1}

---

[53] Daniels and Alberty, p. 361.

APPENDIX C

SPECIFIC CONDUCTANCE VALUES OF NaCl SOLUTIONS AT 25°C USED IN SECTION III D

Cell Constant = θ = 0.306

NaCl Concentration, M x 10^6	Specific Conductance, mhos cm^{-1} x 10^6
3.3	0.46
6.6	0.91
13.2	1.64
19.6	2.65
26.0	3.51
32.3	4.41
44.6	6.02
49.8	6.58
66.2	8.82
99.0	13.2
132	17.5
196	26.1
260	34.5
323	42.5
385	51.0
446	59.1
506	67.1
566	75.0
625	82.6
700	91.5
800	103.8
900	116
1000	128

APPENDIX D

TABLE OF ABBREVIATIONS

Hz	Hertz (cycles per second)
rms	root-mean-square
vdc	volt(s) direct current
vac	volt(s) alternating current
db	decibel(s)
pf	picofarad(s) (10^{-12} farads)
μfd	microfarad(s) (10^{-6} farads)
h	henries (unit of inductance)
mh	millihenries
VTVM	vacuum tube voltmeter
I (or i)	current
f	frequency (in Hz)
w	angular frequency ($=2\pi f$)
μ_o	relative initial permeability
ϵ	dielectric constant
s	standard deviation
ppt	parts per thousand
Ω	ohm(s)
V or E	volt(s)

REFERENCES CITED

1. "The Radio Amateur's Handbook," 44th ed., American Radio Relay League (publisher), 1967.

2. H. V. Malmstadt et al., "Electronics for Scientists," W. A. Benjamin, Inc., New York, 1963.

3. R. L. Weber et al., "Physics for Science and Engineering," McGraw-Hill Book Co., Inc., New York, 1959, p. 409.

4. R. L. Weber et al., "Physics for Science and Engineering," McGraw-Hill Book Co., Inc., New York, 1959, p. 349.

5. C. N. Reilley in P. Delahay, "New Instrumental Methods in Electrochemistry," Interscience Publishers Inc., New York, 1954.

6. W. G. Berl (ed.), "Physical Methods in Chemical Analysis," Vol. 3, Academic Press Inc., New York, 1956.

7. I. M. Kolthoff and P. J. Elving (ed.), "Treatise on Analytical Chemistry," Part I, Vol. 4, Interscience Publishers Inc., New York.

8. E. Pungor, "Oscillometry and Conductometry," Pergamon Press, Oxford, 1965.

9. C. L. Wilson and D. W. Wilson (ed.), "Comprehensive Analytical Chemistry," Elsevier Publishing Co., New York, 1964.

10. A. Timnick et al., Chemistry in Canada 12, 23 (1960).

11. Piccard and Frivold, "Archives des Sciences Physiques et Naturelles" (Series 5) 2, 264 (1920); cited in U. S. Patent 2,542,057.

12. S. Ruben, U. S. Patent 1,610,971, Dec. 14, 1926.

13. G. G. Blake, "Conductimetric Analysis at Radio Frequency," Chemical Publishing Co., Inc., New York, 1952.

14. F. W. Jensen and A. L. Parrack, Ind. Eng. Chem., Anal. Ed. 18, 595 (1946).

15. A. Bellomo, J. Electroanal. Chem. 27, 267 (1970).

16. S. Fujiwara and S. Hayashi, Anal. Chem. 26, 239 (1954).

17. Y. Kamura, Yakugaku Zasshi 74, 1 (1954).

18. M. J. Relis, U. S. Patent 2,542,057, Feb. 20, 1951.

19. Beckman Instruments Co., Inc., Cedar Grove, New Jersey, Model RS7-B.

20. Hytech Marine Products, San Diego, California, Model 6220.

21. S. R. Gupta et al., J. Sci. Instr. 33, 313 (1956).

22. R. Calvert et al., J. Phys. Chem. 62, 47 (1958).

23. V. S. Griffiths, Anal. Chim. Acta 18, 174 (1958).

24. V. S. Griffiths, Talanta 2, 230 (1959).

25. B. Lavagnino and B. Alby, Ann. Chim. 49, 1272 (1959).

26. N. L. Brown and B. V. Hamon, Deep-Sea Research 8, 65 (1961).

27. V. I. Lopatnikov, Soviet Physics (Eng. trans.) 6, 505 (1961).

28. M. De Rossi, Sci. Tec. 6, 31 (1962); C. A. 61, 3754 (1964).

29. C. M. Johnson and G. E. Hart, Rocky Flats Internal Report RFP-657, U. S. Atomic Energy Commission, 1966.

30. C. M. Johnson and G. E. Hart, Anal. Instrum. 4, 23 (1967).

31. A. E. Hackl and H. Deisinger, Allgemeine and Praktishe Chemie 19, 229 (1968).

32. L. Pazsitka et al., Z. Anal. Chem. 245, 103 (1969).

33. K. Park et al., Anal. Chem. 35, 1549 (1963).

34. R. F. Zarilla, "New Instrumentation for Analysis by High Frequency Techniques," thesis, University of Pittsburgh, 1966.

35. D. Owen, "Alternating Current Measurements at Audio and Radio Frequencies," Methuen and Co. Ltd., London, 1957, p. 102.

36. H. W. Hamme et al., J. Chem. Phys. 22, 944 (1954).

37. M. F. C. Ladd and W. H. Lee, Talanta 12, 941 (1965).

38. J. L. Hall, Anal. Chem. 24, 1236 (1952).

39. C. N. Reilley and W. H. McCurdy, Jr., Anal. Chem. 25, 86 (1953).

40. S. C. Clayton et al., Anal. Chim. Acta 14, 269 (1956).

41. L. Meites (ed.), "Handbook of Analytical Chemistry," McGraw-Hill Book Co., New York, 1963.

42. J. C. Clayton *et al.*, Anal. Chim. Acta *14*, 269 (1956).

43. A. H. Collins, Analyst *87*, 733 (1962).

44. A. Campbell and E. C. Childs, "The Measurement of Inductance, Capacitance, and Frequency," Macmillan and Co. Ltd., London, 1935, p. 203.

45. R. Rosenthal (ed.), "Solution Conductivity Handbook," Beckman Instrument Bulletin 4090, 1969, p. 8.

46. A. Schure, "Transformers," J. F. Rider Publisher , Inc., New York, 1961, p. 19.

47. N. A. Lange (ed.), "Handbook of Chemistry," 10th ed., McGraw-Hill Book Co., Inc., New York, 1961, p. 1820.

48. F. Daniels and R. A. Alberty, "Physical Chemistry," 2nd ed., John Wiley and Sons, Inc., New York, 1961, p. 45.

49. N. A. Lange (ed.), "Handbook of Chemistry," 10th ed., McGraw-Hill Book Co., Inc., New York, 1961, p. 1211.

50. D. E. Johnson and C. G. Enke, Anal. Chem. *42*, 329 (1970).

51. I. M. Kolthoff *et al.*, "Quantitative Chemical Analysis," 4th ed., The Macmillan Co. Ltd., London, 1969.

52. N. A. Lange (ed.), "Handbook of Chemistry," 10th ed., McGraw-Hill Book Co., Inc., New York, 1961, p. 1207.

53. J. L. Hall *et al.*, Anal. Chem. *26*, 1539 (1954).

54. Beckman Lab. Instrumentation Catalog 2500-A, June, 1967.

BIBLIOGRAPHY

Beckman Laboratory Instrumentation Catalog 2500-A, June, 1967; Beckman Instruments Co., Inc., Cedar Grove, New Jersey.

Bellomo, A., J. Electroanal. Chem. 27, 267 (1970).

Berl, W. G. (ed.), "Physical Methods in Chemical Analysis," Vol. 3, Academic Press Inc., New York, 1956.

Blaedel, W. J., and Malmstadt, H. V., Anal. Chem. 22, 734 (1950).

Blake, G. G., "Conductimetric Analysis at Radio Frequency," Chemical Publishing Co., Inc., New York, 1952.

Brown, N. L. and Hamon, B. V., Deep-Sea Research 8, 65 (1961).

Calvert, R. *et al.*, J. Phys. Chem. 62, 47 (1958).

Campbell, A. and Childs, E. C., "The Measurement of Inductance, Capacitance, and Frequency," Macmillan and Co. Ltd., London, 1935.

Clayton, S. C. *et al.*, Anal. Chim. Acta 14, 269 (1956).

Collins, A. H., Analyst 87, 733 (1962).

Daniels, F. and Alberty, R. A., "Physical Chemistry," 2nd ed., John Wiley and Sons, Inc., New York, 1961.

De Rossi, M., Sci. Tec. 6, 31 (1962); C. A. 61, 3754 (1964).

Ewing, G. W., "Instrumental Methods of Chemical Analysis," 2nd ed., McGraw-Hill Book Co., Inc., New York, 1960.

Fujiwara, S. and Hayashi, S., Anal. Chem. 26, 239 (1954).

Glasstone, S., "An Introduction to Electrochemistry," D. Van Nostrand Co., Inc., New York, 1942.

Griffiths, V. S., Anal. Chim. Acta 18, 174 (1958).

Griffiths, V. S., Talanta 2, 230 (1959).

Gupta, S. R. *et al.*, J. Sci. Instr. 33, 313 (1956).

Hackl, A. E. and Deisinger, H., Allgemeine and Praktishe Chemie 19, 229 (1968).

Hall, J. L., Anal. Chem. 24, 1236 (1952).

Hall, J. L., et al., Anal. Chem. 26, 1539 (1954).

Hamilton, L. F., and Simpson, S. G., "Quantitative Chemical Analysis," The Macmillan Co., New York, 1958.

Hamme, H. W. et al., J. Chem. Phys. 22, 944 (1954).

Hytech Laboratory Salinometer Model 6220 Specification Sheet; Hytech Marine Products, San Diego, California.

Jensen, F. W. and Parrack, A. L., Ind. Eng. Chem., Anal. Ed. 18, 595 (1946).

Johnson, C. M. and Hart, G. E., Anal. Instrum. 4, 23 (1967).

Johnson, C. M. and Hart, G. E., Rocky Flats Internal Report RFP-657, U. S. Atomic Energy Commission, 1966.

Johnson, D. E. and Enke, C. G., Anal. Chem. 42, 329 (1970).

Kamura, Y., Yakugaku Zasshi 74, 1 (1954).

Kolthoff, I. M. and Elving, P. J. (ed.), "Treatise on Analytical Chemistry," Part I, Vol. 4, Interscience Publishers Inc., New York.

Kolthoff, I. M. et al., "Quantitative Chemical Analysis," 4th ed., The Macmillan Co., Ltd., London, 1969.

Kupka, F., and Slabaugh, W. H., Anal. Chem. 29, 845 (1957).

Kurrelmeyer, B., and Mais, W. H., "Electricity and Magnetism," D. Van Nostrand Co., Inc., Princeton, 1967.

Ladd, M. F. C. and Lee, W. H., Talanta 12, 941 (1965).

Lange, N. A. (ed.), "Handbook of Chemistry," 10th ed., McGraw-Hill Book Co., Inc., New York, 1961.

Lavagnino, B. and Alby, B., Ann. Chim. 49, 1272 (1959).

Lopatnikov, V. I., Soviet Physics (Eng. trans.) 6, 505 (1961).

Malmstadt, H. V. et al., "Electronics for Scientists," W. A. Benjamin, Inc., New York, 1963.

Meites, L. (ed.), "Handbook of Analytical Chemistry," McGraw-Hill Book Co., New York, 1963.

Mellon, M. G., "Chemical Publications," 3rd ed., McGraw-Hill Book Co., Inc., New York, 1958.

Owen, D., "Alternating Current Measurements at Audio and Radio Frequencies," Methuen and Co. Ltd., London, 1957.

Park, K. et al., Anal. Chem. 35, 1549 (1963).

Pazsitka, L. et al., Z. Anal. Chem. 245, 103 (1969).

Piccard and Frivold, "Archives des Sciences Physiques et Naturelles" (Series 5) 2, 264 (1920); cited in U. S. Patent 2,542,057.

Pungor, E., "Oscillometry and Conductometry," Pergamon Press, Oxford, 1965.

"The Radio Amateur's Handbook," 44th ed., American Radio Relay League (publisher), 1967.

Reilley, C. N. in P. Delahay, "New Instrumental Methods in Electro-Chemistry," Interscience Publishers Inc., New York, 1954.

Reilley, C. N. and McCurdy, Jr., W. H., Anal. Chem. 25, 86 (1953).

Relis, M. J., U. S. Patent 2,542,057, Feb. 20, 1951.

Rosenthal, R. (ed.), "Solution Conductivity Handbook," Beckman Instrument Bulletin 4090, 1969.

Ruben, S., U. S. Patent 1,610,971, Dec. 14, 1926.

Schure, A., "Resonant Circuits," John F. Rider Publisher, Inc., New York, 1957.

Schure, A., "Transformers," J. F. Rider Publisher, Inc., New York, 1961.

Schedlovsky, T., in Weissberger, A. (ed), "Physical Methods in Organic Chemistry," Interscience Publishers, Inc., New York, 1946.

Sherrick, P. H., et al., "Manual of Chemical Oscillometry," E. H. Sargent and Co., Chicago, 1954.

Timnick A. et al., Chemistry in Canada 12, 23 (1960).

Weber, R. L. et al., "Physics for Science and Engineering," McGraw-Hill Book Co., Inc., New York, 1959.

Willard, H. H., et al., "Instrumental Methods of Analysis," 4th ed., D. Van Nostrand Co., Inc., Princeton, 1965.

Wilson, C. L. and Wilson, D. W. (ed.), "Comprehensive Analytical Chemistry," Elsevier Publishing Co., New York, 1964.

Zarilla, R. F., "New Instrumentation for Analysis by High Frequency Techniques," thesis, University of Pittsburgh, 1966.